

TRANSPIRATION DYNAMICS OF A SEMIARID URBAN
FOREST ECOSYSTEM IN NORTHERN UTAH, USA

by

Susan Elaine Bush

A dissertation submitted to the faculty of
The University of Utah
in partial fulfillment of the requirements for the degree of

Doctor of Philosophy

Department of Biology

The University of Utah

May 2015

Copyright © Susan Elaine Bush 2015

All Rights Reserved

The University of Utah Graduate School

STATEMENT OF DISSERTATION APPROVAL

The dissertation of Susan Elaine Bush
has been approved by the following supervisory committee members:

<u>James R. Ehleringer</u>	, Chair	<u>05/24/2012</u> Date Approved
<u>David R. Bowling</u>	, Member	<u>05/24/2012</u> Date Approved
<u>Diane E. Pataki</u>	, Member	<u>05/24/2012</u> Date Approved
<u>John S. Sperry</u>	, Member	<u>05/24/2012</u> Date Approved
<u>Philip E. Dennison</u>	, Member	<u>05/24/2012</u> Date Approved

and by M. Denise Dearing, Chair/Dean of
the Department/College/School of Biology

and by David B. Kieda, Dean of The Graduate School.

ABSTRACT

Urbanization of the western United States has been associated with large-scale changes in the species composition and distribution of vegetation on the landscape. Among these changes include the afforestation of land within city boundaries with nonnative cultivars subject to markedly different atmospheric conditions compared to their native habitats and the introduction and expansion of nonnative tree species in riparian regions, both within city boundaries proper and in wild land riparian areas throughout the West. This dissertation is concerned with how these changes have impacted the water use and physiological behavior of tree species in these environments and the associated water use consequences of these changes at multiple temporal and spatial scales.

Multiple sites within the Salt Lake Valley of northern Utah, USA, were instrumented with thermal dissipation probes for measuring sap flow. In addition, porometry, water potential, and other methods were used to further evaluate plant water relations and also the properties and functional status of xylem vasculature. In cultivated landscapes, I found that wood anatomy (ring- versus diffuse-porous xylem) constrained stomatal responses and associated rates of water loss to atmospheric vapor pressure deficit and that differential sensitivity was linked to vulnerability to xylem cavitation. The scaling of sap flux density data to whole-tree and stand water use in an unmanaged riparian forest and across sites in the Salt Lake City urban forest showed significant

variation that was independent of native versus nonnative species status or wood anatomical characteristics. In addition, seasonality differences were observed with respect to the magnitude and timing of water fluxes that were linked to xylem cavitation vulnerability. The results reported here further increase our understanding of the physiology and water use behavior of trees in both urban and natural ecosystems and provide much needed information toward making informed management decisions that impact water resources in urban regions and riparian areas throughout the western US as well as semiarid regions elsewhere.

For Tigerlily and June.

TABLE OF CONTENTS

ABSTRACT.....	iii
LIST OF TABLES.....	viii
ACKNOWLEDGEMENTS.....	ix
Chapters	
1. INTRODUCTION	1
2. WOOD ANATOMY CONSTRAINS STOMATAL RESPONSES TO ATMOSPHERIC VAPOR PRESSURE DEFICIT IN IRRIGATED, URBAN TREES....	5
Abstract.....	6
Introduction.....	6
Materials and methods	7
Results.....	8
Discussion	11
References.....	13
3. CALIBRATION OF THERMAL DISSIPATION SAP FLOW PROBES FOR RING- AND DIFFUSE-POROUS TREES	14
Summary.....	15
Introduction.....	15
Materials and methods	16
Results.....	17
Discussion	20
References.....	23
4. WATER USE AND ECOHYDROLOGY OF CO-OCCURRING RUSSIAN OLIVE AND COTTONWOOD TREES IN AN URBAN RIPARIAN CORRIDOR OF NORTHERN UTAH, USA.....	25
Abstract.....	25
Introduction.....	26
Methods.....	29

Results	34
Discussion	38
References	44
5. WATER USE AND CONTRASTING HYDRAULIC STRATEGIES OF CULTIVATED RING- AND DIFFUSE-POROUS TREES IN A SEMIARID URBAN ECOSYSTEM.....	57
Abstract	57
Introduction	58
Methods	60
Results	64
Discussion	67
References	73

LIST OF TABLES

2.1 Site location, xylem anatomy, water source, mean diameter at breast height (\pm SE), and mean sapwood depth at breast height (\pm SE) of each species.....	7
2.2 Hydraulic conductance (means \pm SE) estimated from midday sap flux and the difference between predawn and midday water potential.....	11
3.1 Characteristics of branch segments used to collect calibration data. Length and diameter are given as mean \pm standard error.....	16
3.2 Mean sapwood area and depth \pm standard error for all branch segments associated with calibration measurements.....	20
3.3 Slope and intercept values \pm standard error of log-transformed calibration data obtained by standard least-squares linear regression.....	20
4.1 Morphological characteristics of measurement trees for the 2004 and 2005 measurement years. Diameter at breast height (DBH), sapwood area, and basal area are given as the mean \pm the standard error.....	47
4.2 Empirical model transpiration results based on leaf and canopy ground areas. Results are shown for the 2004 and 2005 measurement years. Transpiration estimates based on leaf area and canopy ground area have units of $L\ m^{-2}\ d^{-1}$ and $mm\ d^{-1}$, respectively.....	48
5.1 Species, year, and measurement site information for study trees.....	75
5.2 The stand characteristics of measurement trees. The mean \pm the standard error are given.....	76
5.3 Mean July water use \pm the standard error for different scaling metrics.....	77

ACKNOWLEDGEMENTS

I must first acknowledge my advisor, Jim Ehleringer, for the many opportunities and great support he has provided me over the years. He has been a wonderful mentor and friend. I also want to acknowledge Kevin Hultine, who has been incredibly supportive and helpful throughout this process. I am grateful to my committee members John Sperry, Dave Bowling, Diane Pataki, and Phil Dennison for their academic guidance and for providing training and access to lab and field equipment. In addition, it has been a pleasure to be a part of the Ehleringer lab family, where I have had the privilege to work with, and learn from, many great folks.

I am thankful for my mother. She has always been a champion of education. Both she and my lovely father never discouraged me from believing that whatever I wanted to accomplish was within my reach, and for that, and so many other things, I am forever grateful. I must also acknowledge my sisters; I have many. The four strong, beautiful women I grew up with at home, and the other wonderful ladies in my life that I call my sisters too. I am so grateful for all of the support I have received from my family and community of friends.

Lastly, I thank the Biology department for financial support and teaching opportunities and the United States Department of Energy and National Science Foundation for providing additional financial support.

CHAPTER 1

INTRODUCTION

Urbanization in the western US results in large changes in land surface characteristics, including changes in the types and spatial extent of vegetation. In semiarid and arid urban regions of the western US, one of the most striking vegetation changes is the emergence of urban forests, which now extend across large land areas that were previously grasslands or shrublands and that are comprised almost entirely of nonnative tree species. The vast majority of urban forest in the western US was not previously forested, with the likely exception of relatively narrow riparian corridors. These irrigated urban forests are also unusual in that their development would not have been possible without large-scale modification in the amount, timing, and distribution of water on the landscape due to human activity.

The amount of vegetation and availability of water on a landscape has a significant impact on surface energy and water budgets. Measured evapotranspiration rates of semiarid and arid urban ecosystems have been shown to far exceed precipitation inputs due to the mass import of water into these ecosystems and its loss to the atmosphere by either evaporation from impervious or soil surfaces or transpiration from vegetation. However, very little information exists by which to assess the magnitude of these component fluxes. This is especially surprising given that in the western US, these

ecosystems largely rely on an already overappropriated water supply from western riparian ecosystems. Quantifying urban forest transpiration and its associated impact on evapotranspiration fluxes is a critical area of research that is significantly lacking available data.

The complex heterogeneous urban surface, highly diverse mosaic of tree species, and large number of other factors dictated by variable human behavior make quantifying the magnitude of forest transpiration in these ecosystems challenging. Yet because these forests are mostly comprised of nonnative species, where atmospheric vapor pressure deficit (vpd) is extremely high relative to native habitat and water supply for transpiration is often not a limiting factor due to irrigation inputs, these ecosystems also provide the opportunity for employing a common garden approach to examining factors that contribute to plant water use dynamics that may be applicable to other natural ecosystems. The chapters in this dissertation focus on quantifying forest transpiration fluxes in semiarid urban regions, using the Salt Lake City Metropolitan region of northern Utah, US, as typical of the forests that now dominate these urban ecosystems. The overall goal of this thesis is to provide an improved understanding of the factors that influence the magnitude and seasonality of forest transpiration for both urban and nearby natural ecosystems.

The second chapter provides information about differential species responses to increasing vpd for well-irrigated trees, where xylem anatomy seems to play an important role in constraining water loss rates. The results for six species showed that there were two different flux responses to increasing vpd, distinguishable on the basis of wood anatomy type and associated vulnerability to xylem cavitation. Diffuse-porous

species generally showed increasing transpiration rates with increasing vpd, although the magnitude of the response changed over the course of the growing season. In contrast, ring-porous species showed a saturating response to vpd, with very little change in the magnitude of this response occurring over the growing season. These differences were attributed to differences in cavitation vulnerability, where more vulnerable ring-porous species appeared to exercise greater stomatal control of water loss compared to diffuse-porous species.

The focus of the third chapter assesses methodology and the magnitudes of transpiration rates. Transpiration measurements associated with Chapter 2 and the remaining chapters in this thesis were made using thermal dissipation probes. These sensors are commonly used for obtaining sap flux density and estimates of whole-tree and stand water use in forest water balance studies. This method requires the use of an empirically derived equation, which was originally reported as valid for all wood types (ring- and diffuse-porous and tracheid anatomy). However, significant error can arise when large gradients in sap velocity occur along the length of a sensor, or where a large fraction of the sensor length is embedded in nonconducting wood. These are conditions that may be routinely violated in ring-porous trees, and because of this, sensor calibration measurements were made for a set of ring-porous species and also for two diffuse-porous species in order to assess the validity of the original calibration equation. The results of this chapter showed that in all cases the original calibration equation largely underestimated sap flux density in ring-porous species, but was valid for the diffuse-porous species investigated. Calibration equations for use in calculating fluxes for ring-porous species are presented.

Chapters 4 and 5 focus on scaling sap flux density measurements to the whole-tree and whole-plot scales for two different forest types within the Salt Lake Valley urban forest boundaries. Chapter 4 focuses on whole-tree and plot level transpiration dynamics of an unmanaged urban riparian forest consisting of native *Populus fremontii* and invasive *Elaeagnus angustifolia* species. Chapter 5 focuses on whole-tree and plot level transpiration dynamics of cultivated urban tree species associated with landscaped urban area. In both chapters, differences in scaled transpiration fluxes were observed between species. There were also variable seasonal transpiration patterns observed. These results are discussed with respect to impacts on fluxes in both urban and natural forested ecosystems.

CHAPTER 2

WOOD ANATOMY CONSTRAINS STOMATAL RESPONSES TO ATMOSPHERIC VAPOR PRESSURE DEFICIT IN IRRIGATED, URBAN TREES

Springer and Oecologia, Volume 156, 2008, p13-20, "Wood anatomy constrains stomatal responses to atmospheric vapor pressure deficit in irrigated, urban trees," S.E. Bush, D.E. Pataki, K.R. Hultine, A.G. West, J.S. Sperry and J.R. Ehleringer, copyright 2008, with kind permission from Springer Science and Business Media.

Wood anatomy constrains stomatal responses to atmospheric vapor pressure deficit in irrigated, urban trees

Susan E. Bush · Diane E. Pataki · Kevin R. Hultine · Adam G. West ·
John S. Sperry · James R. Ehleringer

Received: 28 July 2007 / Accepted: 8 January 2008
© Springer-Verlag 2008

Abstract Plant transpiration is strongly constrained by hydraulic architecture, which determines the critical threshold for cavitation. Because species vary greatly in vulnerability to cavitation, hydraulic limits to transpiration and stomatal conductance have not generally been incorporated into ecological and climate models. We measured sap flow, leaf transpiration, and vulnerability to cavitation of a variety of tree species in a well-irrigated but semi-arid urban environment in order to evaluate the generality of stomatal responses to high atmospheric vapor pressure deficit (D). We found evidence of broad patterns of stomatal responses to humidity based on systematic differences in vulnerability to cavitation. Ring-porous taxa consistently had vulnerable xylem and showed strong regulation of transpiration in response to D , while diffuse-porous taxa were less vulnerable and transpiration increased nearly linearly with D . These results correspond well to patterns in the distribution of the taxa, such as the prevalence of diffuse-porous species in riparian ecosystems, and also provide a means of representing

maximum transpiration rates at varying D in broad categories of trees.

Keywords Stomatal conductance · Transpiration · Ring-porous · Diffuse-porous · Urban ecology

Introduction

Transpiration rates of whole trees are a major component of the water cycle at the ecosystem, regional, and global scales. At the leaf level, transpiration is controlled by stomata in part to prevent excessive cavitation of xylem. This regulation occurs at the cost of reduced CO_2 supply and consequently has a large influence on photosynthesis and primary productivity. The degree of stomatal opening is strongly constrained by the hydraulic architecture of plants that determines the critical water potential threshold for cavitation (Sperry 2000). While there are many examples of species differences in vulnerability to cavitation, hydraulic constraints on gas exchange have not been evaluated in a large number of species. Yet broad classes of responses across functional types are needed to incorporate hydraulic mechanisms into larger scale models linking biological processes and the water cycle.

Within temperate angiosperm trees, xylem anatomy is broadly divided into plants with ring-porous versus diffuse-porous vessel elements. A major difference in these contrasting xylem anatomies is the diameter distribution of vessel elements. Ring-porous taxa have a bimodal distribution of vessel diameter associated with large, early season vessels and small late-season vessels, while diffuse-porous taxa show very little distinction between the diameter of vessel elements in early versus late wood (Tyree and Zimmerman 2002). Theoretically, we would

Communicated by Manuel Lerdau.

S. E. Bush · K. R. Hultine · A. G. West ·
J. S. Sperry · J. R. Ehleringer
Department of Biology, University of Utah,
Salt Lake City, UT 84112, USA

D. E. Pataki (✉)
Department of Earth System Science and Department of Ecology
and Evolutionary Biology, University of California,
Irvine, CA 92697, USA
e-mail: dpataki@uci.edu

A. G. West
Department of Integrative Biology, University of California,
Berkeley, CA 94720, USA

expect these anatomical differences to result in different hydraulic capacities and transpiration rates (Tyree and Zimmerman 2002). However, previous attempts to quantify whole tree transpiration rate differences among trees with contrasting anatomies have yielded mixed results, with no clear systematic differences (Oren and Pataki 2001; Pataki and Oren 2003).

In this study we exploited a relatively new ecological environment to determine whether diffuse-porous trees systematically have different stomatal sensitivity to vapor pressure deficit (D) than ring-porous trees based on categorically different hydraulic constraints. Cities in arid and semi-arid regions are commonly associated with afforestation that replaces the native desert and grassland vegetation with irrigated forests (Nowak et al. 1996). In these ecosystems, non-native species experience D environments that greatly exceed the upper limits associated with their native habitats today, and in all likelihood at any time during their evolutionary histories. Urban forests in the western United States are unusual in that they comprise almost entirely non-native deciduous tree species from mesic environments, and their continued presence relies primarily on irrigation water to sustain soil moisture. From a management perspective, transpiration rates of urban trees are of great interest in the selection of water-conserving species. From an ecological perspective, we utilized this environment to test the hypothesis that differences in angiosperm xylem anatomy were a constraint on transpiration rates in moist soils in the high D environment of the Salt Lake Valley, Utah, where both ring-porous and diffuse-porous trees are routinely cultivated.

Materials and methods

Study site

The Salt Lake Valley (latitude 40.66; longitude 111.55; elevation 1,275–1,550 m) is a metropolitan area located in northern Utah, USA. The climate is semi-arid, with a mean annual temperature and precipitation of 11.1°C and

411 mm, respectively (Alder et al. 1998). Mean daytime D may exceed 5 kPa during the growing season in the Salt Lake Valley, whereas mean daytime D in mesic environments rarely exceeds 2 kPa. Sap flux measurements were made at three different locations in the Salt Lake Valley during the 2003 and 2004 growing seasons.

The “Campus” and “Red Butte” sites were measured in 2003. These sites were landscaped and regularly irrigated. The “Riparian” site was measured in 2004 and was a riparian forest along a major river corridor that runs from south to north across the middle of the valley. The Campus site was located at the University of Utah and consisted of diffuse-porous *Platanus acerifolia* (Ait.) Willd. and ring-porous *Gleditsia triacanthos* L. planted within a turfgrass lawn. The Red Butte site was located at the University of Utah Research Park at the mouth of Red Butte Canyon and consisted of diffuse-porous *Acer platanoides* L. and ring-porous *Quercus rubra* L. planted in turfgrass and interspersed with small groves of irrigated *Quercus gambelii* Nutt. The Riparian site was located in a riparian forest of *Populus fremontii* Wats. growing along the Jordan River in Sandy, Utah. Of these species, both *P. fremontii* and *Q. gambelii* were native to the study region. The mean diameter of study trees is given in Table 1.

Sap flux measurements

At each site, 20-mm-long thermal dissipation probes according to Granier (1987) were used to measure sap flux density (J_s) for ten individuals of each species. Sensor pairs were inserted radially at breast height (1.4 m), with a vertical separation of 15 cm. The axial direction of insertion was selected at random. The temperature difference associated with each sensor pair was measured every 30 s and averaged every 30 min with a datalogger (CR23X; Campbell Scientific, Logan, Utah) during June and up to and including September. J_s ($\text{g m}^{-2} \text{s}^{-1}$) was calculated according to the empirically derived equation (Granier 1987):

Table 1 Site location, xylem anatomy, water source, mean diameter at breast height (\pm SE), and mean sapwood depth at breast height (\pm SE) of each species

Species	Xylem anatomy	Site	Water source	Mean diameter (cm)	Mean sapwood depth (cm)
<i>Platanus acerifolia</i>	Diffuse	Campus	Irrigated	25.0 \pm 1.8	8.7 \pm 0.9
<i>Acer platanoides</i>	Diffuse	Red Butte	Irrigated	26.5 \pm 0.7	8.8 \pm 0.6
<i>Populus fremontii</i>	Diffuse	Riparian	Riparian	30.3 \pm 3.2	5.5 \pm 0.6
<i>Gleditsia triacanthos</i>	Ring	Campus	Irrigated	20.8 \pm 1.1	3.2 \pm 0.2
<i>Quercus gambelii</i>	Ring	Red Butte	Irrigated	13.5 \pm 0.5	2.8 \pm 0.2
<i>Quercus rubra</i>	Ring	Red Butte	Irrigated	21.4 \pm 1.1	3.1 \pm 0.2

$$J_s = 119(\Delta T_m / \Delta T - 1)^{1.231} \quad (1)$$

where ΔT is the temperature difference between the sensor probes and ΔT_m is the temperature difference between the sensor probes under zero-flow conditions. Trees were cored using an increment borer at the conclusion of the experiment to estimate sapwood depth visually at the sensor location. In all cases, the sensor depth did not exceed sapwood depth (Table 1).

Atmospheric and soil moisture measurements

Temperature and relative humidity were measured continuously at all three study locations (HMP35C, HMP45A; Vaisala, Helsinki). Measurement frequency and output was the same as for sap flux measurements. Time domain reflectometry probes (CS616; Campbell Scientific) integrating the top 30 cm of soil were used to monitor the seasonal course of soil moisture at the Campus and Red Butte sites. Eight probes, five at the Campus site and three at the Red Butte site, were distributed at different locations across each site. Measurements were made every 10 min and averaged every 30 min. In addition, irrigation water was collected in graduated cylinders at the Campus and Red Butte sites from the last week of August up to and including the third week of September. A small amount of oil was placed in the cylinders to minimize evaporation. Three cylinders were placed at each site. Soil water availability was monitored at the Riparian site with depth to the water table measurements using an onsite piezometer.

Water potential measurements

Predawn and midday water potential were measured on a monthly basis throughout the growing season for each species. Single leaves from five individual trees per species were cut using a sharp razor blade and measured immediately following excision using a Scholander-type pressure chamber (PMS, Corvallis, Ore.). In situ hydraulic conductance was estimated from sap flow measurements and the water potential gradient as measured by predawn and midday water potential according to Pataki et al. (2000).

Gas exchange measurements

Leaf-level gas exchange was measured with a steady state porometer (LI-1600; LI-COR Biosciences) from mid June up to and including early July 2006 between 1000 and 1600 hours for two of the six species in this study. Because

of the logistical difficulty of characterizing whole-canopy stomatal conductance with leaf-level measurements on many replicate trees, *P. acerifolia* and *Q. rubra* were selected as representative species having diffuse-porous and ring-porous wood anatomy, respectively. Average species-level responses to ambient D conditions for these two species were evaluated from consecutive measurements of three trees per species, where four independent, south-facing, leaf measurements were made per tree for a given measurement period. Porometry measurements were made relatively early in the growing season to avoid potentially confounding effects of significant changes in leaf-level transpiration rates over time, but late enough in the season to capture high ambient D conditions.

Vulnerability curve measurements

Vulnerability to cavitation was measured according to the centrifuge method described in Alder et al. (1997). Six stem segments from independent trees for each species were collected before dawn and placed in large plastic bags where they remained until analyzed within a 3-day period. In order to reduce water loss from the stems during storage, a wet paper towel was placed inside the bags, and bags were stored in a walk-in refrigerator. Where possible, only stems representing current year growth were collected. In addition, stem cross-sectional areas were combined with vulnerability curve measurements to assess differences in stem area specific conductivity among species.

Results

Temperature, humidity, and D were very similar at the Campus and Red Butte sites, which were measured simultaneously in 2003 (Fig. 1). Although the Riparian site was measured in 2004, the seasonal pattern was similar. Mean daytime D reached a maximum of 5 kPa in July (Fig. 1). Volumetric water content measurements showed intra- and inter-site specific variation at the Campus and Red Butte sites (Fig. 2), with mean values generally ranging between 20 and 30%. No clear pattern of seasonal decline in volumetric water content was observed, with the exception of a brief drier period at the Red Butte site in September (Fig. 2, days 254–264). The average amount of irrigation recorded at each site from the last week of August up to and including the third week of September was 300 and 310 mm, respectively. However, the amount of irrigation was probably underestimated, as on several occasions the cylinders were filled to capacity and the maximum cylinder height was recorded. At the riparian site, the depth to the water table was ~ 1 m throughout the

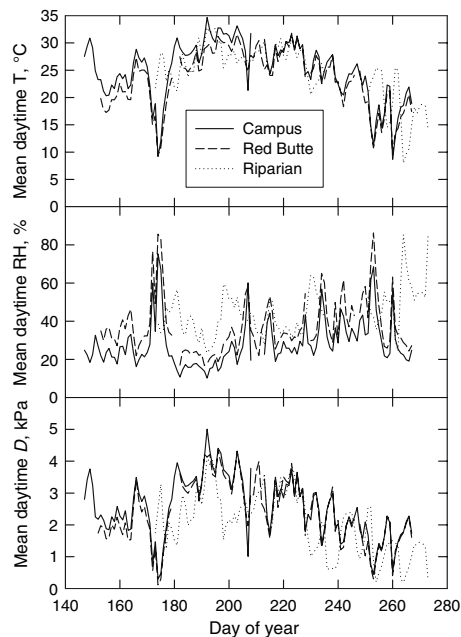


Fig. 1 Daytime average temperature (T), relative humidity (RH), and vapor pressure deficit (D) at each site during the study period. The Campus and Red Butte sites were measured in 2003 and the Riparian site was measured in 2004

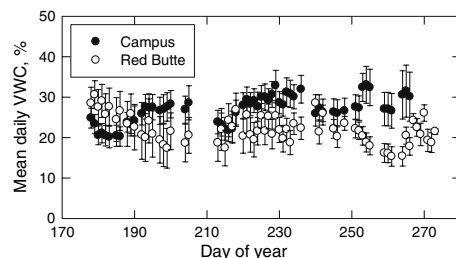


Fig. 2 The seasonal course of volumetric water content (VWC) from 0–30 cm for the two irrigated sites. Data are shown \pm SE

measurement period based on measurements from an onsite piezometer.

Measured predawn water potential showed some variation over the course of the measurement period (Fig. 3), with all species showing some decline by September. However, the absolute values remained relatively positive and ranged between -0.3 and -0.8 MPa (Fig. 3). There

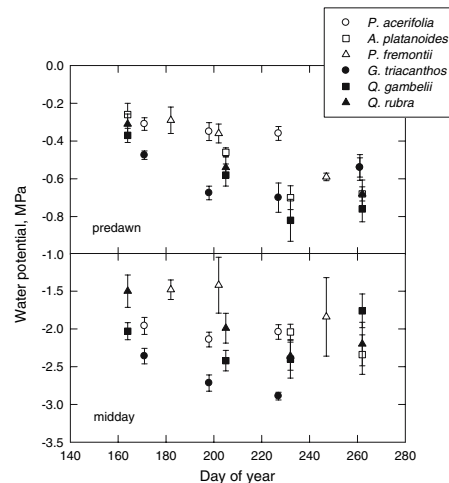


Fig. 3 The seasonal course of predawn and midday water potential measurements. All species were measured in 2003 except *Populus fremontii*, which was measured in 2004. Ring-porous species are shown with closed symbols and diffuse-porous species are shown with open symbols. Error bars represent the SE

were no differences between June and July measurement periods for all species (ANOVA, $P > 0.05$) except *G. triacanthos*, which showed a small mean difference of 0.2 MPa (ANOVA, $P < 0.05$). The largest mean difference observed for any species over the entire measurement period was 0.45 MPa for *Q. gambelii* between June and August. Midday leaf water potentials did not show a clear seasonal pattern and ranged from -1.5 to -3 MPa (Fig. 3). Both predawn and midday water potential were more negative in ring-porous than diffuse-porous species (predawn, -0.63 ± 0.03 and -0.45 ± 0.02 MPa; midday, -2.2 ± 0.08 and -1.6 ± 0.08 MPa; $P < 0.05$). There were no significant differences among species within wood anatomy groups (ANOVA, $P > 0.05$).

Species differed in both the magnitude and the seasonal variation of J_s . The diffuse-porous species showed high J_s in the outer 20 mm of sapwood, but also showed large declines during the growing season for *P. acerifolia* and *A. platanoides* (Fig. 4). In contrast, J_s of *G. triacanthos*, *Q. gambelii*, and *Q. rubra* was relatively low and constant throughout the season (Fig. 4). These species differences appeared to be related to two distinct patterns of responses of daily J_s to average daytime D . In diffuse-porous species, seasonal declines in J_s were related to the seasonal decline in D , in that J_s of diffuse-porous species was closely correlated with D (Fig. 5). Surprisingly, even at the highest D , the diffuse-porous trees showed very little stomatal control

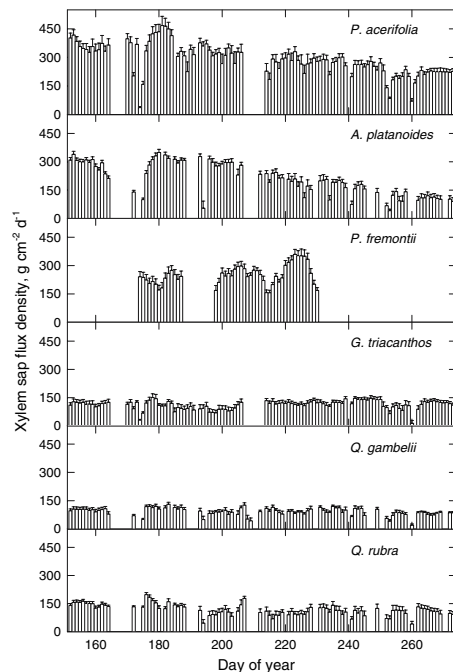


Fig. 4 Average daily sap flux density during the growing season for each species. All species were measured during the 2003 growing season except *P. fremontii*, which was measured in 2004. Error bars represent the SE. *d* Day

of transpiration as evidenced by the linearity of the J_s response to D . However, a reduction in J_s was observed for diffuse-porous species as the growing season progressed (Fig. 5). In contrast, ring-porous species showed a saturating response to increasing D , reaching maximum J_s near D values that are commonly associated with the maximum D in mesic ecosystems, around 2 kPa. Additionally, maximum J_s of ring-porous trees did not show any appreciable decline over the course of the growing season (Fig. 5). There was a significant decline in calculated in situ hydraulic conductance of *P. acerifolia* between June and July and *A. platanooides* between August and September (paired *t*-test, $P < 0.05$; Table 2). The other species did not show significant declines in hydraulic conductance between sampling periods.

There has been some discussion about the appropriate methodology for applying sap flux measurements to ring-porous trees (Clearwater et al. 1999; Granier et al. 1994). The basis for methodological concerns is twofold. First, large radial differences in the J_s along the sensor length

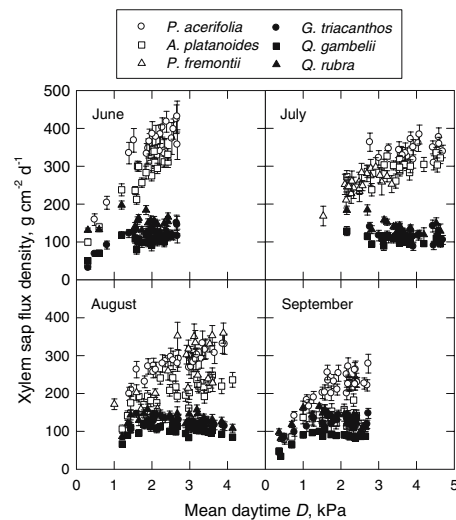


Fig. 5 Average daily sap flux density for diffuse-porous (open symbols) and ring-porous (closed symbols) species in response to average daytime D for June, July, August, and September

may lead to errors in interpreting and scaling measurements to whole trees, and to comparing species with contrasting wood anatomy. Radial trends have been reported for ring-porous species, although results have not always been consistent (Clearwater et al. 1999; Lu et al. 2004; Phillips et al. 1996). A related issue is whether J_s is underestimated in ring-porous trees if transpiration is concentrated largely in the current year vessels, which is difficult to measure. While more information is needed to resolve these issues, several studies have shown good agreement between sap flux measurements in ring-porous trees and independent measurements of transpiration including ventilated chambers and stem water absorption (Goulden and Field 1994; Granier et al. 1994). Regardless of this, systematic underestimation of sap flux in the ring porous species in this study would not explain the saturating response at high D if errors in estimating sap flux of ring-porous trees are independent of D . Differences in stomatal responses to humidity were also observed with independent leaf-level gas exchange measurements (Fig. 6). There was a linear increase in transpiration in response to increasing D for diffuse-porous *P. acerifolia* ($P < 0.001$; Fig. 6), but no response to increasing D for ring-porous *Q. rubra* ($P > 0.1$; Fig. 5).

Vulnerability to cavitation measurements also showed two categories of responses to decreasing water potential. In ring-porous species, lower relative hydraulic

Table 2 Hydraulic conductance (means \pm SE) estimated from midday sap flux and the difference between predawn and midday water potential

Species	Day of year	Hydraulic conductance ($\text{g m}^{-2} \text{s}^{-1} \text{MPa}^{-1}$)
<i>P. acerifolia</i> ^a	171	84.1 \pm 15.0
	198	28.1 \pm 7.0
	227	31.3 \pm 5.4
	261	47.5 \pm 11.0
<i>A. platanoides</i> ^a	232	50.8 \pm 8.2
	262	28.2 \pm 5.6
<i>P. fremontii</i> ^a	182	22.7 \pm 7.5
	202	50.3 \pm 3.0
<i>G. triacanthos</i> ^b	171	19.1 \pm 2.5
	198	11.4 \pm 2.5
	227	15.1 \pm 2.9
<i>Q. gambelii</i> ^b	164	13.0 \pm 0.9
	205	18.8 \pm 1.8
	232	19.6 \pm 3.9
	262	39.8 \pm 12.2
<i>Q. rubra</i> ^b	164	21.4 \pm 0.8
	205	20.1 \pm 0.3
	232	25.0 \pm 2.7
	262	28.2 \pm 5.8

^a Diffuse-porous species

^b Ring-porous species

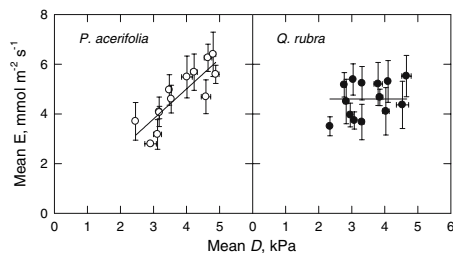


Fig. 6 Leaf-level transpiration (E) for diffuse-porous (*Platanus acerifolia*; left panel) and ring-porous (*Quercus rubra*; right panel) trees in response to ambient D conditions. The slope of the relationship between transpiration and D was significant for *P. acerifolia* ($P < 0.001$), but not for *Q. rubra* ($P = 0.168$)

conductance was sustained at negative stem water potentials than in diffuse-porous species (Fig. 7, upper panel). In addition, stem area-specific conductivity for ring-porous species showed higher potential conducting efficiency at the cost of increased vulnerability to cavitation, whereas diffuse-porous species showed less vulnerability to cavitation at the cost of lower potential conducting efficiency

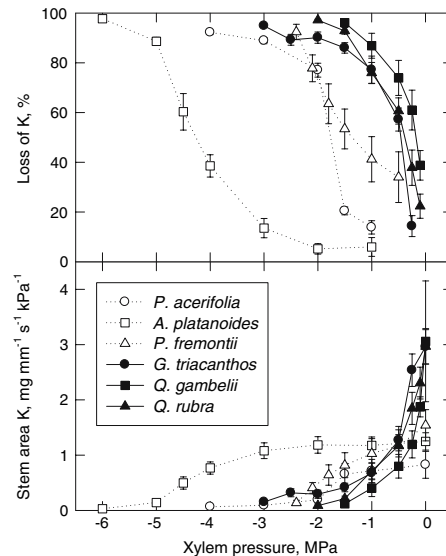


Fig. 7 The cavitation vulnerability of xylem (upper panel) and absolute stem area specific hydraulic conductance (lower panel) for diffuse-porous (open symbols) and ring-porous (closed symbols) species with increasing xylem tension

(Fig. 7, lower panel). Differences among species within a given wood type were also observed, particularly for diffuse-porous species. However, the categorically different responses observed between wood types were not driven by any single species, as all diffuse-porous species showed a more gradual change in % loss conductivity and stem area-specific conductivity with decreasing xylem pressure relative to ring-porous species, particularly between 0 and -0.5 MPa (Fig. 7).

Discussion

Our results show two categories of J_s responses to D across wood anatomy types that we attribute to differences in stomatal sensitivity to D , with the most pronounced differences occurring at D values that exceed those generally found in the native range of mesic trees (Fig. 5). In general, previous studies of the response of transpiration to D have been associated with a relatively small D range. Our measured J_s rates are comparable to previously measured values of J_s under conditions of low D (Hultine et al. 2007; Bovard et al. 2005; Catovsky et al. 2002; Oren and Pataki 2001; Oren et al. 1999; Pataki and Oren 2003; Phillips et al.

1996). However, the small range in D associated with most previous sap flow measurements as well as studies of stomatal responses of leaves to D (e.g., Franks and Farquhar 1999) has made it difficult to determine whether there are clear differences in the sensitivity of ring vs. diffuse-porous trees. While there is some indication of differences in stomatal sensitivity to D among diffuse vs. ring-porous species at low D (Oren and Pataki 2001; Oren et al. 1999), a survey of the available literature yields limited results because of the lack of data of stomatal responses of ring-porous species to very high D exceeding 3 kPa. Additional measurements in a broader range of taxa and biomes are needed to confirm the generality of these results; however, they are supported by observed patterns in the distribution of the species. In semi-arid environments, riparian trees currently overwhelmingly comprise diffuse-porous species. Our results suggest that this is a competitive advantage: diffuse-porous species can maintain high rates of stomatal conductance and therefore continue photosynthesis under highly desiccating atmospheric conditions.

Independent leaf-level transpiration measurements showed patterns of transpiration response to increasing D that were similar to those obtained with J_s measurements (Figs. 5, 6). While differences in the magnitude of transpiration were observed at the leaf scale relative to the whole plant scale (Figs. 5, 6), likely attributable to methodological or scaling factors (particularly variations in leaf-sapwood area ratios), the pattern of response to increasing D (linear for diffuse-porous and saturating for ring-porous) remained consistent. These results provide further evidence that the observed patterns of J_s in response to D result from differences in stomatal sensitivity to D between wood anatomy types. However, additional measurements of leaf-level transpiration will be needed to determine the extent of this response at smaller temporal and spatial scales.

The contrasting patterns of J_s with increasing D shown by ring and diffuse-porous trees are likely related to differences in the vulnerability of these species to xylem cavitation (Fig. 7). The notion that there may be a safety versus efficiency tradeoff in xylem transport that is related to the size of conducting xylem conduits has long been proposed (Tyree and Zimmerman 2002). Larger diameter conduits have the capacity for greater efficiency in sap transport, while smaller diameter conduits are generally more resistant to xylem cavitation events. While the exact mechanisms are still the focus of ongoing research, differences in vulnerability to cavitation between ring and diffuse-porous species were recently described by Hacke et al. (2006) and Li et al. (2007) and confirmed here (Fig. 7). Hence, diffuse-porous trees can tolerate the negative water potentials that develop in xylem when stomata remain open at high D . These differences may not be

manifested in bulk leaf midday water potential, which did not differ greatly among the taxa (Fig. 3). Our results also cannot be explained by age differences among species, as there were no systematic differences in age between ring and diffuse-porous species in this study.

The consequence of lack of stomatal regulation in diffuse-porous trees was that some cavitation was apparent by late summer, as evidenced by reduced rates of J_s (Figs. 4, 5) and a relatively constant predawn to midday water potential difference resulting in lower values of calculated, in situ hydraulic conductance (Table 2). There was little indication of progressive soil drought during the growing season that would have caused additional water stress. While there was a small decline in predawn water potential at both of the landscaped sites as the growing season progressed, this decline was unlikely to account for the reduced J_s rates, as the timing of the change in water potential and J_s did not coincide. Additionally, nighttime transpiration precludes the use of predawn water potential measurements as a proxy for soil water potential, which would also introduce errors into the calculation of hydraulic conductance. There was some evidence of nighttime sap flow during the study period (data not shown); during these periods, ΔT_m from Eq. (1) was prescribed from earlier periods when D approached zero, as in Daley and Phillips (2006). However, despite the difficulty in estimating effective plant soil water potential and hydraulic conductance in semi-arid environments, progressive cavitation resulting from lack of stomatal regulation of water loss seems to be the best explanation for the change in the relationship between J_s and D in diffuse-porous species late in the growing season.

Previous studies have suggested deeper rooting in ring-porous than in diffuse-porous trees (Abrams 1990; Burns and Honkala 1990; Pallardy and Rhoads 1993), although this has been difficult to quantify in mixed species stands. In our study, there was little evidence of deeper rooting in ring-porous species, as predawn water potential was more rather than less negative in ring-porous compared to diffuse-porous trees (Fig. 2). However, the absolute differences among taxa were small and water potentials remained relatively high due to irrigation. Here, we show that differences in J_s responses to D persist in the absence of large differences in access to water among the taxa. In addition, our results suggest that a tendency for ring-porous trees to be more deeply rooted would be advantageous given their more vulnerable transport system. The degree to which ring-porous species systematically have deeper rooting distributions relative to diffuse-porous species as a consequence of differences in cavitation vulnerability is not known and warrants further study. In addition, the diffuse-porous species measured in this study had consistently greater sapwood depths than the ring-porous species

(Table 1), which may be an additional mechanism for coping with water stress. In particular, root-to-sapwood area and leaf-to-sapwood area ratios are important aspects of allometry that may govern plant responses to water stress; however, they are very difficult to measure in mature trees. Additional data are needed across the taxa to determine if variations are consistent by wood type.

From a whole ecosystem perspective, our results suggest that changes in D due to altered temperature and/or humidity would have different effects on ring and diffuse-porous species. Provided that soil moisture is not limiting, an increase in D would correspond to increased water vapor fluxes from forested areas dominated by diffuse-porous trees, whereas transpiration of forests dominated by ring-porous trees would show little change. In the long-term, sustained shifts in average D may ultimately impact competition for water resources and affect the distribution of species.

In general, models of stomatal response to humidity have relied on empirical parameters to describe a phenomenon that is well understood mechanistically (Buckley 2005). It is well known that stomatal closure at decreasing humidity is a mechanism to regulate plant water status and avoid damaging effects of water stress such as excessive cavitation (Sperry 2000; Sperry et al. 1998). This mechanism has not been incorporated into most ecological and land surface models because vulnerability to cavitation has been described as highly species specific and difficult to generalize across broad functional classes. Here we provide evidence that stomatal response to humidity may indeed be predictable based on functional types of two broad classes of deciduous trees. While these results apply specifically to conditions of high soil moisture, they provide a basis for describing the maximum rate of transpiration under non-limiting soil moisture, but varying atmospheric conditions.

Acknowledgements We thank Tim Dance and Angela Allred for their assistance with fieldwork and sensor construction. This work was funded by the U.S. National Science Foundation grants ATM-02157658 and IBN-0416297.

References

- Abrams MD (1990) Adaptations and responses to drought in *Quercus* species of North America. *Tree Physiol* 7:227–238
- Alder NN, Pockman WT, Sperry JS, Nuismer S (1997) Use of centrifugal force in the study of xylem cavitation. *J Exp Bot* 48:665–674
- Alder WJ, et al. (1998) Climate of Salt Lake City, UT. In: NOAA technical memorandum NRS WR-152
- Bovard BD, Curtis PS, Vogel CS, Su H-B, Schmid HP (2005) Environmental controls on sap flow in a northern hardwood forest. *Tree Physiol* 25:31–38
- Buckley TH (2005) The control of stomata by water balance. *New Phytol* 168:275–292
- Burns RM, Honkala BH (1990) *Silvics of North America*. USDA Forest Service, Washington
- Catovsky S, Holbrook NM, Bazzaz FA (2002) Coupling whole-tree transpiration and canopy photosynthesis in coniferous and broad-leaved tree species. *Can J For Res* 32:295–309
- Clearwater MJ, Meinzer FC, Abbadie L, Andrade JL, Goldstein G, Holbrook NM (1999) Potential errors in measurement of nonuniform sap flow using heat dissipation probes. *Tree Physiol* 19:681–687
- Daley MJ, Phillips NG (2006) Interspecific variation in nighttime transpiration and stomatal conductance in a mixed New England deciduous forest. *Tree Physiol* 26:411–419
- Franks PJ, Farquhar GD (1999) A relationship between humidity response, growth form, and photosynthetic operating point in C3 plants. *Plant Cell Environ* 22:1337–1349
- Goulden ML, Field CB (1994) Three methods for monitoring the gas exchange of individual tree canopies: ventilated-chamber, sap-flow and Penman-Monteith measurements on evergreen oaks. *Funct Ecol* 8:125–135
- Granier A (1987) Evaluation of transpiration in a Douglas-fir stand by means of sap flow measurements. *Tree Physiol* 3:309–320
- Granier A et al (1994) Axial and radial water flow in the trunks of oak trees: a quantitative and qualitative analysis. *Tree Physiol* 14:1383–1396
- Hacke UG, Sperry JS, Wheeler JK, Castro L (2006) Scaling of angiosperm xylem structure with safety and efficiency. *Tree Physiol* 26:689–701
- Hultine KR, Bush SE, West AG, Ehleringer JR (2007) Effect of gender on sap-flux-scaled transpiration in a dominant riparian tree species: Box elder (*Acer negundo*). *J Geophys Res* 112:G03S06. doi:10.1029/2006JG000232
- Li Y, Sperry JS, Taneda H, Bush SE, Hacke UG (2007) Evaluation of centrifugal methods for measuring xylem cavitation in conifers, diffuse- and ring-porous angiosperms. *New Phytol* 177:558–568
- Lu P, Urban L, Ping Z (2004) Granier's thermal dissipation probe (TDP) method for measuring sap flow in trees: theory and practice. *Acta Bot Sin* 46:631–646
- Nowak DJ, Rowntree RA, McPherson EG, Sisinni SM, Kerkmann ER, Stevens JC (1996) Measuring and analyzing urban tree cover. *Landsc Urban Plan* 36:49–57
- Oren R, Pataki DE (2001) Transpiration in response to variation in microclimate and soil moisture in southeastern deciduous forests. *Oecologia* 127:549–559
- Oren R et al (1999) Survey and synthesis of intra- and interspecific variation in stomatal sensitivity to vapour pressure deficit. *Plant Cell Environ* 22:1515–1526
- Pallardy SG, Rhoads JL (1993) Morphological adaptations to drought in seedlings of deciduous angiosperms. *Can J For Res* 23:1766–1774
- Pataki DE, Oren R (2003) Species differences in stomatal control of water loss at the canopy scale in a mature bottomland deciduous forest. *Adv Water Resour* 26:1267–1278
- Pataki DE, Oren R, Smith WK (2000) Sap flux of co-occurring species in a western subalpine forest during seasonal soil drought. *Ecology* 81:2557–2566
- Phillips N, Oren R, Zimmerman R (1996) Radial patterns of xylem sap flow in non-, diffuse- and ring-porous tree species. *Plant Cell Environ* 19:983–990
- Sperry JS (2000) Hydraulic constraints on plant gas exchange. *Agric For Meteorol* 104:13–23
- Sperry JS, Adler FR, Campbell GS, Compstock JP (1998) Limitation of plant water use by rhizosphere and xylem conductance: results from a model. *Plant Cell Environ* 21:347–359
- Tyree MT, Zimmerman MH (2002) *Xylem structure and the ascent of sap*. Springer, New York

CHAPTER 3

CALIBRATION OF THERMAL DISSIPATION SAP FLOW PROBES FOR RING- AND DIFFUSE-POROUS TREES

S.E. Bush, K.R. Hultine, J.S. Sperry, and J.R. Ehleringer, "Calibration of thermal dissipation sap flow probes for ring- and diffuse-porous trees," *Tree Physiology*, 2010, Volume 30: 1545-1554, by permission of Oxford University Press.

Calibration of thermal dissipation sap flow probes for ring- and diffuse-porous trees

SUSAN E. BUSH,¹ KEVIN R. HULTINE, JOHN S. SPERRY and JAMES R. EHLERINGER

Department of Biology, University of Utah, Salt Lake City, UT 84112, USA

¹ Corresponding author (sbush@biology.utah.edu)

Received May 11, 2010; accepted September 21, 2010; handling Editor Nathan Phillips

Summary Thermal dissipation probes (the Granier method) are routinely used in forest ecology and water balance studies to estimate whole-tree transpiration. This method utilizes an empirically derived equation to measure sap flux density, which has been reported as independent of wood characteristics. However, errors in calculated sap flux density may occur when large gradients in sap velocity occur along the sensor length or when sensors are inserted into non-conducting wood. These may be conditions routinely associated with ring-porous species, yet there are few cases in which the original calibration has been validated for ring-porous species. We report results from laboratory calibration measurements conducted on excised stems of four ring-porous species and two diffuse-porous species. Our calibration results for ring-porous species were considerably different compared with the original calibration equation. Calibration equation coefficients obtained in this study differed by as much as two to almost three orders of magnitude when compared with the original equation of Granier. Coefficients also differed between ring-porous species across all pressure gradient conditions considered; however, no differences between calibration slopes were observed for data collected within the range of expected in situ pressure gradients. In addition, dye perfusions showed that in three of the four ring-porous species considered, active sapwood was limited to the outermost growth ring. In contrast, our calibration results for diffuse-porous species showed generally good agreement with the empirically derived Granier calibration, and dye perfusions showed that active sapwood was associated with many annual growth rings. Our results suggest that the original calibration of Granier is not universally applicable to all species and xylem types and that previous estimates of absolute rates of water use for ring-porous species obtained using the original calibration coefficients may be associated with substantial error.

Keywords: *Elaeagnus angustifolia*, *Gleditsia triacanthos*, Granier, *Populus fremontii*, *Quercus gambelii*, sap flux, *Sophora japonica*, *Tilia cordata*, transpiration, validation.

Introduction

Thermal dissipation probes (the Granier method) are routinely used in forest ecology and water balance studies to estimate whole-tree transpiration. The method involves measuring the temperature difference between a heated and a reference sensor, which are inserted radially into sapwood. Sap flux density is calculated according to an empirically derived equation originally validated for two gymnosperm species (*Pseudotsuga menziesii* (Mirb.) Franco, Douglas fir and *Pinus nigra* Arnold, Austrian pine) and one ring-porous angiosperm species (*Quercus pedunculata* Ehrh., English oak) (Granier 1985). The calibration has since been validated with measurements showing generally good agreement with the original calibration for many other woody species (Cabibel and Do 1991, Lu and Chacko 1998, Braun and Schmid 1999, Clearwater et al. 1999, Catovsky et al. 2002, Lu et al. 2002, McCulloh et al. 2007). Goulden and Field (1994) reported calibration data for excised stems of *Quercus agrifolia* Nee (California live oak) that had calibration slopes that differed from the original calibration, where the use of the Granier equation would have resulted in underestimated sap flux density. However, the original design had been modified such that the heated sensor received only a fraction of the power compared with the original design. The validity of the original calibration has also been supported by results from studies showing generally good quantitative agreement between water flux estimates obtained with the Granier method compared with other sap flow methods, water absorption, branch bag measurements, eddy covariance measurements and catchment-scale water balance, as well as between sap flux-derived canopy stomatal conductance and porometry-derived stomatal conductance (Granier et al. 1990, 1994, Kostner et al. 1996, Saugier et al. 1997, Tournebize and Boistard 1998, Ewers et al. 2007, Ford et al. 2007). However, results of calibration measurements conducted on excised stems of *Quercus gambelii* Nutt. (Gambel oak) and *Acer grandidentatum* Nutt. (Bigtooth maple) differed substantially relative to the original calibration of Granier

(Taneda and Sperry 2008), in which differences were attributed at least in part to sensor contact with non-conducting wood. More recently, Steppe et al. (2010) and Hultine et al. (2010b) reported calibration results that differed from the original calibration for excised stems of *Fagus grandifolia* and *Tamarix ramosissima* × *chinensis*, respectively. In all three aforementioned studies, the Granier equation underestimated sap flux density.

Large errors in calculated sap flux density can occur in cases in which steep gradients in sap velocity occur along the sensor length or in which a portion of the sensor is inserted into non-conducting wood (Clearwater et al. 1999). Although the original calibration of Granier has been reported to be independent of wood characteristics (Granier et al. 1990), steep velocity gradients along the sensor length and sensor contact with non-conducting wood are conditions that may be encountered more often in ring-porous species relative to species with diffuse porous or tracheid wood anatomy. This is because ring-porous wood has a vessel diameter distribution that is bimodal, with high conducting capacity, large diameter, early season vessels and lower conducting capacity, smaller diameter, late season vessels, leading to potentially very steep gradients in sap velocity across the conducting sapwood in a single growth ring (Tyree and Zimmermann 2002). In fact, previous studies have documented large gradients in sap velocity that are associated with depths equivalent to the typical length of a Granier sensor (20 mm) and cases in which most of the fluid flow through the xylem of ring-porous species was associated with current year vessels (Ellmore and Ewers 1986, Cermak et al. 1992, Granier et al. 1994, Cermak and Nadezhdina 1998, Jaquish and Ewers 2001, Gebauer et al. 2008).

Despite these considerations, most of the reports validating the initial calibration equation are associated with diffuse-porous, agricultural cultivars or tropical species. Validation of the initial calibration for ring-porous taxa is largely absent in the literature and, to our knowledge, is limited to the ring-porous genera *Quercus* and the *Castanea sativa* species. In this article, we report results from laboratory calibration experiments conducted on four ring- and two diffuse-porous tree species. Our objective was to assess the applicability of the original empirical calibration equation reported by Granier to ring-porous trees representing different genera. In addition, because we expected that the potential errors mentioned above were less likely to be associated with diffuse-porous or tracheid-only species, we also report here the results of calibration measurements for two diffuse-porous species.

Materials and methods

Plant material

Calibration measurements were made during the 2008 and 2009 growing seasons using excised branch segments from four ring-porous species and two diffuse-porous species.

The ring-porous species included *Elaeagnus angustifolia* L. (Russian olive, $n=7$), *Gleditsia triacanthos* L. (Honey locust, $n=6$), *Q. gambelii* Nutt. (Gambel oak, $n=6$) and *Sophora japonica* L. (Japanese pagoda, $n=6$), and the two diffuse-porous species included *Populus fremontii* S. Watson (Fremont cottonwood, $n=6$) and *Tilia cordata* Mill. (Littleleaf linden, $n=5$). Plant material was collected from five sites located either in or near Salt Lake Valley, UT, USA (latitude 40°66'; longitude 111°55'; elevation 1275–1550 m). The Salt Lake Valley is a metropolitan area, with a semi-arid climate. Mean annual temperature and precipitation are 11.1 °C and 411 mm, respectively (Alder et al. 1998). The sites included a riparian area associated with the Jordan river corridor, which runs south to north across the center of Salt Lake Valley (*E. angustifolia*), three irrigated, landscaped sites including a Salt Lake City park (*T. cordata*), the University of Utah campus (*G. triacanthos*, *S. japonica*), a site at the base of Red Butte Canyon Research Natural Area (*Q. gambelii*) and, lastly, a site located inside Red Butte Canyon Research Natural Area, just east of Salt Lake City (*P. fremontii*).

Material preparation and experimental apparatus

Stem segments ~3 m in length and 4–6 cm in diameter at the center were cut in air, bagged after foliage removal and taken back to the laboratory, where they were re-cut underwater to remove 1 m lengths on either side of the final measurement segment. Table 1 provides characteristics of the final measurement segments for each species. In the laboratory, both ends of each measurement segment were shaved with a sharp razor blade underwater. Stem segments were then fastened upright to a ring stand using clamps. The lower end of each stem segment was submerged in a beaker of filtered 20 mM KCl solution that rested on a balance (LP34000P, Sartorius, Goettingen, Germany), such that the stem segment did not touch any part of the beaker. The balance was used to make gravimetric measurements of water flow through the stem segments concurrently with sap flow measurements using Granier sensors (described below). The top (downstream end) of each stem segment

Table 1. Characteristics of branch segments used to collect calibration data. Length and diameter are given as mean ± standard error.

Species	Wood type	Length (cm)	Diameter (cm)	N
<i>E. angustifolia</i>	Ring-porous	57.5 ± 10.0	4.36 ± 0.30	7
<i>G. triacanthos</i>	Ring-porous	74.1 ± 5.0	5.06 ± 0.26	6
<i>Q. gambelii</i>	Ring-porous	79.6 ± 8.3	4.37 ± 0.08	6
<i>S. japonica</i>	Ring-porous	76.1 ± 1.5	4.47 ± 0.22	6
<i>P. fremontii</i>	Diffuse-porous	76.8 ± 1.9	5.08 ± 0.15	6
<i>T. cordata</i>	Diffuse-porous	80.6 ± 2.2	4.83 ± 0.15	5

The sample size represents the number of segments per species, where segments were collected from independent trees.

was stripped of bark and connected with tubing to a vacuum pump via a 4 l Erlenmeyer vacuum flask.

Sap flow measurements

Stem segments were instrumented with heat dissipation probes to measure sap flux density according to Granier:

$$F_d = ak^b \quad (1)$$

where F_d is sap flux density in $\text{g cm}^{-2} \text{s}^{-1}$, a the coefficient (0.0119), b the scaling exponent (1.23) and k a dimensionless quantity related to the temperature difference between a heated and reference probe:

$$k = \frac{\Delta T_{\max}}{\Delta T} - 1 \quad (2)$$

where ΔT is the temperature difference between the sensor probes and ΔT_{\max} is the temperature difference between the sensor probes under zero flow conditions. A constant 0.2 W of power was delivered to the heated probes via a coiled constantan heating element. In order to calculate sap flux density, conducting sapwood area was obtained from dye perfusions (see below). Both 10 mm (*S. japonica*) and 20 mm (*E. angustifolia*, *G. triacanthos*, *P. fremontii*, *Q. gambelii* and *T. cordata*) length probes were used for calibration measurements in order to be consistent with the size of sensors used previously in field installations (Bush et al. 2008, Hultine et al. 2010a). Our goal was not to assess the differences between the use of 10 and 20 mm probes, but rather to assess whether either type yielded calibration results consistent with the widely used empirical calibration equation. Sensor pairs were inserted radially into each stem segment, with a vertical separation of 15 cm. The temperature difference associated with each sensor pair was measured every 5 s, and 5 min averages were stored using a datalogger (CR23X, Campbell Scientific Inc., Logan, UT, USA).

A range of sap flux density values was obtained for each stem segment by changing the vacuum pressure of the system. The applied pressure gradient ranged from 0.001 to 0.14 MPa m^{-1} . This bracketed the expected range of in situ frictional gradients. Trunks and large branches are generally thought to experience a frictional pressure gradient of the order of one or two times the hydrostatic slope (~ 0.01 MPa m^{-1}), with greater gradients in smaller branches (Tyree and Zimmermann 2002). Following each change in vacuum pressure, the pressure and flow rate were kept constant for a minimum of 20 min before gravimetric and thermal dissipation probe data were recorded. The maximum temperature difference between each sensor pair was recorded under zero flow conditions, following the experimental procedure. In order to determine the zero flow value, stems remained in the same position associated with flow measurements, where they were left overnight with the upstream (lower) end of each stem still submerged in a beaker of water. The

time required to obtain a stable zero flow value took anywhere from less than an hour to several hours depending on the measurement segment.

Sapwood area determination

In order to determine sapwood area, stems were submerged in a beaker of Safranin O solution (0.1%) following a series of flow rate measurements, and dye was pulled by vacuum through each stem until it was visible in the downstream reservoir (Erlenmeyer vacuum flask). In most cases, dye was pulled through the stems for an additional 5–10 min after it was visible in the downstream reservoir. Directly following the dye perfusions, the stems were again submerged in KCl solution and flushed for the same time period in order to inhibit the spread of dye to inactive xylem. Measurement segments were then sectioned using a band saw, and images of cross-sections located near the heated sensors were obtained using a scanner. Scanned images were used to calculate the total conducting sapwood area with Image J software (Image J, NIH, USA, <http://rsbweb.nih.gov/ij/>).

Calculations and statistical analysis

A correction to calculate the temperature difference and sap flux density associated with active sapwood was applied to diffuse-porous calibration data, where the active sapwood depth was less than the sensor length according to Clearwater et al. (1999):

$$\Delta T_{\text{sw}} = \frac{\Delta T - d\Delta T_m}{c} \quad (3)$$

where ΔT_{sw} is the temperature difference between the portion of the heated and reference sensors associated with active sapwood, ΔT_m the temperature difference between the portion of the heated and reference sensors associated with inactive xylem and c and d the fraction of the sensor length associated with active and inactive xylem, respectively.

Statistical analyses were performed using GraphPad Prism software (www.graphpad.com). Species calibration curves were obtained by fitting a least-squares power function to pooled data of all measurement segments for each species. Comparison of calibration data across species was made by log transforming the data, followed by performing standard least-squares regression, where differences in slopes (exponent b) and intercepts ($\ln(\text{coefficient } a)$) were assessed.

Results

Ring-porous species

Calibration results were different from the Granier calibration for all ring-porous species considered in this study. In contrast to coefficient a of the Granier equation (0.0119, Eq. (1)), the coefficient a obtained from all measurements, combined by

species, varied from 0.93 to 5.81, exceeding the Granier coefficient by two to almost three orders of magnitude. Values obtained for exponent b were more similar to the reported Granier value and ranged from 1.24 to 1.88 (Figure 1). We also observed a fairly high degree of variation across stems obtained from different trees of the same species. However, in general, there was less variability in measured sap flux density values at the low end of the applied pressure range with correspondingly smaller k values (Figure 1).

Our results from dye perfusions generally showed that only the current year xylem was active in the ring-porous species (Figure 2). The only exception to this pattern was *E. angustifolia*, where some active xylem was present in previous growth rings (Figure 2a). However, the active xylem in previous years growth comprised only a small fraction of the total stained area. The average conducting sapwood area ranged from 0.35 ± 0.06 to 1.70 ± 0.18 cm², whereas the average sapwood depth ranged from 0.88 ± 0.04 to 1.63 ± 0.23 mm (Table 2 and Figure 2).

Calibration differences between ring-porous species varied depending on the range of applied pressure gradients used in the laboratory to induce different flow conditions. Species-specific differences in the scaling exponent b and coefficient a were assessed by comparing the slopes and intercepts of log-transformed regression

models for each species. Differences in the scaling exponent b were observed when data across the entire pressure gradient range were considered ($0.001\text{--}0.14$ MPa m⁻¹, Table 3, $P < 0.05$). However, no statistical differences in b were observed between species for data within the expected range of in situ pressure gradients (<0.02 MPa m⁻¹, Table 3, $P > 0.05$). This was also true for all data collected within the pressure gradient ranges of <0.03 and <0.04 MPa m⁻¹ (Table 3, $P > 0.05$). The point at which statistical differences in b between species were observed occurred when data associated with a pressure gradient range of up to 0.05 MPa m⁻¹ and greater were included in the analysis (Table 3, $P < 0.05$). Species-specific differences in coefficient a were observed across all pressure gradient ranges considered (Table 3, $P < 0.05$). However, when *E. angustifolia* was removed from the regression comparison, no differences in intercepts were observed between *G. triacanthos*, *Q. gambelii* and *S. japonica* at the lower end of the pressure gradient ranges considered (<0.02 and 0.03 MPa m⁻¹, $P > 0.05$).

The calibration equation coefficients and scaling exponents obtained depended on the range of applied pressure gradients considered (Figure 3 and Table 3). In general, increasing the range of data included according to pressure gradient conditions was associated with increasing a and b values (Figure 3 and Table 3).

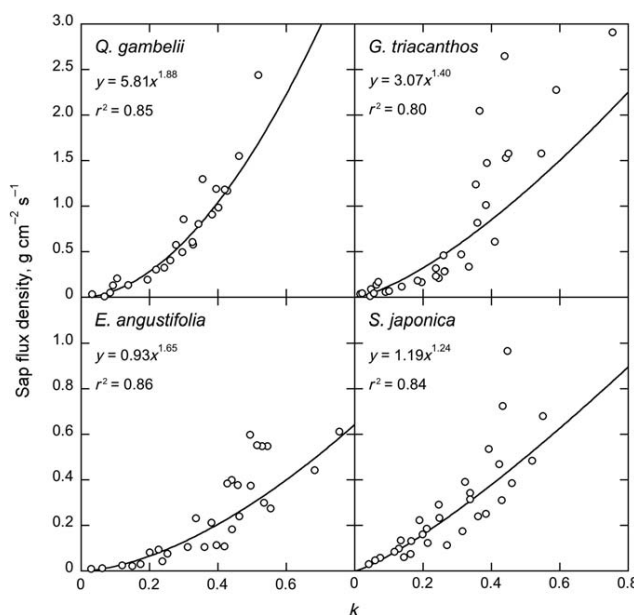


Figure 1. Relationship between sap flux density and k obtained for excised branch segments of ring-porous species. Solid lines represent curve fits of least-squares power functions.

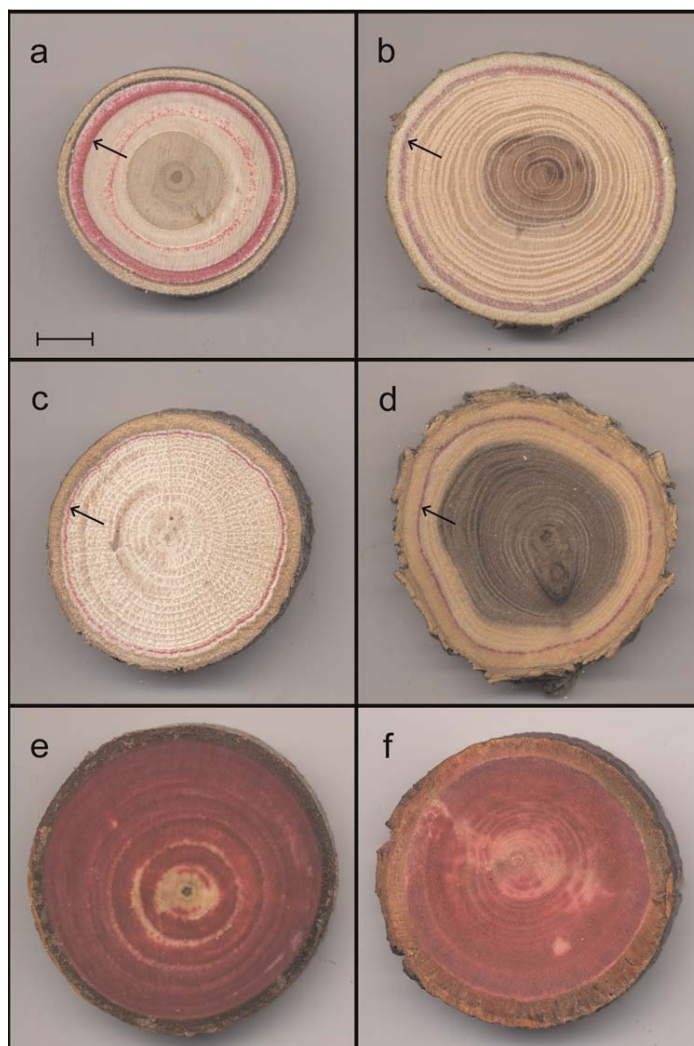


Figure 2. Images of representative branch cross-sections obtained from the location between the heated and reference thermal dissipation probes for both ring-porous and diffuse-porous species. (a–d) Ring-porous species *E. angustifolia*, *G. triacanthos*, *Q. gambelii* and *S. japonica*, respectively. (e and f) Diffuse-porous species *P. fremontii* and *T. cordata*, respectively. Active sapwood area is shown as the stained area indicated with arrows. The scale bar represents a length of 1 cm.

Diffuse-porous species

Calibration results for diffuse-porous species were generally in good agreement with Granier's calibration (Figure 4). In addition, comparison of coefficient *a* and exponent *b* values

yielded no differences across the entire range of pressure gradient conditions considered ($P > 0.05$). In most cases, the active sapwood depth was less than the sensor length (20 mm) for both *P. fremontii* and *T. cordata*. Because of

Table 2. Mean sapwood area and depth \pm standard error for all branch segments associated with calibration measurements.

Species	Wood type	Sapwood area (cm ²)	Sapwood depth (mm)	N
<i>E. angustifolia</i>	Ring-porous	1.70 \pm 0.18	1.63 \pm 0.23	7
<i>G. triacanthos</i>	Ring-porous	0.73 \pm 0.09	0.98 \pm 0.09	6
<i>Q. gambelii</i>	Ring-porous	0.35 \pm 0.06	0.88 \pm 0.04	6
<i>S. japonica</i>	Ring-porous	0.51 \pm 0.12	1.08 \pm 0.14	6
<i>P. fremontii</i>	Diffuse-porous	16.02 \pm 1.01	12.80 \pm 1.46	6
<i>T. cordata</i>	Diffuse-porous	13.08 \pm 0.75	15.20 \pm 0.80	5

Table 3. Slope and intercept values \pm standard error of log-transformed calibration data obtained by standard least-squares linear regression.

Pressure gradient range (MPa m ⁻¹)	Species	Slope	Intercept	r ²
<0.02 ^a	<i>E. angustifolia</i>	1.09 \pm 0.16	-1.42 \pm 0.34	0.91
	<i>G. triacanthos</i>	0.87 \pm 0.25	-0.51 \pm 0.69	0.59
	<i>Q. gambelii</i>	1.55 \pm 0.61	0.84 \pm 1.43	0.57
	<i>S. japonica</i>	0.94 \pm 0.14	-0.56 \pm 0.28	0.82
<0.03 ^a	<i>E. angustifolia</i>	1.15 \pm 0.15	-1.20 \pm 0.30	0.86
	<i>G. triacanthos</i>	0.91 \pm 0.21	-0.23 \pm 0.52	0.60
	<i>Q. gambelii</i>	1.65 \pm 0.47	1.10 \pm 1.05	0.68
	<i>S. japonica</i>	1.08 \pm 0.13	-0.21 \pm 0.23	0.82
<0.04 ^a	<i>E. angustifolia</i>	1.16 \pm 0.14	-1.18 \pm 0.26	0.88
	<i>G. triacanthos</i>	1.00 \pm 0.19	0.03 \pm 0.45	0.66
	<i>Q. gambelii</i>	1.70 \pm 0.29	1.33 \pm 0.58	0.76
	<i>S. japonica</i>	1.16 \pm 0.11	0.00 \pm 0.18	0.83
<0.05 ^{a,b}	<i>E. angustifolia</i>	1.29 \pm 0.14	-0.88 \pm 0.25	0.87
	<i>G. triacanthos</i>	1.07 \pm 0.17	0.24 \pm 0.40	0.70
	<i>Q. gambelii</i>	1.72 \pm 0.27	1.39 \pm 0.53	0.77
	<i>S. japonica</i>	1.24 \pm 0.10	0.17 \pm 0.16	0.84
<0.15 (all data) ^{a,b}	<i>E. angustifolia</i>	1.65 \pm 0.13	-0.07 \pm 0.17	0.86
	<i>G. triacanthos</i>	1.40 \pm 0.13	1.12 \pm 0.24	0.80
	<i>Q. gambelii</i>	1.88 \pm 0.17	1.76 \pm 0.27	0.85
	<i>S. japonica</i>	1.24 \pm 0.10	0.17 \pm 0.16	0.84

The slope data correspond to the scaling exponent b , and the antilog of the intercept corresponds to coefficient a . Different ranges in applied pressure gradient conditions associated with data collection are shown.

^aSpecies-specific differences in intercept values were observed over all pressure gradient ranges analyzed.

^bSpecies-specific statistical differences between slope values (exponent b) were not observed until the pressure gradient range included all data collected <0.05 MPa m⁻¹.

this, the use of the Granier equation initially underestimated sap flux density for both species. However, the active sapwood depth was large enough that it was possible to apply the correction according to Clearwater et al. (1999, Eq. (3)), which brought the calibration results for both species within the range consistent with the original Granier calibration.

Dye perfusion results for both *P. fremontii* and *T. cordata* showed that xylem representing multiple years of growth was active (Figure 2). This was the case for all the measurement segments of both species considered. In addition,

xylem associated with previous years' growth was often stained uniformly throughout. The average active sapwood area was 16.02 ± 1.01 and 13.08 ± 0.75 cm² for *P. fremontii* and *T. cordata*, respectively.

Discussion

Calibration data for all four ring-porous species gave equations that were substantially different from the original Granier equation, particularly with respect to coefficient a , where differences of two to three orders of magnitude were observed (Figure 1 and Table 3). These results are not consistent with the originally reported results of Granier or subsequent work (Granier 1985, Cabibel and Do 1991, Catovsky et al. 2002). However, Taneda and Sperry (2008) also obtained calibration results that differed substantially from Granier's equation for *Q. gambelii*, where reported coefficient a values ranged from 2.38×10^{-3} to 1.81×10^{-2} m s⁻¹ (corresponding to 0.238–1.81 in g cm⁻² s⁻¹ units reported here) and exponent b values ranged from 1.05 to 1.50 for different stems. The exact values for coefficient a and exponent b reported by Taneda and Sperry were smaller relative to those reported here, which may have been associated with differences in applied pressure gradients for measurement stems. However, both Taneda and Sperry (2008) and the current study showed that the largest differences compared with the original Granier equation were associated with the coefficient a value, where in both cases, differences that exceeded two orders of magnitude were observed, and the use of the Granier equation would have resulted in substantial underestimation of sap flux density.

Sap flux density values associated with ring-porous calibration measurements in this study were quite high, although much of the data were collected under pressure gradient conditions that likely exceed those experienced in situ. However, measured k values associated with previous field installations (Bush et al. 2008), and the same populations of ring-porous species considered here, were generally <0.5 . Field measured k values combined with species-specific calibration curves indicated in almost all cases that, even when all of the calibration data were considered (up to applied pressure gradients of 0.14 MPa m⁻¹), flux rates did not exceed maximum midday velocities previously reported for trees with wide vessels (up to 13 mm s⁻¹ or 1.3 in g cm⁻² s⁻¹ units reported here) (Tyree and Zimmermann 2002).

The large calibration differences observed are likely due to the small conducting sapwood area and small sapwood depth relative to the total sensor length obtained in all cases for the ring-porous species (Figure 2 and Table 2). The stained sapwood area ranged from 0.35 ± 0.06 to 1.70 ± 0.18 cm² for the entire cross-sectional area of the measurement segments and was generally limited to current year xylem. The stained area was substantially smaller than the apparent sapwood based on visual distinction between

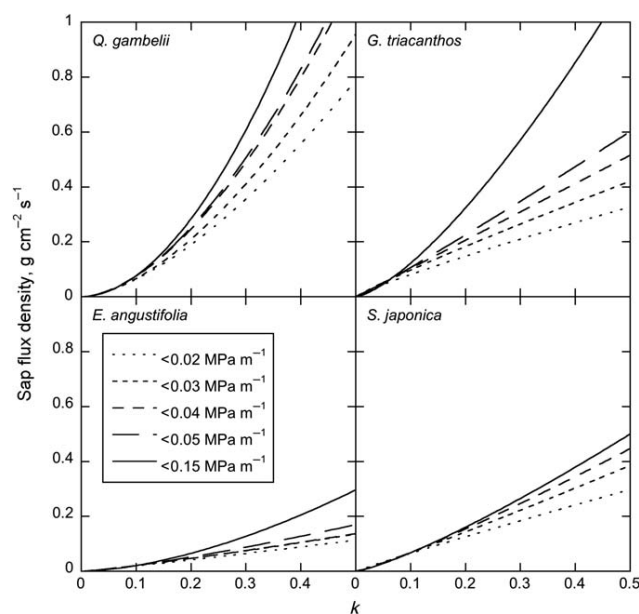


Figure 3. Influence of the range of applied pressure gradient conditions associated with calibration data collection on calibration results. Lines show least-squares power functions fitted to different pressure gradient ranges for all ring-porous species considered. The coefficients and r^2 values are given in Table 3 (slope and antilog of intercept values correspond to exponent b and coefficient a , respectively). No slope differences (exponent b) were observed for data collected below a pressure gradient of 0.04 MPa m^{-1} . However, differences in intercepts were observed over all analyzed pressure gradient ranges.

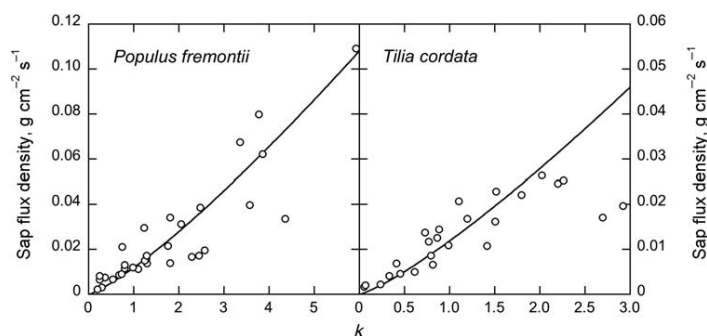


Figure 4. Relationship between sap flux density and k obtained for excised branch segments of diffuse-porous species. The solid line represents the original Granier calibration. Data shown were corrected according to Clearwater et al. (1999) for all stems where sensor length exceeded active sapwood depth.

darker heartwood (where present) and lighter sapwood over the cross-sectional area of the stem (Figure 2 and Table 2). In addition, the average sapwood depth was substantially smaller than the sensor length for both the 10 and 20 mm

probes used (Table 2). Correcting for this problem according to Clearwater et al. (1999) was not possible because the active sapwood depth was so small that the corrected temperature difference between the sensor probes, representing

the area in contact with active sapwood, becomes a negative value. This also has implications for scaling sap flux data to the whole-tree and stand levels. Our data suggest that sap flux data should be scaled using total sapwood area associated with current year xylem, unless there is evidence to suggest that xylem from previous years' growth is substantially contributing to whole-tree sap flow.

Our results also showed species-specific differences between ring-porous species, which varied depending on the range of applied pressure gradients considered. Exponent b values were only different between species when data associated with a pressure gradient range of up to 0.05 MPa m^{-1} and above (likely in excess of native gradients) were included. Below a 0.04 MPa m^{-1} cut-off, all species were statistically the same. Coefficient a values differed between species across all pressure gradient ranges considered. However, the removal of *E. angustifolia* from the regression comparison showed no differences in coefficient a between the remaining three ring-porous species at pressure gradient ranges of <0.02 and $<0.03 \text{ MPa m}^{-1}$. In addition, obtained a and b coefficients were sensitive to the pressure gradient range considered, where increasing the range of pressure gradients associated with data collection was associated with increasing values of both a and b (Figure 3 and Table 3). Because of these results, we suggest that thermal dissipation probes used to measure absolute rates of water use in ring-porous species should be independently calibrated where possible and that calibration data used to derive equation coefficients be constrained to include only applied pressure gradient conditions likely associated with in situ pressure gradients. Our results differed considerably from the widely used Granier equation, particularly with respect to the coefficient a values, and suggest that previous calculations of absolute rates of water uptake in ring-porous species using the Granier coefficients may be substantially underestimated.

It is not clear why our results were markedly different from the previous calibrations for *Quercus* species and *C. sativa* (Granier 1985; Cabibel and Do 1991; Catovsky et al. 2002). It is possible that if a large number of early season vessels were open at both ends of the measurement segments used in the current study, observed sap flux density could have been considerably higher due to decreased resistance in the flow path, with correspondingly little or no flow occurring in the much higher resistance pathways associated with late wood. However, to minimize this potential effect, our final measurement segments were relatively long, ranging on average from 57.5 ± 10.0 to $79.6 \pm 8.3 \text{ cm}$ (Table 1). Furthermore, if a large fraction of early season vessels were open at both ends of the measurement segments, we would expect that the stained xylem would include open-ended, early season vessels from previous years' growth as well, provided that vessel length distributions were unchanged across growth rings and tyloses formation was not a large factor. However, this was not observed, as stained xylem was generally limited to current

year growth. We cannot rule out the possibility that tyloses were not a factor, as the measurement segments in this study were not examined for their presence. In addition, because we did not generate vessel length distributions for each species and for this diameter size class, we cannot completely eliminate the possibility of open-ended vessels in our final measurement segments. Still, if our measured sap flux density values were in fact higher than what would be observed in situ, we would expect that the value obtained for k would increase accordingly and would not necessarily expect increased sap velocity conditions to have a large impact on the calibration results, unless the relationship between sap flux density and k changes considerably at high sap velocities.

In contrast to our results associated with ring-porous species, we found that the calibration results for the two diffuse-porous species agreed well with the original Granier calibration (Figure 4). Our results also provide further support for the use of the Clearwater equation (Eq. (3)) to correct for errors associated with installations, where the length of thermal dissipation probes exceeds the active sapwood depth. Our results reported here for diffuse-porous species are also consistent with many earlier reports that provided subsequent validation of the Granier calibration for a number of diffuse-porous species (Cabibel and Do 1991, Lu and Chacko 1998, Braun and Schmid 1999, Clearwater et al. 1999, McCulloh et al. 2007). Recently, however, Steppe et al. (2010) found that the original calibration underestimated sap flux density in *F. grandifolia* on average by 60% when compared with paired gravimetric measurements. In addition, calibration data collected on excised stems of *T. ramosissima* × *chinensis* (Hultine et al. 2010b) also showed that the Granier equation underestimated sap flux density by 50%. The average value obtained for coefficient a in the latter case was $240 \text{ g m}^{-2} \text{ s}^{-1}$ (compared with 119 for the Granier equation in the same units) and 1.16 for the scaling exponent b . While the results for diffuse-porous species reported here were consistent with the Granier equation and many other previous reports, the results of Steppe et al. (2010) and Hultine et al. (2010b) indicate that the Granier equation is not universally applicable to diffuse-porous species. However, the differences reported in Steppe et al. (2010) and Hultine et al. (2010b) (60 and 50%, respectively), while significant, are much smaller relative to differences reported for ring-porous species in Taneda and Sperry (2008) and this study (in excess of two orders of magnitude).

It is important to note that the calibration data reported here are associated with excised branch segments, where substantial circumferential variability in sap flow may occur due to the presence of compression or tension wood, which was not accounted for in this study. The degree to which calibration results may vary depending on sampling location in a given tree (branches vs. boles, for example) is still largely unknown. To our knowledge, we are the first to

report calibration data for five of the six species in this study. The number of species, genera and xylem types examined, particularly with respect to the ring-porous species, for which data were relatively scarce and potentially higher error relative to other xylem types may be expected based on anatomical features of the xylem and theoretical considerations (Clearwater et al. 1999), represents a step forward in advancing our overall understanding of the widely used Granier method and its potential limitations.

Thermal dissipation probes are widely used for calculating sap flow of trees and forest stands. However, our results show that it should not be assumed that the original calibration is appropriate in all cases. We found that the original calibration did not accurately calculate sap flow for all four ring-porous species considered in this study. In addition, we found species-specific differences in calibration results between ring-porous species, particularly with respect to the equation coefficient α . We also show that the Granier calibration was consistent with calibration data collected for two diffuse-porous species in this study. We suggest that independent calibration of the Granier method should be conducted where possible, as the data reported here and elsewhere suggest that the use of the original Granier equation is not universally applicable across species and xylem types.

Acknowledgments

We thank the Sandy City, UT, administration, Williams Pipeline Co. and the University of Utah grounds department for access to plant material.

Funding

This research was supported, in part, through the Terrestrial Carbon Processes (TCP) program by the Office of Science (BER), US Department of Energy under Grant No. DE-FG02-06ER64309.

References

- Alder, W.J., L. Nierenberg, S.T. Buchanan, W. Cope, J.A. Cisco, C.C. Schmidt, A. Smith and W. Figgins. 1998. Climate of Salt Lake City, UT. NOAA Technical Memorandum NRS WR-152.
- Braun, P. and J. Schmid. 1999. Sap flow measurements in grapevines (*Vitis vinifera* L.) 2. Granier measurements. *Plant Soil* 215:47–55.
- Bush, S.E., D.E. Pataki, K.R. Hultine, A.G. West, J.S. Sperry and J.R. Ehleringer. 2008. Wood anatomy constrains stomatal responses to atmospheric vapor pressure deficit in irrigated, urban trees. *Oecologia* 156:13–20.
- Cabibel, B. and F. Do. 1991. Mesures thermiques des flux de seve dans les troncs et les racines et fonctionnement hydrique des arbres. I. Analyse theorique des erreurs sur la mesure des flux et validation des mesures en presence de gradients thermiques extérieurs. *Agronomie* 11:669–678.
- Catovsky, S., N.M. Holbrook and F.A. Bazzaz. 2002. Coupling whole-tree transpiration and canopy photosynthesis in coniferous and broad-leaved tree species. *Can. J. For. Res.* 32:295–309.
- Cermak, J. and N. Nadezhkina. 1998. Sapwood as the scaling parameter-defining according to xylem water content or radial pattern of sap flow? *Ann. For. Sci.* 55:509–521.
- Cermak, J., E. Cienciala, J. Kucera and J. Hallgren. 1992. Radial velocity profiles of water flow in trunks of Norway spruce and oak and the response of spruce to severing. *Tree Physiol.* 10:367–380.
- Clearwater, M.J., F.C. Meinzer, J.L. Andrade, G. Goldstein and N. M. Holbrook. 1999. Potential errors in measurement of nonuniform sap flow using heat dissipation probes. *Tree Physiol.* 19:681–687.
- Ellmore, G.S. and F.W. Ewers. 1986. Fluid flow in the outermost xylem increment of a ring-porous tree, *Ulmus americana*. *Am. J. Bot.* 73:1771–1774.
- Ewers, B.E., R. Oren, H.-S. Kim, G. Bohrer and C.-T. Lai. 2007. Effects of hydraulic architecture and spatial variation in light on mean stomatal conductance of tree branches and crowns. *Plant Cell Environ.* 30:483–496.
- Ford, C.R., R.M. Hubbard, B.D. Kloeppel and J.M. Vose. 2007. A comparison of sap flux-based evapotranspiration estimates with catchment-scale water balance. *Agric. For. Meteorol.* 145:176–185.
- Gebauer, T., V. Horna and C. Leuschner. 2008. Variability in radial sap flux density patterns and sapwood area among seven co-occurring temperate broad-leaved tree species. *Tree Physiol.* 28:1821–1830.
- Goulden, M.L. and C.B. Field. 1994. Three methods for monitoring the gas exchange of individual tree canopies: ventilated chamber, sap-flow and Penman-Monteith measurements on evergreen oaks. *Funct. Ecol.* 8:125–135.
- Granier, A. 1985. Une nouvelle methode pour la mesure du flux de seve brute le tronc des arbres. *Ann. For. Sci.* 42:193–200.
- Granier, A., T. Anfodillo, M. Sabatti, H. Cochard, E. Dreyer, M. Tomasi, R. Valentini and N. Breda. 1994. Axial and radial water flow in the trunks of oak trees: a quantitative and qualitative analysis. *Tree Physiol.* 14:1383–1396.
- Granier, A., V. Bobay, J.H.C. Gash, J. Gelpe, B. Saugier and W.J. Shuttleworth. 1990. Vapour flux density and transpiration rate comparisons in a stand of Maritime pine (*Pinus pinaster* Ait.) in Les Landes forest. *Agric. For. Meteorol.* 51:309–319.
- Hultine, K.R., S.E. Bush and J.R. Ehleringer. 2010a. Ecophysiology of riparian cottonwood and willow before, during and after two years of soil water removal. *Ecol. Appl.* 20:347–361.
- Hultine, K.R., P.L. Nagler, K. Morino, S.E. Bush, K.G. Burch, P.E. Dennison, E.P. Glenn and J.R. Ehleringer. 2010b. Sap flux-scaled transpiration by tamarisk (*Tamarix* spp.) before, during and after episodic defoliation by the saltcedar leaf beetle (*Diorhabda carinulata*). *Agric. For. Meteorol.* 150:1467–1475.
- Jaquish, L.L. and F.W. Ewers. 2001. Seasonal conductivity and embolism in the roots and stems of two clonal ring-porous trees, *Sassafras albidum* (Lauraceae) and *Rhus typhina* (Anacardiaceae). *Am. J. Bot.* 88:206–212.
- Kostner, B., P. Biron, R. Siegwolf and A. Granier. 1996. Estimates of water vapor flux and canopy conductance of Scots pine at the tree level utilizing different xylem sap flow methods. *Theor. Appl. Climatol.* 53:105–113.
- Lu, P. and E. Chacko. 1998. Evaluation of Granier's sap flux sensor in young mango trees. *Agronomie* 18:461–471.
- Lu, P., K. Woo and Z. Liu. 2002. Estimation of whole-plant transpiration of bananas using sap flow measurements. *J. Exp. Bot.* 53:1771–1779.
- McCulloh, K.A., K. Winter, F.C. Meinzer, M. Garcia, J. Aranda and B. Lachenbruch. 2007. A comparison of daily water use estimates derived from constant-heat sap-flow probe values and

- gravimetric measurements in pot-grown saplings. *Tree Physiol.* 27:1355–1360.
- Saugier, B., A. Granier, J.Y. Pontailler, E. Dufrene and D.D. Baldocchi. 1997. Transpiration of a boreal pine forest measured by branch bag, sap flow and micrometeorological methods. *Tree Physiol.* 17:511–519.
- Steppe, K., D.J.W. De Pauw, T.M. Doody and R.O. Teskey. 2010. A comparison of sap flux density using thermal dissipation, heat pulse velocity and heat field deformation methods. *Agric. For. Meteorol.* 150:1046–1056.
- Taneda, H. and J.S. Sperry. 2008. A case-study of water transport in co-occurring ring- versus diffuse-porous trees: contrasts in water-status, conducting capacity, cavitation and vessel refilling. *Tree Physiol.* 28:1641–1651.
- Tournebise, R. and S. Boistard. 1998. Comparison of two sap flow methods for the estimation of tree transpiration. *Ann. For. Sci.* 55:707–713.
- Tyree, M.T. and M.H. Zimmermann. 2002. Xylem structure and the ascent of sap. Springer Series in Wood Science. Ed. T.E. Timell. Springer, New York.

CHAPTER 4

WATER USE AND ECOHYDROLOGY OF CO-OCCURING RUSSIAN OLIVE AND COTTONWOOD TREES IN AN URBAN RIPARIAN CORRIDOR OF NORTHERN UTAH, USA

Abstract

Elaeagnus angustifolia (Russian olive) is an invasive tree species that is widespread throughout Western US riparian ecosystems. Despite its large geographic extent and dominance in these systems, very little is known regarding the ecohydrological consequences of its presence and its water use behavior compared to native taxa. Here I report water use of *E. angustifolia* and native *Populus fremontii* (Fremont Cottonwood) stands obtained from sap flux measurements made over the course of two growing seasons in a riparian ecosystem located in northern Utah, USA. I found that *E. angustifolia* and *P. fremontii* had very similar rates of water use when scaled per unit basal area, but that water use per unit leaf area and canopy ground area were lower for *E. angustifolia* compared to *P. fremontii*. The impact of observed water use differences between *E. angustifolia* and *P. fremontii* on current and future transpiration fluxes from riparian forests in the Western US is discussed.

Introduction

Riparian ecosystems in the arid western US are highly valued for their freshwater resources that support biodiversity and wildlife habitat in both natural and urban ecosystems (Knopf et al. 1988; Naiman et al. 1993; Sabo et al. 2010). However, water managers are increasingly under pressure to divert limited water supplies for municipal and agricultural development. Consequently, large-scale modification of riparian ecosystems have been ongoing for the purpose of changing the availability and distribution of water throughout the West (Sabo et al. 2010). Compounding these challenges are a combination of global environmental change processes including the spread of nonnative species, shifts in climate (causing lower spring snowmelt and higher evaporative demand), and increased land use. These ongoing challenges have stimulated significant interest in water budget accounting of western riparian river systems including improved estimates of evapotranspiration (*ET*) across multiple scales (Goodrich et al. 2000; Jackson et al. 2001; Dahm et al. 2002; Cleverly et al. 2006; Barnett et al. 2008; Hultine et al. 2010; Sabo et al. 2010; Hultine and Bush 2011).

Riparian forest transpiration makes up a large fraction of the evapotranspiration flux in riparian ecosystems (Dahm et al. 2002) and comprises a disproportionate amount of the evapotranspiration flux in semiarid and arid regions (Scott et al. 2004; Huxman et al. 2005; Williams et al. 2006). Historically, western riparian forests in semiarid and arid regions were most commonly comprised of *Populus* spp. (cottonwood) and *Salix* spp. (willow) assemblages (Webb et al. 2007). However, since the middle of the twentieth century, nonnative tree species have become increasingly common throughout riparian ecosystems of the western landscape; the most notable examples being *Tamarix* spp.

(tamarisk) and *Elaeagnus angustifolia* (Russian olive). These species are currently widespread and are estimated to be the third and fourth most frequently occurring and the second and fifth most dominant woody species in western riparian regions, respectively (Friedman et al. 2005).

Considerable attention has been paid for understanding the ecohydrologic consequences of *Tamarix* spp., but despite the widespread distribution of *E. angustifolia*, there has been little attention focused on its potential impact on ecohydrology of western US rivers and streams (Hultine and Bush 2011). One challenge that impedes studies of *E. angustifolia* water use is that this species rarely occurs in monocultures that are large enough to deploy either micrometeorological approaches, such as eddy covariance flux measurements, or remote sensing techniques in order to estimate *ET*. An alternative approach is to upscale measurements of stem sap flux since the flux through plant stems is proportional to the transpiration flux from the canopy. Upscaled transpiration rates calculated from sap flux measurements show that riparian tree species, including *Populus* spp., *Salix* spp., and *Tamarix* spp., transpire anywhere from 1.0–9.0 mm day⁻¹ (Sala et al. 1996; Schaeffer et al., 2000; Pataki et al. 2005; Gazal et al. 2006; Nagler et al. 2007, 2008, 2009; Hultine et al. 2007, 2010a, 2010b; Pattison et al. 2011). Preliminary data suggest that *E. angustifolia* transpiration on a per-basal-area basis may be considerably higher than co-occurring *Populus* (Hultine and Bush 2011), but to our knowledge there are no comprehensive published data that compare water use patterns of *E. angustifolia* with other dominant riparian species.

The importance for characterizing *E. angustifolia* water use patterns in the western US is amplified by the likely increase in the distribution and abundance of this

species over time. Habitat suitability assessments suggest that *E. angustifolia* can tolerate a broader range of sunlight, soil water, and soil quality conditions compared to native taxa (Katz and Shafroth 2003; Reynolds and Cooper 2010; Jarnevich and Reynolds 2011; Nagler et al. 2011). Moreover, intensive *Tamarix* control programs, including the use of a widely distributed biological control, *Diorhabda carinulata* Brullé (northern tamarisk leaf beetle), are potentially expanding the realized niche for *E. angustifolia* throughout large areas of the Western US (Hultine et al., 2010c; Hultine and Bush 2011). The likely future expansion in distribution and overall cover of *E. angustifolia*, coupled with diminishing water supplies in riverine systems, establishes a critical need for quantifying water use patterns of this species and its potential impact on ecohydrology in riparian ecosystems.

The majority of studies that report water use dynamics of *E. angustifolia* have been associated with sites within Eurasia and generally associated with suboptimal growing conditions including poor soil quality of degraded croplands, highly saline water sources, and arid desert geographic locations (Xu et al. 1998; Chen et al. 2004; Khamzina et al. 2009; Zhao and Liu 2010; Ma et al. 2011). Studies that report information on water use dynamics of *E. angustifolia* in the western US have been scarce. Hultine and Bush (2011) reported that *E. angustifolia* water use on a per-basal-area basis may be considerably higher than co-occurring *Populus*. Likewise, Allen et al. (2005) provided estimates of evapotranspiration for an *E. angustifolia* stand in the Middle Rio Grande Basin derived from remote sensing data.

In this paper, I compare patterns of sap flux-scaled water use between nonnative *E. angustifolia* and native *Populus fremontii* that were co-occurring in an urban riparian

area in northern Utah, USA. My goal was to evaluate the potential ecohydrological impact of *P. fremontii* replacement by *E. angustifolia* that is occurring, or is predicted to occur, over the next several decades (Jarnevich and Reynolds 2011; Nagler et al. 2011). Results from this research will shed light on the impacts of *E. angustifolia* on water resources as this species continues to spread throughout the western US.

Methods

Study area

The study site was located in a riparian area along the Jordan River in Salt Lake Valley, UT, USA (latitude 40.66; longitude 111.55; elevation 1,275–1,550 m). The Salt Lake Valley is a megapolitan area with a semiarid climate; mean annual temperature and precipitation are 11.0 °C and 409 mm, respectively (<http://www.wrh.noaa.gov/slc/climate/slcclimate/SLC/>). The study site was an unmanaged area, with a tree canopy largely comprised of *E. angustifolia*. There was also a stand of *P. fremontii* located directly adjacent to the Jordan River (Figure 4.1). Ten trees of both species were instrumented with sap flow sensors and monitored during the 2004 and 2005 growing seasons. Tree morphological characteristics are given in Table 4.1.

Sap flow

Sap flow measurements were made using Granier-type thermal dissipation probes, where the temperature difference between a heated and reference sensor pair is empirically related to sap flux density (J_s , $\text{g m}^{-2} \text{s}^{-1}$) according to the following:

$$J_s = 119(\Delta T_m / \Delta T - 1)^{1.231} \quad (4.1)$$

where ΔT is the temperature difference between the heated and reference sensors and ΔT_m is the temperature difference between the heated and reference sensors measured under zero-flow conditions (Granier 1987). Equation 4.1 was used to obtain J_s for *P. fremontii* trees, where laboratory calibrations validated the use of this equation for this species. However, a modified version of this equation was used to calculate J_s for *E. angustifolia* according to Bush et al. (2010), which was based on *E. angustifolia*-specific calibration measurements. Trees were instrumented with 20-mm length probes, separated vertically by 15 cm. The direction of sensor-pair placement around the bole of the trees was randomized. Measurements were made every 30 s, and half-hour means were stored with a datalogger (CR23X; Campbell Scientific, Logan, Utah).

Whole-tree water use

Whole-tree water use was determined by multiplying J_s by total cross-sectional conducting sapwood area. Cross-sectional conducting sapwood area was obtained by using species-specific allometric equations generated from an adjacent stand (Figure 4.2) combined with tree diameter measured at breast height (DBH, ~1.4 m). Allometric data for sapwood area were obtained with an increment borer, where cores from 26 *P. fremontii* trees and 16 *E. angustifolia* trees were used to measure sapwood depth. Sapwood depth was assessed visually based on the apparent sapwood to heartwood transition and translucence for *P. fremontii* individuals, whereas sapwood depth for *E. angustifolia* individuals was based on the ring-width of the measurement year. This

approach was consistent with results from previous studies, where *P. fremontii* was shown to have active xylem associated with multiple years of growth, and *E. angustifolia* was shown to have active xylem limited to the current-year growth ring (Trafton 2005; Bush et al. 2010). Because the sapwood depth of *P. fremontii* trees exceeded the length of sap flow probes, radial variation in sap flux density was accounted for according to Pataki et al. (2011). DBH was measured for all trees instrumented with sap flow sensors in 2004. However, because the site was bulldozed for development following the 2005 season and before increased diameter estimates were obtained for individual trees, in order to calculate conducting sapwood area for 2005, average annual growth for the 2005 growing season from an adjacent stand combined with 2004 diameter data was used to obtain tree diameter data for 2005.

Meteorological measurements

Temperature and relative humidity were measured at the study site using an HMP45C temperature and relative humidity probe in combination with an aspirated radiation shield (Vaisala, Finland). These measurements were made and stored at the same frequency as sap flow measurements and were used to calculate atmospheric vapor pressure deficit (vpd). Photosynthetically active radiation (PAR) data were obtained from a meteorological station associated with Mesowest (<http://mesowest.utah.edu>), located within the Salt Lake Valley ~14 km distant from the study site. All-wave radiation obtained from the station was converted to PAR according to Al-Shooshan (1997). Because comparison of PAR data obtained from multiple meteorological stations within the Salt Lake Valley showed very little difference between PAR datasets, it was assumed

that the PAR data obtained were generally representative of the conditions at the measurement site.

Leaf area

Leaf area was obtained in 2004 by placing leaf collection bins below the canopy, where leaves were collected at the end of the growing season. A subset of collected litter was used to obtain specific leaf area. Leaf area for calculation of specific leaf area was obtained using scanned images of a subset of leaves and Image J software (<http://rsbweb.nih.gov/ij/>). The total combined litter from all bins was sorted by species and weighed to obtain total leaf area for each species. Total leaf area for each species was then divided by total bin ground area to obtain leaf area index for each species.

Water potential

Water potential data were obtained on a monthly basis throughout the 2004 and 2005 growing seasons for five individuals of each species using a Scholander-type pressure chamber (PMS, Albany, OR). Predawn measurements were made between the hours of 2 and 5 a.m., and midday measurements were made between the hours of 11 a.m. and 2 p.m. Leaves that were collected for midday measurements were obtained from sunlit portions of the tree canopy where possible. Small branch segments were collected using a pole pruner and immediately placed in a bag containing a wet paper towel for transport to the pressure chamber, where a single cut with a razor blade was used to excise leaves for measurement.

Stand transpiration

Total stand transpiration was determined by scaling average tree water use per canopy ground area and per leaf area to the entire plot area. Because the stand of *P. fremontii* was associated with a linear arrangement of trees parallel to the river, outermost measurement trees of both species were used to define the borders of a rectangular plot area. An aerial image of the site associated with the 2005 growing season was used to measure total canopy area of each species within the plot using Image J software (<http://rsbweb.nih.gov/ij/>). Total leaf area for each species was obtained by multiplying LAI by total canopy area for each species.

Annual transpiration

In order to estimate stand water use beyond the periods of measurement for the entire 2004 and 2005 growing seasons and to provide a method of estimating transpiration of these species beyond the boundaries of the measurement plot in this study, empirical relationships between water use per unit leaf area and per unit canopy ground area relative to meteorological data and time of year were obtained using least squares multiple linear regression. Variable inputs included PAR, log-transformed vpd, and day of year (DOY), as all three were found to have a significant impact on model results. Log-transformed vpd was used as a model input instead of vpd, as the relationship between water use and vpd showed significant departure from linearity, particularly for *E. angustifolia*. Water use per unit leaf area and per unit canopy area data were selected for the empirical relationship output, as leaf area and canopy ground area are well suited for linking with data that can be obtained for different locations and at

much larger spatial scales from remotely sensed data products.

Results

Meteorological variables were generally similar in magnitude for the 2004 and 2005 growing seasons (Figure 4.3). No differences were detected between mean daytime conditions when compared by month between the 2 years, with the exception of July relative humidity, where mean July relative humidity was 38.9% in 2004 versus 31.9% for 2005 (unpaired t-test, $p < 0.05$).

Water potential varied between species and throughout each growing season (Figure 4.4). *E. angustifolia* had consistently lower water potential values compared to *P. fremontii* for both predawn and midday measurements (Figure 4.4). *E. angustifolia* predawn water potential ranged from -0.60 ± 0.05 MPa to -0.94 ± 0.02 MPa in 2004 and -0.56 ± 0.04 MPa to -0.74 ± 0.04 MPa in 2005, while *P. fremontii* values ranged from -0.29 ± 0.03 to -0.59 ± 0.01 MPa in 2004 and from -0.39 ± 0.03 to -0.44 ± 0.04 MPa in 2005. Midday water potential values ranged from -2.08 ± 0.24 to -3.16 ± 0.05 MPa in 2004 and from -1.80 ± 0.09 to -2.54 ± 0.10 MPa in 2005 for *E. angustifolia*. *P. fremontii* midday values ranged from -1.48 ± 0.06 to -1.84 ± 0.24 MPa in 2004 and from -1.54 ± 0.04 to -1.66 ± 0.11 MPa in 2005. No significant differences were observed between June and July time periods for *E. angustifolia* predawn and midday measurements for the 2004 growing season (Figure 4.4, repeated measures ANOVA, $p > 0.05$). However, there were significant declines observed between the June versus September and July versus September time periods (Figure 4.4, repeated measures ANOVA, $p < 0.05$). *E. angustifolia* measurements obtained in 2005 showed a difference between June versus

July and June versus August measurement periods (repeated measures ANOVA, $p < 0.05$), but no difference was observed between the July and August time periods for both predawn and midday data (repeated measures ANOVA, $p > 0.05$). *P. fremontii* predawn data obtained in 2004 showed no significant difference between the June and July measurement periods (repeated measures ANOVA, $p > 0.05$), but significant differences were observed between June versus September and July versus September (repeated measures ANOVA, $p < 0.05$). No significant differences were observed between predawn water potential values during the 2005 measurement season, and no significant differences in midday values were observed throughout both the 2004 and 2005 measurement seasons (Figure 4.4, repeated measures ANOVA, $p > 0.05$). Although soil moisture was not measured on site, depth to groundwater as monitored from a piezometer in the middle of the measurement plot was less than 1 m throughout both growing seasons.

The magnitude and variability of whole-tree water use differed between species for both the 2004 and 2005 measurement years. Average whole-tree water use ranged from 19.1 ± 3.7 to 38.4 ± 5.3 L d⁻¹ and from 19.1 ± 10.7 to 45.3 ± 7.5 L d⁻¹ for *E. angustifolia* in 2004 and 2005, respectively. *P. fremontii* whole-tree water use was greater and more variable compared to *E. angustifolia* for both years and ranged from 45.2 ± 4.0 to 122.2 ± 26.2 L d⁻¹ and 44.2 ± 11.2 to 167.3 ± 47.5 L d⁻¹ for the 2004 and 2005 measurement years, respectively (Figure 4.5). Average whole-tree water use was significantly higher in *P. fremontii* relative to *E. angustifolia*, where the average daily water use in 2004 and 2005 was 90.3 ± 2.7 and 108.0 ± 2.7 L d⁻¹ for *P. fremontii* compared to 31.8 ± 0.8 and 35.7 ± 0.6 L d⁻¹ for *E. angustifolia* in 2004 and 2005 (Figure

4.5, unpaired t-test, $p < 0.05$).

Significant differences in average seasonal water use per unit basal area, leaf area, and ground-based canopy area were observed between species (Figure 4.6, unpaired t-test, $p < 0.05$), with the exception of water use per unit basal area during the 2005 growing season (Figure 4.6, unpaired t-test, $p > 0.05$). *E. angustifolia* showed slightly higher daily water use per unit basal area for the 2004 measurement season with values ranging from 0.08 ± 0.01 to 0.17 ± 0.01 L cm⁻² compared to 0.07 ± 0.01 to 0.16 ± 0.01 L cm⁻² for *P. fremontii*. However, no differences were observed during the 2005 growing season, with values ranging from 0.09 ± 0.01 to 0.17 ± 0.01 L cm⁻² and 0.05 ± 0.01 to 0.19 ± 0.05 L cm⁻² for *E. angustifolia* and *P. fremontii*, respectively. Average seasonal daily water use per basal area was 0.14 ± 0.004 and 0.14 ± 0.002 L cm⁻² for *E. angustifolia* in 2004 and 2005 compared to 0.12 ± 0.003 and 0.14 ± 0.003 L cm⁻² for *P. fremontii* (unpaired t-test, $p < 0.05$).

P. fremontii showed significantly higher daily average water use per unit leaf area for both measurement seasons compared to *E. angustifolia*. Average seasonal daily values for *P. fremontii* were 1.76 ± 0.05 and 2.06 ± 0.05 L m⁻² compared to 1.38 ± 0.04 and 1.61 ± 0.03 L m⁻² for *E. angustifolia* in 2004 and 2005, respectively (Figure 4.6, unpaired t-test, $p < 0.05$). Daily values ranged from 1.07 ± 0.14 to 2.34 ± 0.41 L m⁻² in 2004 and 0.74 ± 0.15 to 2.85 ± 0.98 L m⁻² in 2005 for *P. fremontii* and from 0.84 ± 0.18 to 1.68 ± 0.28 and 0.62 ± 0.28 to 1.99 ± 0.43 L m⁻² for *E. angustifolia* during the 2004 and 2005 measurement seasons.

P. fremontii also showed higher water use per unit canopy area compared to *E. angustifolia* for both measurement years (Figure 4.6, unpaired t-test, $p < 0.05$), with 3.20

± 0.09 and $3.75 \pm 0.09 \text{ mm d}^{-1}$ in 2004 and 2005 for *P. fremontii* relative to 1.71 ± 0.04 and $2.00 \pm 0.04 \text{ mm d}^{-1}$ for *E. angustifolia*. Daily water use per canopy area varied from 1.94 ± 0.26 to $4.24 \pm 0.75 \text{ mm d}^{-1}$ and 1.35 ± 0.28 to $5.17 \pm 1.77 \text{ mm d}^{-1}$ in 2004 and 2005 for *P. fremontii* compared to 1.05 ± 0.23 to $2.10 \pm 0.35 \text{ mm d}^{-1}$ and 0.78 ± 0.35 to $2.48 \pm 0.53 \text{ mm d}^{-1}$ for *E. angustifolia*. *E. angustifolia* and *P. fremontii* showed very similar contributions to whole-plot tree transpiration for both total leaf area based and total canopy area based estimates (Figure 4.7, unpaired t-test, $p < 0.05$). No difference in whole-plot transpiration estimates based on total leaf or canopy area was observed between species during the 2004 growing season (Figure 4.7, unpaired t-test, $p > 0.05$). In contrast, *E. angustifolia* showed higher contributions to whole-plot transpiration for both total leaf and canopy area estimates in 2005, although differences in the absolute values were small. Total leaf area based transpiration of *E. angustifolia* ranged from 0.42 to 0.84 mm d^{-1} with a mean of $0.69 \pm 0.02 \text{ mm d}^{-1}$ in 2004 and from 0.52 to 0.99 mm d^{-1} with a mean of $0.83 \pm 0.01 \text{ mm d}^{-1}$ in 2005. Total leaf area based transpiration of *P. fremontii* ranged from 0.40 to 0.87 mm d^{-1} with a mean of $0.66 \pm 0.02 \text{ mm d}^{-1}$ in 2004 and from 0.28 to 1.05 mm d^{-1} with a mean of $0.76 \pm 0.02 \text{ mm d}^{-1}$ in 2005. Similar results were found for differences between species whole-plot transpiration based on total canopy ground area of each species within the plot. *E. angustifolia* showed a range of 0.42 to 0.84 mm d^{-1} and a mean of $0.68 \pm 0.02 \text{ mm d}^{-1}$ in 2004 and a range of 0.52 to 0.99 mm d^{-1} with a mean of $0.83 \pm 0.01 \text{ mm d}^{-1}$ in 2005. *P. fremontii* showed values ranging from 0.40 to 0.85 mm d^{-1} with a mean of $0.65 \pm 0.02 \text{ mm d}^{-1}$ in 2004 and a range of 0.28 to 1.05 mm d^{-1} with a mean of $0.76 \pm 0.02 \text{ mm d}^{-1}$ in 2005. Comparison of total plot tree transpiration based on leaf and canopy areas yielded similar results, with both scaling

methods yielding average daily tree transpiration of 1.33 and 1.32 mm d⁻¹ in 2004 for canopy and leaf based area estimates and 1.59 mm d⁻¹ in 2005 for both canopy and leaf based area estimates.

Modeled transpiration results that incorporated PAR, log-transformed vpd, and day of year as variable inputs produced significant relationships that explained greater than 50% of the variance in water use for both measurement years and by model type (leaf and canopy area based, Table 4.2). In addition, transpiration values from model outputs showed generally good agreement with measured values (Figure 4.8).

Discussion

Seasonal water use dynamics differed between *E. angustifolia* and *P. fremontii* in this study (Figures 4.5 and 4.6). Whole-tree water use was greater and more dynamic for *P. fremontii* compared to *E. angustifolia*, with average daily water use between 44.2 ± 11.2 and 167.3 ± 47.5 L d⁻¹ and 19.1 ± 3.7 and 45.3 ± 7.5 L d⁻¹, respectively, over the course of the entire study period (Figure 4.5). These data are consistent with previously reported water-use estimates for *P. fremontii* trees of similar size (Schaeffer et al. 2000), although comparable estimates for *E. angustifolia* stands in the western US appear to be lacking in the literature. Whole-tree water use has been estimated for *E. angustifolia* in two studies with sites located in Eurasia, where Khamzina et al. (2009) estimated water use of saplings to be between 16 and 23 L d⁻¹ for a plantation site in Uzbekistan. Chen et al. (2004) reported daily water use for a single tree of similar size compared to measurement trees in this study that approached peak rates of 60 L d⁻¹ during the growing season for a site in Northwest China.

In addition, results from this study showed very similar rates of transpiration per unit basal area, with only slightly higher values for *E. angustifolia* compared to *P. fremontii* during the 2004 growing season (Figure 4.6). In contrast, we found that *P. fremontii* had consistently higher transpiration per unit leaf and canopy ground area compared to *E. angustifolia* for the entire study period.

These data suggest that changes in stand water use associated with the establishment of *E. angustifolia* along river reaches depends primarily on two factors: 1) differences in stand density between species and 2) the spatial extent of *E. angustifolia* at a given site. In the first case, stand water use associated with either partial or total replacement of *P. fremontii* with *E. angustifolia* would result in lower stand water use from riparian forests along western US river systems. One exception to that would likely be given total replace of *P. fremontii* with *E. angustifolia* and then only if the stand density of *E. angustifolia* far exceeds *P. fremontii*. However, water-use measurements collected in an adjacent plot, with representative monostands of each species indicated the opposite to be true. Total basal area to ground area measurements taken in multiple subplots associated with the same neighboring stands used to generate allometric scaling relationships showed that on average, basal area to ground area of *P. fremontii* was greater than four times higher relative to *E. angustifolia*. The basal area to ground area average of three plots of *P. fremontii* was $45.2 \pm 7.5 \text{ cm}^2 \text{ m}^{-2}$ compared to $9.9 \pm 0.6 \text{ cm}^2 \text{ m}^{-2}$ for *E. angustifolia*. However, in the second case, if the spatial extent of riparian forest zone increases due to greater drought tolerance of *E. angustifolia* such that the total amount of area occupied by riparian trees expands beyond the original riparian corridor boundary, or changes in stand density where *E. angustifolia* becomes established and

persists as an understory species along with *P. fremontii* or other woody species, the overall water use of riparian forests would likely increase. In the case of establishment of *E. angustifolia* as an understory species, however, this would likely result in replacement of *P. fremontii* canopy area with *E. angustifolia* over time, as *E. angustifolia* appears to be capable of generating self-replacing stands because of its apparent shade tolerance, while *P. fremontii* in contrast, requires moist, high irradiance conditions generated by fluvial disturbance of floodplain area.

The seasonal patterns of whole-tree and site based transpiration reported here appear to be representative of conditions associated with little or no apparent drought stress as indicated by water potential data (Figure 4.3). Water potential values at the end of the 2004 growing season were slightly lower relative to 2005, but overall, predawn water potential values were fairly stable across both measurement seasons. However, *E. angustifolia* did show consistently lower predawn water potential values relative to *P. fremontii*, although the overall differences were small. It is possible this could be due to differences in water source and rooting depth distribution of *E. angustifolia* relative to *P. fremontii*, or spatial variability in water table depth across the measurement plot. Predawn and midday water potential data reported by Trafton (2005) for *E. angustifolia* were consistent with the pattern reported here, where *E. angustifolia* showed lower predawn and midday water potential values over the course of two growing seasons relative to native taxa. In that case, the isotopic composition of stem water obtained for *E. angustifolia* individuals having a diameter exceeding 3.5 cm indicated use of ground water, which varied in depth across multiple locations to a maximum depth of 1.5 m across both measurement seasons. In the current study, the water table monitored from a

well located near the center of the measurement plot never dropped below 1 m throughout the measurement period, and all measurement trees were much larger than 3.5 cm, so unless there was a high degree of spatial variability in the depth to ground water across the plot, it is not likely that the differences in predawn water potential between species were attributable to differences in water availability.

E. angustifolia and *P. fremontii* had a similar impact on total tree transpiration at the whole-plot level at this study location, although *E. angustifolia* had a slightly greater contribution during the 2005 growing season (Figure 4.7). This is because although *E. angustifolia* had lower water use overall for all metrics considered relative to *P. fremontii*, it covered a much larger fraction of the site area (Figure 4.1). Estimates of water use based on total leaf and canopy ground area of the site yielded similar results, where *E. angustifolia* transpiration varied from 0.42 to 0.99 mm d⁻¹ and *P. fremontii* transpiration varied from 0.28 to 1.05 mm d⁻¹ over the course of both measurement seasons (Figure 4.7). In order to estimate the contribution of each species to transpiration across the entire measurement seasons, measured transpiration was used to generate an empirical relationship of transpiration on a canopy and leaf area basis as a function of vpd, PAR, and time variables (Figure 4.8). Estimated total tree transpiration based on the empirical relationship and actual canopy coverage relative to whole plot area for both growing seasons was 188.6 and 239.2 mm in 2004 and 2005, respectively, with *E. angustifolia* and *P. fremontii* contributions of 99.1 and 89.5 mm in 2004 and 117.0 and 122.2 mm for 2005, respectively. Average daily tree transpiration of the study plot for the entire growing season period was 1.3 and 1.6 mm d⁻¹ for the 2004 and 2005 growing seasons, respectively. Whole season water use estimates were also generated assuming

conditions of complete canopy coverage for each species independently and yielded whole season transpiration estimates for *E. angustifolia* of 248 and 293 mm with an average daily rate of 1.7 and 2.0 mm d⁻¹ for the 2004 and 2005 growing seasons. Corresponding whole season estimates for *P. fremontii* were 447 and 611 mm, with daily rates of 3.1 and 4.1 mm d⁻¹ for 2004 and 2005, respectively. These results compare generally well with other estimates of stand transpiration for *P. fremontii*. Pataki et al. (Pataki et al. 2005) estimated canopy transpiration for *P. fremontii* stands in Moab, Utah, to be 4.8 and 9.3 mm d⁻¹ for a canopy subject to high salinity and competition with *Tamarix ramosissima* relative to a control stand. Gazal et al. (2006) reported seasonal transpiration of *P. fremontii* stands along the San Pedro River in Arizona with estimates of 966 mm and 484 mm for perennial and intermittent stream site locations. Daily estimates generally ranged from ~ 2.5 to 6.5 mm d⁻¹ for the perennial site and ~ 0 to 3 mm d⁻¹ for the intermittent stream location. Nagler et al. (2007) reported transpiration rates for a restoration plantation of *P. fremontii* on the lower Colorado River, with daily estimated water use that ranged between 6 and 10 mm d⁻¹, integrating to 1240 mm on an annual basis. Estimates of stand transpiration for *E. angustifolia* have been reported by Trafton (2005), with daily values of 4.9 mm d⁻¹ compared to 2.6 mm d⁻¹ for *P. deltoides* and 2.3 mm d⁻¹ for *Salix exigua* at the same study location. The only other stand estimate available in the literature for *E. angustifolia* is from Allen et al. (2005), where total evapotranspiration from a *E. angustifolia* stand along the Middle Rio Grande derived from remote sensing data was 1442 mm yr⁻¹, with an estimated peak of 7.5 mm d⁻¹ during the June time period. This estimate would have included soil and open water evaporation and understory transpiration if applicable, although no site-specific information regarding

the species composition of the study area was provided. In addition, empirical relationship results reported here provide a method to estimate transpiration rates of *E. angustifolia* and *P. fremontii* for areas that extend beyond the boundaries of the current study site when coupled with estimates of species canopy area or leaf area obtained from aerial photographs or remote sensing data and also provide a means to estimate the contribution of each species to total evapotranspiration in areas where it is directly measured or calculated via remote sensing methods.

The spatial extent of *E. angustifolia* on the western US riparian landscape is already significant. However, there is ample evidence suggesting that this species has the capacity for a much more extensive distribution in the future, especially given its apparent higher tolerance to drought, poor soil quality, high water source salinity, and establishment in full shade relative to native riparian taxa in the western US (Katz and Shafroth 2003; Reynolds and Cooper 2010; Jarnevich and Reynolds 2011; Nagler et al. 2011). The results reported here suggest that *E. angustifolia* could have a substantial impact on water resources particularly in areas where its stand density or spatial extent on the landscape exceeds that of native *P. fremontii*. Because varying meteorological conditions, soil water and nutrient availability, and soil texture can have a large impact transpiration dynamics of stands, additional data are still needed to assess the variability in water use of *E. angustifolia* for different geographic locations and compared to different native taxa of the western US. In order to better understand the overall impacts of current and future distribution of *E. angustifolia* on western water resources, estimates of its contribution to total evapotranspiration fluxes at much larger spatial scales are needed. Model results reported here could provide a means to quantify the contribution of

P. fremontii and *E. angustifolia* transpiration fluxes to total evapotranspiration at various spatial scales for river basins in the western US.

References

- Barnett, TP, Pierce, DW, Hidalgo, HG, Bonfils, C, Santer, BD, Das, T, Bala, G, Wood, AW, Nozawa, T, Mirin, AA, Cayan, DR, Dettinger, MD. 2008. Human-induced changes in the hydrology of the Western United States. *Science*. 319:1080–1083.
- Bush, SE, Hultine, KR, Sperry, JS, Ehleringer, JR. 2010. Calibration of thermal dissipation sap flow probes for ring- and diffuse-porous trees. *Tree Physiol*. 30:1545–1554.
- Chen, R, Kang, E, Zhang, Z, Zhao, W, Song, K, Zhang, J, Lan, Y. 2004. Estimation of tree transpiration and response of tree conductance to meteorological variables in desert-oasis system of Northwest China. *Sci China, Ser D: Earth Sci*. 47:9–20.
- Cleverly, J R, Dahm, CN, Thibault, JR, McDonnell, DE, Allred Coonrod, JE. 2006. Riparian ecohydrology: regulation of water flux from the ground to the atmosphere in the Middle Rio Grande, New Mexico. *Hydrol Processes*. 20:3207–3225.
- Dahm, CN, Cleverly, JR, Allred Coonrod, JE, Thibault, JR, McDonnell, DE, Gilroy, DJ. 2002. Evapotranspiration at the land/water interface in a semi-arid drainage basin. *Freshwater Biology*. 47:831–843.
- Friedman, JM, Auble, GT, Shafroth, PB, Scott, ML, Merigliano, MF, Freehling, MD, Griffin, ER. 2005. Dominance of non-native riparian trees in western USA. *Biol Invasions*. 7:747–751.
- Goodrich, DC, Scott, R, Qi, J, Goff, B, Unkrich, CL, Moran, MS, Williams, DG, Schaeffer, SM, Snyder, K, MacNish, R, Maddock, T, Pool, D, Chehbouni, A, Cooper, DI, Eichinger, WE, Shuttleworth, WJ, Kerr, Y, Marsett, R, Ni, W. 2000. Seasonal estimates of riparian evapotranspiration using remote and in situ measurements. *Agric For Meteorol*. 105:281–309.
- Granier, A. 1987. Evaluation of transpiration in a Douglas-fir stand by means of sap flow measurements. *Tree Physiol*. 3:309–320.
- Hultine, KR, Bush, SE. 2011. Ecohydrological consequences of non-native riparian vegetation in the southwestern United States: a review from an ecophysiological perspective. *Water Resour Res*. 47:W07542 (07541–07513).

- Hultine, KR, Nagler, PL, Morino, K, Bush, SE, Burtch, KG, Dennison, PE, Glenn, EP, Ehleringer, JR. 2010. Sap flux-scaled transpiration by tamarisk (*Tamarix* spp.) before, during and after episodic defoliation by the saltcedar leaf beetle (*Diorhabda carinulata*). *Agric For Meteorol.* 150:1467–1475.
- Jackson, RB, Carpenter, SR, Dahm, CN, McKnight, DM, Naiman, RJ, Postel, SL, Running, SW. 2001. Water in a changing world. *Ecol Appl.* 11:1027–1045.
- Jarnevich, CS, Reynolds, LV. 2011. Challenges of predicting the potential distribution of a slow-spreading invader: a habitat suitability map for an invasive riparian tree. *Biol Invasions.* 2011:153–163.
- Katz, GL, Shafroth, PB. 2003. Biology, ecology and management of *Elaeagnus angustifolia* L. (Russian olive) in Western North America. *Wetlands.* 23:763–777.
- Khamzina, A, Sommer, R, Lamers, JPA, Vlek, PLG. 2009. Transpiration and early growth of tree plantations established on degraded cropland over shallow saline groundwater table in northwest Uzbekistan. *Agric For Meteorol.* 149:1865–1874.
- Knopf, FL, Johnson, R, Rich, T, Samson, FB, Szaro, RC. 1988. Conservation of riparian ecosystems in the United States. *Wilson Bull.* 100:272–284.
- Ma, JX, Chen, YN, Li, WH, Huang, X, Zhu, CG, Ma, XD. 2012. Sap flow characteristics of four typical species in desert shelter forest and their responses to environmental factors. *Environ Earth Sci.* 67:151–160.
- Nagler, PL, Glenn, EP, Jarnevich, CS, Shafroth, PB. 2011. Distribution and abundance of Saltcedar and Russian Olive in the Western United States. *Crit Rev Plant Sci.* 30:508–523.
- Naiman, RJ, Decamps, H, Pollock, M. 1993. The role of riparian corridors in maintaining regional biodiversity. *Ecol Appl.* 3:209–212.
- Pataki, DE, Bush, SE, Gardner, P, Solomon, DK, Ehleringer, JR. 2005. Ecohydrology in a Colorado River riparian forest: implications for the decline of *Populus fremontii*. *Ecol Appl.* 15:1009–1018.
- Pataki, DE, McCarthy, HR, Litvak, E, Pincetl, S. 2011. Transpiration of urban forests in the Los Angeles metropolitan area. *Ecol Appl.* 21:661–677.
- Reynolds, LV, Cooper, DJ. 2010. Environmental tolerance of an invasive riparian tree and its potential for continued spread in the southwestern US. *J Veg Sci.* 21:733–743.
- Sabo, JL, Sinha, T, Bowling, LC, Schoups, GHW, Wallender, WW, Campana, ME, Cherkauer, KA, Fuller, PL, Graf, WL, Hopmans, JW, Kominoski, JS, Taylor, C,

- Trimble, SW, Webb, RH, Wohl, EE. 2010. Reclaiming freshwater sustainability in the Cadillac Desert. *Proc Natl Acad Sci U.S.A.* 107:21263–21270.
- Schaeffer, SM, Williams, DG, Goodrich, DC. 2000. Transpiration of cottonwood/willow forest estimated from sap flux. *Agric For Meteorol.* 105:257–270.
- Trafton, AN. 2005. Water relations of native and non-native tree species along the Middle Rio Grande, New Mexico, USA. University of New Mexico master's thesis.
- Webb, RH, Leake, SA, Turner, RM. 2007. The ribbon of green: change in riparian vegetation in the southwestern United States. Tucson (AZ): The University of Arizona Press 480 p.
- Xu, X, Zhang, R, Xue, X, Zhao, M. 1998. Determination of evapotranspiration in the desert area using lysimeters. *Commun Soil Sci and Plant Anal.* 29:1–13.
- Zhao, W, Liu, B. 2010. The response of sap flow in shrubs to rainfall pulses in the desert region of China. *Agric For Meteorol.* 150:1297–1306.

Table 4.1

Morphological characteristics of measurement trees for the 2004 and 2005 measurement years. Diameter at breast height (DBH), sapwood area, and basal area are given as the mean \pm the standard error.

Species	Year	DBH (cm)	Sapwood area (cm ²)	Basal area (cm ²)	LAI (m ² m ⁻²)	n
<i>E. angustifolia</i>	2004	16.8 \pm 1.2	18.6 \pm 2.4	232.5 \pm 31.9	1.25	10
<i>P. fremontii</i>	2004	29.5 \pm 3.6	463.5 \pm 112.3	773.8 \pm 213.4	1.82	10
<i>E. angustifolia</i>	2005	17.6 \pm 1.3	20.4 \pm 2.8	253.6 \pm 35.3	na	10
<i>P. fremontii</i>	2005	31.0 \pm 3.6	503.2 \pm 116.6	846.2 \pm 223.0	na	10

Table 4.2

Empirical model transpiration results based on leaf and canopy ground areas. Results are shown for the 2004 and 2005 measurement years. Transpiration estimates based on leaf area and canopy ground area have units of $L\ m^{-2}\ d^{-1}$ and $mm\ d^{-1}$, respectively.

Year	Species	Model type	Model variable	Coefficient	R ²	P
2004	<i>Elaeagnus</i>	leaf	constant ln(vpd) PAR DOY	0.5007 0.1595 0.00909 0.001852	0.55	<0.0001
2004	<i>Populus</i>	leaf	constant ln(vpd) PAR DOY	-0.2384 0.4472 0.01775 0.003819	0.6	<0.0001
2005	<i>Elaeagnus</i>	leaf	constant ln(vpd) PAR DOY	1.522 0.1624 0.007211 -0.001303	0.54	<0.0001
2005	<i>Populus</i>	leaf	constant ln(vpd) PAR DOY	2.607 0.3753 0.01661 -0.007143	0.49	<0.0001
2004	<i>Elaeagnus</i>	canopy	constant ln(vpd) PAR DOY	-0.3455 0.3417 0.009883 0.006522	0.53	<0.0001
2004	<i>Populus</i>	canopy	constant ln(vpd) PAR DOY	-0.4889 0.7117 0.03524 0.006859	0.62	<0.0001
2005	<i>Elaeagnus</i>	canopy	constant ln(vpd) PAR DOY	0.5563 0.2846 0.006381 0.00445	0.5	<0.0001
2005	<i>Populus</i>	canopy	constant ln(vpd) PAR DOY	4.911 0.665 0.02918 -0.0135	0.49	<0.0001

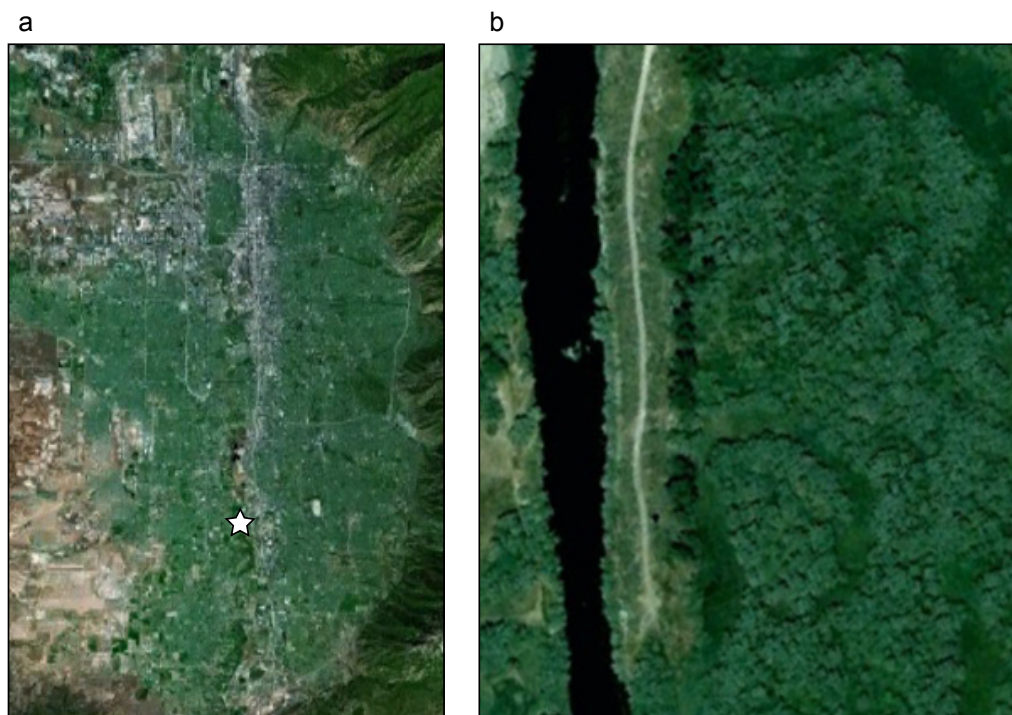


Figure 4.1: The field site location within Salt Lake Valley, UT, USA (a) and an aerial view of the site, where the extent of *E. angustifolia* (light green) and *P. fremontii* (dark green) canopies are distinguishable (b).

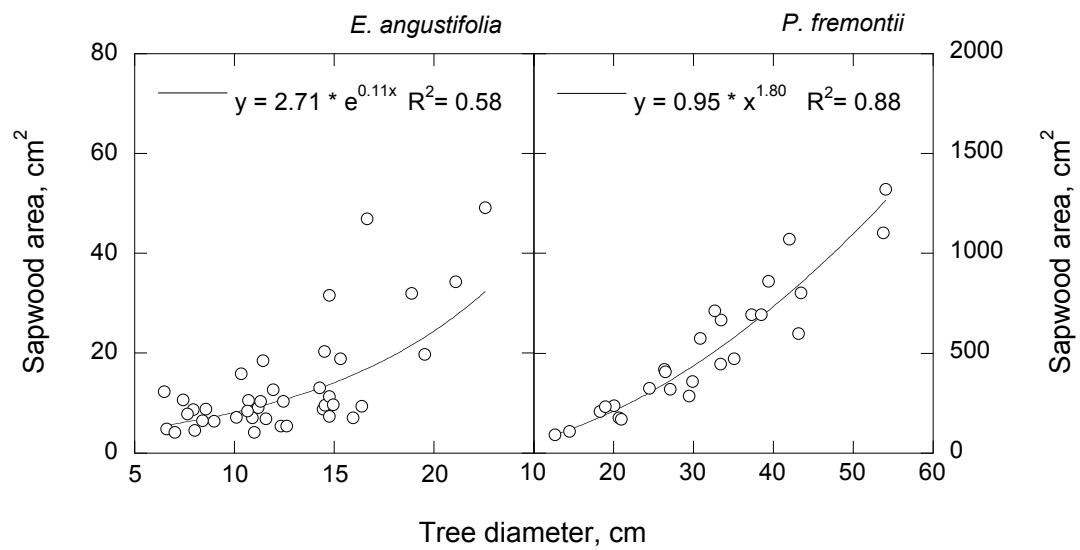


Figure 4.2: The allometric relationship between sapwood area and tree diameter for *E. angustifolia* and *P. fremontii* species. Sapwood area data for *E. angustifolia* represent the areas associated with current-year sapwood. Best-fit nonlinear regressions were used to generate the allometric equations.

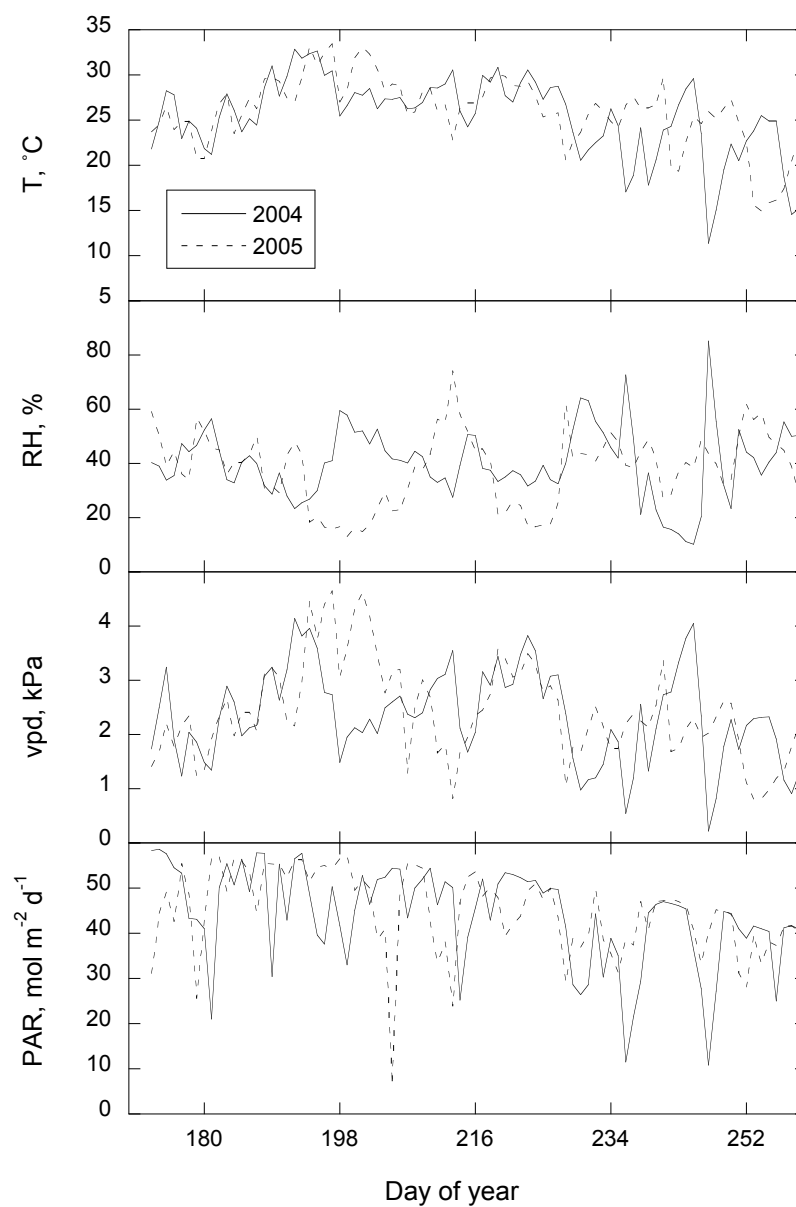


Figure 4.3: Average daytime temperature (T), relative humidity (RH), vapor pressure deficit (vpd), and daily sum of photosynthetically active radiation (PAR) spanning the measurement time periods during the 2004 and 2005 growing seasons.

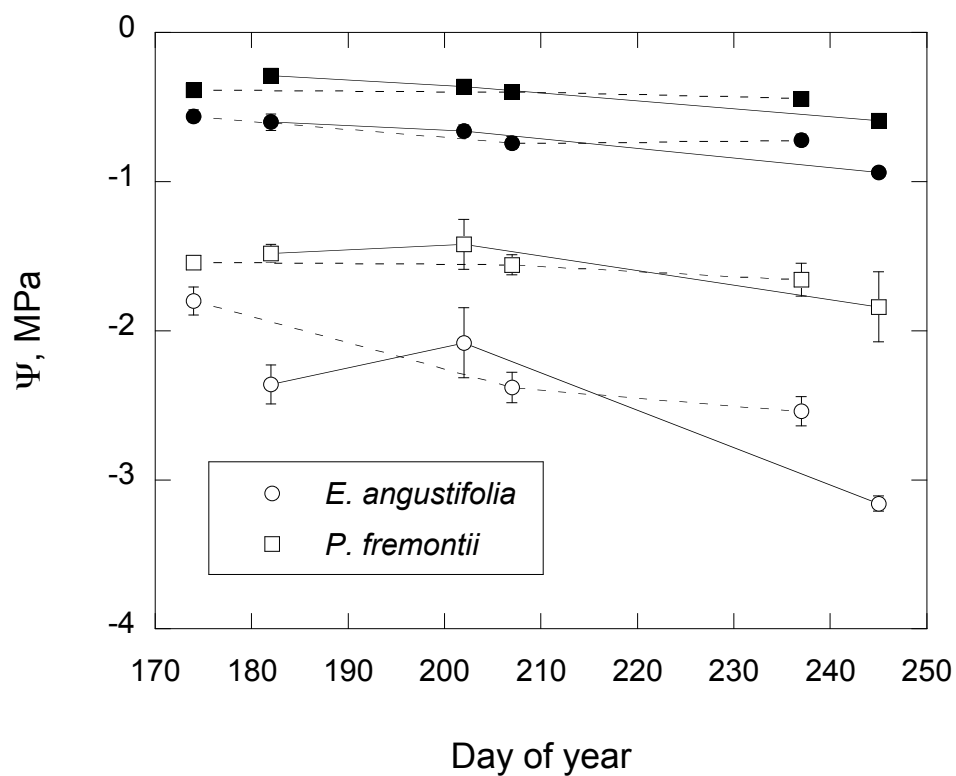


Figure 4.4: The seasonal course of predawn and midday water potential for the 2004 and 2005 growing seasons. Closed symbols represent predawn data, and open symbols represent midday data. Solid lines show data collected during the 2004 growing season and dotted lines show data collected during the 2005 growing season. Error bars represent the standard error of the mean.

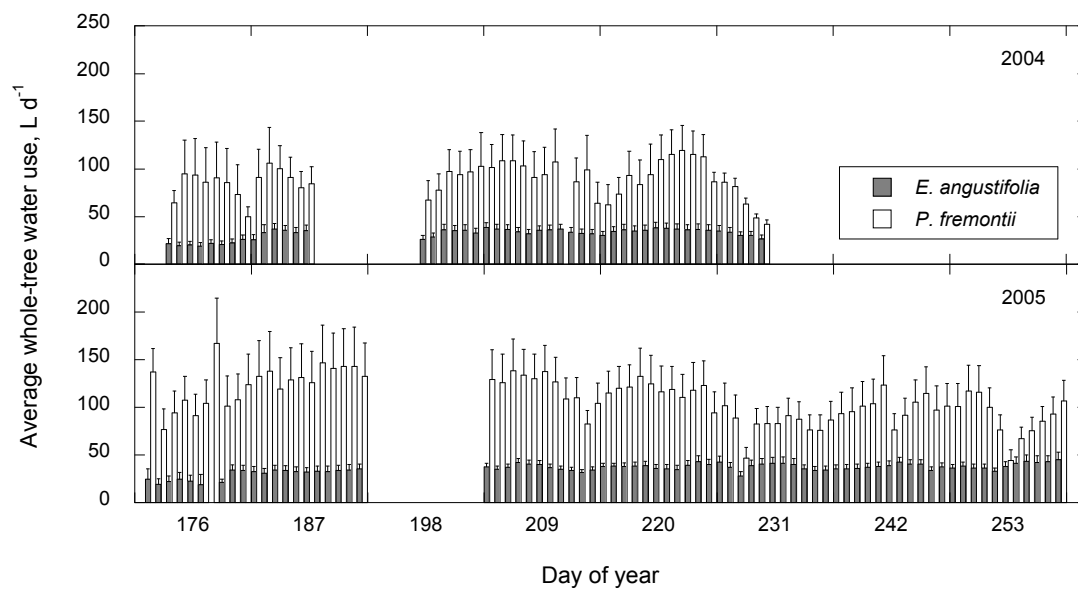


Figure 4.5: The seasonal course of whole-tree water use. Error bars represent the standard error of the mean.

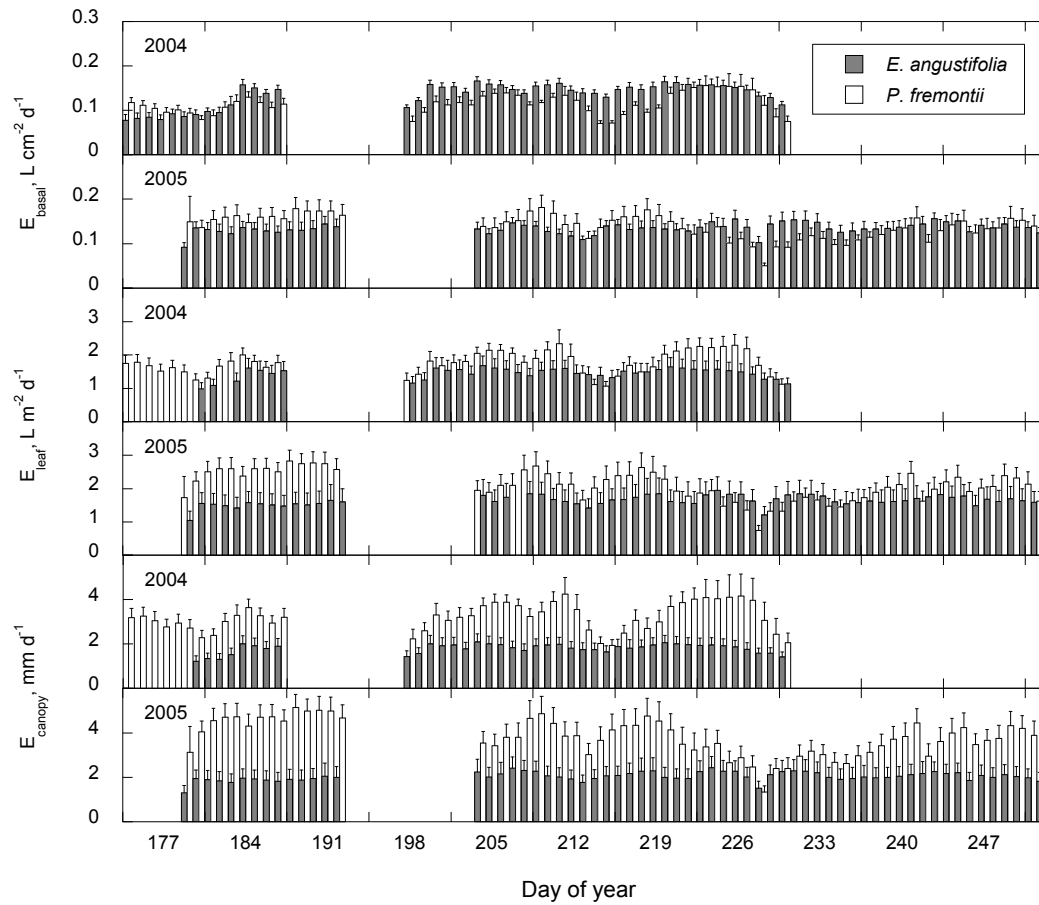


Figure 4.6: The seasonal course of whole-tree water use per unit basal area, ground-based canopy area, and leaf area. Error bars represent the standard error of the mean.

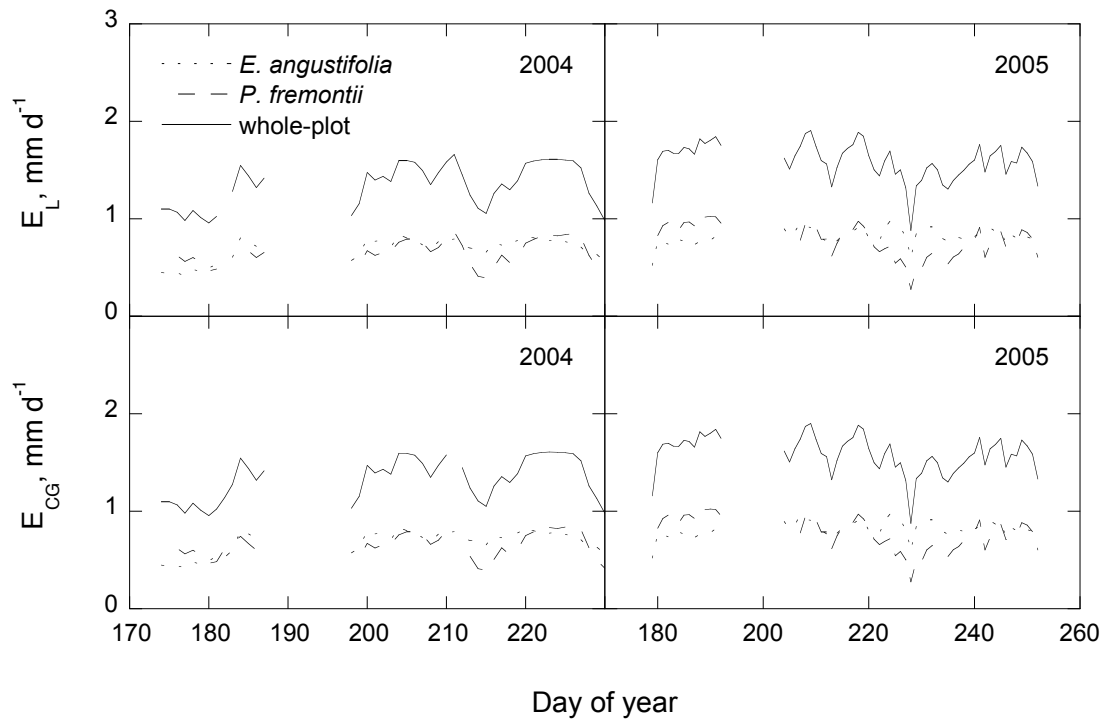


Figure 4.7: Whole-plot tree transpiration over the course of the 2004 and 2005 growing seasons. Estimates based on data scaled by total canopy ground area (CG) and leaf area (L) within the plot boundaries are shown.

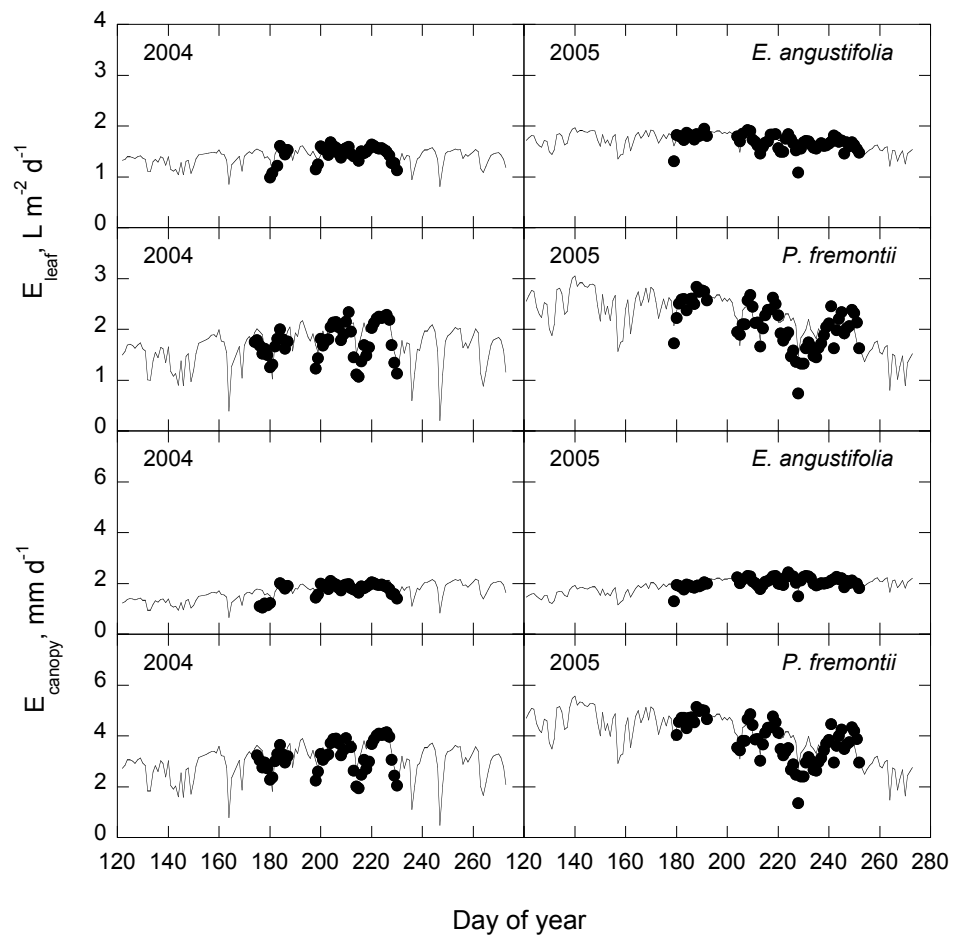


Figure 4.8: Empirical model results for transpiration per unit ground-based canopy area and leaf area for the 2004 and 2005 growing seasons. The solid lines represent model output data for the entire growing season time periods for both years. Actual measurements are shown with closed, circle symbols.

CHAPTER 5

WATER USE AND CONTRASTING HYDRAULIC STRATEGIES OF CULTIVATED RING- AND DIFFUSE-POROUS TREES IN A SEMIARID URBAN ECOSYSTEM

Abstract

Knowledge of forest transpiration magnitude and seasonality dynamics in semiarid cities is important for the selection of water conserving species and urban landscape management and improved understanding of the role of urban forests in urban microclimate and energy balance. Seasonal transpiration rates of nine tree species from multiple landscaped sites in Salt Lake City, UT, USA are reported here, including ring-porous *Gleditsia. triacanthos*, *Quercus. rubra*, *Fraxinus. americana*, *Celtis. occidentalis*, and *Sophora. japonica*, and diffuse-porous *Platanus. acerifolia*, *Acer. platanoides*, *Tilia. cordata*, and *Carpinus. betulus*. Large differences were observed in average whole-tree water use across seasonal time periods, as well as water use expressed on a basal-, crown-, and stand-area basis. In addition, no systematic differences in transpiration magnitude were observed between ring- and diffuse-porous wood anatomical categories. However, differences in seasonality were observed between ring- and diffuse-porous species, where in general, ring-porous species showed little to no decline in transpiration rates over the course of the growing season. In contrast, diffuse-porous species showed a range of responses with a general pattern of a seasonal decline in water use. Differences

in patterns of seasonal decline in water use for both ring- and diffuse-porous species appear to be linked to xylem cavitation vulnerability.

Introduction

Cities in the western US are often dominated by planted trees, even though these ecoregions were originally tree-less grasslands, shrublands, and deserts. As a result of human choices and market forces, urban forests of semiarid and arid regions of the western US are associated with high species diversity and can be comprised almost entirely of nonnative trees. The vast presence of trees occupying neighborhoods where there were none before, coupled with a supply of irrigation water and a climate that is markedly different relative to their native climates, undoubtedly impacts the magnitude of transpiration fluxes in these areas. Semiarid and arid cities of the western US also rely on the import of large quantities of water to sustain human enterprise, where water used for irrigation and outdoor use can be significant (Pataki et al. 2011a). Increasing urbanization associated with population growth and changes in water availability due to changes in climate are expected to increase the demand for already overappropriated water resources (Jackson et al. 2001; Barnett et al. 2008; Sabo et al. 2010). Because urban forests provide many positive benefits, including evaporative cooling, reduction of surface temperatures, erosion control and mitigation of runoff, and aesthetics among others (Peters and McFadden 2010; Pataki et al. 2011b), but require a share of limited water resources, information about the magnitude of water use for different species in these regions is needed. In addition to providing information that is important in identifying water conserving species, this information is important to better understand the overall impact

of forest transpiration in terms of water balance (i.e., supply requirements and seasonal water loss patterns) at spatial scales from the individual parcel to that of a city. Such information is needed if we are to address the water challenges that face the western US, which requires that we understand how comparable forest transpiration fluxes are between cities and how different these fluxes are compared to natural forest ecosystems.

Previous studies of water use dynamic of urban trees have generally focused on leaf-level gas exchange or measurements associated small or containerized trees (Vrecenak and Herrington 1984; Whitlow and Bassuk 1988; Zajicek and Heilman 1991; Kjelgren and Clark 1993; Devitt et al. 1994; Devitt et al. 1995a, 1995b; Close et al. 1996; Costello et al. 1996; Barradas 2000; Cermak et al. 2000; Cregg and Dix 2001; Johnson et al. 2001; Martin and Stabler 2002; Celestian and Martin 2005). Sap flux measurements of mature, landscaped trees are limited, but recent studies have begun to provide a much needed picture of factors that influence the magnitude of urban forest transpiration (Bush et al. 2008; McCarthy and Pataki 2010; Peters et al. 2010; McCarthy et al. 2011; Pataki et al. 2011c). From these, it is clear that there is a high degree of variability between species and across sites. It is also clear that some of this variability is associated with differences in site conditions, such as whether the site was irrigated or not, differences in soil nutrient dynamics, or differences in atmospheric conditions (principally atmospheric vapor pressure deficit). Furthermore, there is evidence that some of the variation can be attributed to intrinsic differences between species that appear to be linked to either place of geographic origin or wood type. How these factors, alone or together, scale to impact the magnitude of forest transpiration requires further investigation. While Bush et al. (2008) showed distinctly different patterns of sap flux response to atmospheric vapor

pressure deficit that were discernable by wood type, it was not clear if that apparent pattern led to fundamentally different amounts of water use between species in that environment, as those data were not scaled to the whole-tree or whole-site level. The objectives of this study were to evaluate whole-tree and whole-site water use of irrigated urban trees in the Salt Lake City urban forest to assess whether previously reported sap flux density responses yielded fundamentally different patterns of water use at the whole-tree and whole-site scale over time to assess the degree of variability between sites within the Salt Lake City study area and provide a means to compare land area based estimates of forest water use to other urban and natural forested ecosystems.

Methods

Study sites

Ten tree species were instrumented with sap flow sensors to measure transpiration rates at six different sites during the 2003 and 2007 growing seasons. Trees were associated with irrigated urban landscaped sites in Salt Lake City, UT, USA (latitude 40.66; longitude 111.55; elevation 1,275-1,550 m). Salt Lake City has a semiarid climate with mean annual temperature and precipitation of 11.0 °C and 409 mm, respectively (<http://www.wrh.noaa.gov/slc/climate/slccclimate/SLC/>). The measurement sites were located on the University of Utah campus (North campus, located just south of the Merrill Engineering building, Marriott Library, Practice field, located just east of Milton Bennion Hall, and Golf course, located just north of the Eccles Broadcast Center), and two were located nearby, just outside of the University of Utah campus proper, in a Salt Lake City park (Sunnyside, located just southeast of Spence Eccles Field House) and the

University of Utah Research Park area (Williams, located just west of Red Butte Garden and Arboretum) (Figure 5.1). Measurement species included ring-porous species, *Gleditsia triacanthos* (Honey locust), *Quercus gambelii* (Gambel oak), *Quercus rubra* (Red oak), *Celtis occidentalis* (Common hackberry), *Sophora japonica* (Japanese pagoda), and *Fraxinus americana* (White ash), and diffuse-porous species, *Platanus acerifolia* (London plane), *Acer platanoides* (Norway maple), *Carpinus betulus* (European hornbeam), and *Tilia cordata* (Littleleaf linden). Specific site, species type and locations, and tree stand characteristics are provided in Tables 5.1 and 5.2.

Meteorological measurements

Temperature and relative humidity measurements associated with the 2003 growing season were obtained at both study sites and were previously described in Bush et al. (2008). Temperature and relative humidity measurements associated with the 2007 growing season were obtained from a meteorological station located on the University of Utah campus (<http://mesowest.utah.edu>), where 5-minute average data were available associated with the North campus site location and with a temperature and relative humidity sensor (HMP45C, Vaisala, Finland) located at the Sunnyside study site. Temperature and relative humidity measurements at the Sunnyside location were measured according to the same frequency as sap flow measurements at that site (30 s). Data obtained from another meteorological station located on campus, associated with the University of Utah Biology growth facility (Red Butte Canyon Station #1) were used to fill in data gaps associated with periods of time during the growing season when sap flow was not measured. Photosynthetically active radiation data were obtained from the

University of Utah Biology growth facility in 2007, and data for 2003 were obtained from a meteorological station located off campus. Comparison of offsite data and data obtained from the growth site for 2007 showed very little difference and was assumed to be representative of conditions on campus (<http://mesowest.utah.edu>, station MSI01).

Sap flow

Trees were instrumented with Granier-type thermal dissipation sap flow sensors that were 2 cm in length with the exception of the installations associated with *C. occidentalis*, *S. japonica*, and *F. americana*, all of which were instrumented with 1 cm length probes. Sap flux density for diffuse-porous species was calculated according to the empirically derived equation (Granier 1987):

$$J_s = 119(\Delta T_m / \Delta T - 1)^{1.231} \quad (5.1)$$

where J_s is sap flux density ($\text{g m}^{-2} \text{s}^{-1}$), ΔT is the recorded temperature difference between the heated and reference sensor, and ΔT_m is the recorded temperature difference between the heated and reference sensor under zero flow conditions. Sap flux density for ring-porous species was calculated according to empirically derived equations of the same form according to Bush et al. (2010), where the entire current year sapwood area of calibration stems was used to obtain sap flux density instead of dyed area in order to be consistent with field-based sapwood area measurements of ring-porous species. Species-specific equations were employed where possible. In cases where species-specific equations were not available, the calibration coefficient and scaling exponent for

calculating J_s was obtained by pooling all ring-porous calibration data. Sap flow measurements were made every 30 s, and half hour means were stored using a datalogger (CR21X and CR23X, Campbell Scientific, Logan, UT).

Whole-tree water use, water use per crown area, and whole-plot transpiration

In order to calculate whole-tree transpiration, J_s was multiplied by total conducting sapwood area, which was obtained by measuring sapwood depth from tree cores collected using an increment borer. In the case of diffuse-porous species, sapwood depth values were determined based on visual inspection of tree cores for apparent sapwood to heartwood transitional area and core translucence. Radial variation in J_s with increasing sapwood depth was accounted for according to Pataki et al. (2011c). Sapwood depth for ring-porous species was obtained differently. Because dye perfusion measurements from a previous study indicated that conductive sapwood area was limited to the current year xylem (Bush et al. 2010), large diameter tree cores (~1 cm) were collected for every individual ring-porous tree that was instrumented with sap flow sensors. These cores were then cut in half with a band saw to expose the width of annual rings and scanned. Scanned images were processed using Image J software (<http://rsbweb.nih.gov/ij/>) to obtain sapwood depth for the year associated with sap flow measurements. Whole tree water use expressed on a crown area basis was obtained by dividing whole-tree water use by ground area below the canopy defined by the dripline. Whole-plot water use was obtained by calculating the sum of total water use of trees within the plot boundary divided by total plot area. Plot areas were defined for each

species by calculating the area occupied by each species using aerial imagery (Google Earth), ground-based measurements, and Image J software. Defining whole-plot boundaries for each species was based on the edge of the canopies of measurement trees associated with groups of trees at a given site.

Hydraulic measurements

In order to assess species differences in xylem cavitation vulnerability, stem hydraulic conductivity measurements were collected according to Alder et al. (1997) for eight of the 10 species reported here. A total of six stem segments were collected before dawn from independent trees of each species. Stem material was immediately placed in large plastic bags containing wet paper towels before transporting the material back to the laboratory. Stem material was stored in a walk-in refrigerator until time of measurement, which occurred within 3 days of time of collection. Hydraulic measurements were used to generate vulnerability curves from which the xylem pressure associated with 50% loss in hydraulic conductivity (p_{50}) relative to maximum was calculated, as this is a common metric used to assess differences in cavitation vulnerability between species.

Results

Meteorological data for both sites and for each measurement year showed generally good agreement. There were small differences observed between temperature, relative humidity, and vpd for the two sites associated with the 2003 growing season. The North Campus site had higher average temperature and vpd by 1.6 °C and 0.1 kPa and lower relative humidity by 9% compared to the Williams site (Figure 5.2, paired t-

test, $p > 0.05$). No statistical differences were observed for mean daytime temperature or vpd for the 2007 growing season (paired t-test, $p > 0.05$, Figure 5.2). However, a small difference in mean daytime relative humidity was observed between sites, where the North campus site on average was 5.1% greater than the Sunnyside location (paired t-test, $p > 0.05$). The month of July had the highest average mean daytime temperature and vpd conditions for both measurement years, with values of $30.2^\circ \pm 0.5$ and $28.1^\circ \pm 0.4$ C and 3.6 ± 0.1 and 3.4 ± 0.1 kPa for the North campus site and Williams site, respectively, the 2003 growing season. The North campus site and Sunnyside sites had corresponding values of $30.1^\circ \pm 0.4$ and $29.9^\circ \pm 0.4$ C and 4.4 ± 0.1 and 4.3 ± 0.1 kPa, respectively, for average July mean daytime temperature and vpd conditions during the 2007 growing season.

Differences in whole-tree water use, water use per basal area, water use per crown area, and whole plot water use were observed across sites from both measurement years. Average whole-tree water use for species across the entire period of measurement varied, where *Q. gambelii* showed the lowest seasonal average water use of 13.4 ± 0.2 L d⁻¹, and *C. occidentalis* had the largest average water use of 172.7 ± 5.7 L d⁻¹ (Figures 5.3 and 5.4). Average water use per basal and crown area also showed large differences between species. Average seasonal water use per basal area was lowest for *S. japonica* with an average of 0.08 ± 0.002 L cm⁻² d⁻¹ and highest for *F. Americana* with 0.36 ± 0.007 L cm⁻² d⁻¹ (Figures 5.5 and 5.6). Average water use per crown area was highest for *F. Americana* at 9.9 ± 0.2 mm d⁻¹ and was lowest for *S. japonica* at 0.9 ± 0.03 mm d⁻¹ (Figures 5.7 and 5.8). The highest average whole plot water use was 1.9 ± 0.04 mm d⁻¹ associated with *C. betulus* and the lowest average value was 0.9 ± 0.01 mm d⁻¹ associated with both *Q.*

rubra. Because the length of the measurement period varied by species and between years, average data were generated for the month of July for each year for all species in order to directly compare mean water use differences between species (Table 5.3). The month of July was selected because it was the month with the highest average vpd for both years and there were few data gaps during that time period for all species. In general, there were no clear patterns observed that appeared to be linked to the species geographic place of origin (mesic, temperate vs. xeric, for example) or by xylem type. As with the seasonal average data, the same relationships for species with the highest and lowest rates of water use for each type of scaled measure were consistent with average July results. For example, *C. occidentalis* had the highest average July whole tree water use and *Q. gambelii* had the lowest water use (Table 5.3).

Differences in seasonal patterns of water use based on different scaling metrics and as a function of vpd varied across species in this study (Figures 5.3–5.11). Some species showed pronounced declines in water use over time (e.g., *A. platanoides*) compared to others that showed relatively little change in the magnitude of water use over time (e.g., *Q. gambelii*). There also appeared to be changes in the magnitude of seasonal water use over time relative to changes in vpd that varied between species (Figure 5.11). In order to evaluate whether there was a relationship between xylem vulnerability to cavitation and seasonal patterns of water use, J_s data for each species were scaled as the percent maximum daytime J_s observed over the entire study period for each species and limited to high vpd conditions (mean daytime vpd > 3). These data were plotted against day of year time. The resulting slope for each species showed a statistically significant relationship as a function of p50 (Figure 5.12, linear least squares

regression, $p < 0.05$).

Discussion

Differences were observed in water use of species for all scaling metrics considered in this study (Figures 5.3–5.10). While differences in patterns of response of J_s to increasing vpd have been reported previously for ring- versus diffuse-porous tree species in the Salt Lake Valley urban ecosystem (Bush et al. 2008) and in other urban studies of tree water use (Peters et al. 2010), the data reported here do not suggest that in general the magnitude of fluxes differ categorically between ring and diffuse-porous trees (Figures 5.3–5.10, Table 5.3). Average daily whole-tree water use for the entire measurement periods in 2003 and 2007 varied from $13.4 \pm 0.2 \text{ L d}^{-1}$ to $172.7 \pm 5.7 \text{ L d}^{-1}$ across species, while water use per basal area ranged from $0.08 \pm 0.002 \text{ L cm}^{-2} \text{ d}^{-1}$ to $0.36 \pm 0.007 \text{ L cm}^{-2} \text{ d}^{-1}$. These results are consistent with previously reported values for trees of the same size class across functional types and a broad range of species from different geographic locations ecosystem types (Wullschleger et al. 1998). However, water use per basal area for *Q. gambelii*, the only native tree species of the region reported here, was lower than reported values for a natural stand located in Red Butte Canyon Research Natural Area located at higher elevation, just east of Salt Lake City (Taneda and Sperry 2008). Comparable results of water use estimates associated with other studies of urban trees are limited. Pataki et al. (2011) reported water use for *G. triacanthos* and *P. hybrida* (Londonplane - referred to as *P. acerifolia* here), both species common to this study, for study sites in Los Angeles, CA. Average *G. triacanthos* and *P. hybrida* water use was 89.9 and 176.9 L d^{-1} , respectively, during the month of August for the Los Angeles sites

and differed from average values for the month of July in Salt Lake City, where *P. acerifolia* had comparatively lower water use and *G. triacanthos* had higher water use (Table 5.3). The differences in *P. acerifolia* could be attributable to the fact that the trees measured in Salt Lake City were smaller relative to those in Los Angeles. However, differences in size do not explain the differences in average water use for *G. triacanthos*, as *G. triacanthos* trees were smaller in Salt Lake City relative to Los Angeles, but had higher water use. It is possible that other site-specific variables such as soil textural or nutrient properties or different methods for obtaining whole-tree water use of ring-porous species compared to that study may account for the differences. It is also possible that differences in the magnitude of mean daytime vpd over which data were averaged in each location may be a contributing factor (July–August mean for the Los Angeles site was 1.3 kPa compared to 3.1 kPa for the July–August average vpd at the North campus site in Salt Lake City).

Water use per crown area was generally similar between species in this study with the exception of data associated with *C. betulus* and *F. americana* (Figures 5.7 and 5.8, Table 5.3). The large difference between these two species and the rest of the species in this study was attributable to differences in canopy structure. Both *C. betulus* and *F. americana* had columnar shaped canopy crowns, while all others had varying shapes of broad crowns. Data for *Q. gambelii* on a per canopy area or plot area basis were not available because this was the only species where the trees were growing in small stands, not isolated crowns, and for which individual crown areas or stand densities were not determined. Peters et al. (2010) reported water use per crown area for urban deciduous broadleaf species in St. Paul Minnesota to be $\sim 1 \text{ mm d}^{-1}$, which is generally smaller than

reported here for trees in Salt Lake City with the exception of *Q. rubra* and *S. japonica* species. This is not surprising given the very different climate and atmospheric conditions between the two study locations. Data for both water use per crown area and whole-plot water use were reported in this study as they each provide useful information.

Transpiration per unit crown area is a useful metric, particularly for urban foresters and land managers, as it allows for understanding to what degree transpiration rates may be expected to vary between species for the amount of space that they occupy. While transpiration on a whole-plot or landscape basis is important for understanding the impact of the urban forest on evapotranspiration fluxes per unit land area, it is heavily influenced by stand density, which varies widely in urban ecosystems, and determining associated plot area is much more difficult relative to natural stands (Pataki et al. 2011c). Average whole-plot estimates of tree transpiration for this study ranged from $0.9 \pm 0.01 \text{ mm d}^{-1}$ for the *Q. rubra* stand to $2.1 \pm 0.05 \text{ mm d}^{-1}$ for the *F. americana* stand. Overall, the estimates provided here are generally higher compared to whole-plot estimates provided by Pataki et al. (2011) for study sites in Los Angeles, where whole-plot transpiration was as high as $\sim 2 \text{ mm d}^{-1}$, but in most cases was below 1 mm d^{-1} . As was previously mentioned, these differences could be attributable to differences in species and stand density between sites and differences in environmental conditions between sites. In addition, the data reported here are not dissimilar to estimates of canopy transpiration reported for a wide range of natural deciduous forest ecosystems that have rates of generally $< 4 \text{ mm d}^{-1}$ (Wilson et al. 2001; Ewers et al. 2002; Bovard et al. 2005; Schipka et al. 2005; Wullschleger and Hanson 2006; Asbjornsen et al. 2007; Bowden and Bauerle 2008; Gebauer et al. 2012).

Differences in the patterns of seasonal water use between species were observed

in this study (Figures 5.3–5.8), where the variability was not explained by changes in water availability, as the trees were all associated with irrigated sites, or by meteorological conditions alone (Figure 5.11). In general, ring-porous species as a group showed less change in water use over time compared to diffuse-porous species. This is similar to what was observed and previously reported by Bush et al. (2008) and Peters et al. (2010) in two different cities. In contrast, diffuse-porous species showed change in water use versus mean daytime vpd over time, where the degree to which the magnitude was reduced relative to vpd appeared to vary across species. For example, *A. platanoides* showed a marked seasonal decline in transpiration magnitude versus vpd, while *C. betulus* did not. One explanation for the observed decrease in flux that would be consistent with the suggestion that ring-porous species exercise greater stomatal control given their greater vulnerability to xylem cavitation (Bush et al. 2010; Litvak et al. 2012) compared to diffuse-porous species is that reduced stomatal control of diffuse-porous species comes at the cost of incurring damage to the vascular system over time, accompanied by a reduction in whole-plant hydraulic conductance. The degree to which that occurs in diffuse-porous species may also be linked to varying degrees of vulnerability to cavitation, given that as a group diffuse-porous species exhibit a much broader range in vulnerability to cavitation (some quite vulnerable, some far less so) relative to ring-porous species. The climate of Salt Lake City provides a good environment by which to look for such differences. This is because mean daytime vpd conditions are generally high and, equally important, if not more so, sustained throughout much of the growing season (Figure 5.2). By filtering daily transpiration to include only days associated with very high vpd conditions (mean daytime vpd >3) assessing the

change in transpiration over time should yield differences between these functional types for the reasons discussed above. In order to obtain a quantity representative of change in J_s over time and keep the scale the same between species for comparison, change in J_s was scaled relative to the maximum J_s measured over the whole-seasonal time period for each species. Data limited to mean daytime vpd conditions > 3 were examined for the change in the percent maximum J_s over time (day of year). The slope of this relationship ($dJ_{s\%max}/dt$) was plotted against p50 for each species considered in this study. The relationship between the slope of the percent change in transpiration over time versus p50 was significant and showed that species with greater vulnerability to cavitation showed little change in the magnitude of flux over time relative to species with less vulnerable xylem (Figure 5.12). These differences were also distinct by wood type. In this case, ring-porous trees appear to be display isohydric behavior, which is consistent with their more vulnerable xylem relative to diffuse-porous species. Diffuse-porous species showed patterns that are consistent with varying degrees of anisohydry, which may also be explained by the fact that there is a large amount of variation in the vulnerability of diffuse-porous vasculature to xylem cavitation including species that are very vulnerable and often associated with riparian habitats to species that are comparatively very resistant. These results suggest that the hydraulic architecture and associated vulnerability to cavitation may explain differences in distinctly different patterns of seasonal water use observed across species in semiarid urban ecosystems not subject to limited water availability and to other natural forested ecosystems given similar conditions of high soil moisture availability.

These data also suggest that the selection of ring- versus diffuse-porous species

would impact the seasonality of transpiration fluxes in semi-arid and arid urban regions differently. Although during the hottest month in this study, there were not any marked differences between ring- and diffuse-porous fluxes, the whole-season time series suggest that semiarid and arid urban forests comprised mostly of diffuse-porous species would be associated with a higher early season transpiration pulse, decreasing over time, the rate of which would be linked to the composition of diffuse-porous species and their associated cavitation vulnerability. In contrast, a forest of ring-porous species would likely generate a less variable and sustained transpiration flux. The result may be fluxes of similar magnitude at the annual scale for each type, but the timing and seasonality of fluxes may be quite different. A forest comprised entirely of diffuse-porous species relative to ring-porous species would also likely have a distinctly higher early season flux due to differences in leaf phenology, given that ring-porous trees generally leaf out later than diffuse-porous species (Wang et al. 1992).

These results are of interest for a number of reasons. From a practical perspective, data here were presented using metrics that are easy to measure and provide urban foresters and land managers with water use information for species commonly planted in the Salt Lake Valley urban ecosystem, but many of which are also commonly planted in urban ecosystems of other geographic regions. These data are also important in that they provide additional and much needed information regarding the magnitude of transpiration at the forest stand scale. Lastly, the results reported here suggest a link between seasonal patterns of water use and vulnerability to cavitation that may be applicable to a broader range of ecosystem types and improve the overall understanding of the factors that impact seasonal changes in both urban and natural forested ecosystems over time.

References

- Asbjornsen, H, Tomer, MD, Gomez-Cardenas, M, Brudvig, LA, Greenan, CM, Schilling, K. 2007. Tree and stand transpiration in a Midwestern bur oak savanna after elm encroachment and restoration thinning. *For Ecol and Manage.* 247:209–219.
- Barnett, TP, Pierce, DW, Hidalgo, HG, Bonfils, C, Santer, BD, Das, T, Bala, G, Wood, AW, Nozawa, T, Mirin, AA, Cayan, DR, Dettinger, MG. 2008. Human-induced changes in the hydrology of the Western United States. *Science.* 319:1080–1083.
- Bovard, BD, Curtis, PS, Vogel, CS, Su, H-B, Schmid, HP. 2005. Environmental controls on sap flow in a northern hardwood forest. *Tree Physiol.* 25:31–38.
- Bowden, JD, Bauerle, WL. 2008. Measuring and modeling the variation in species-specific transpiration in temperate deciduous hardwoods. *Tree Physiol.* 28:1675–1683.
- Bush, SE, Hultine, KR, Sperry, JS, Ehleringer, JR. 2010. Calibration of thermal dissipation sap flow probes for ring- and diffuse-porous trees. *Tree Physiol.* 30:1545–1554.
- Bush, SE, Pataki, DE, Hultine, KR, West, AG, Sperry, JS, Ehleringer, JR. 2008. Wood anatomy constrains stomatal responses to atmospheric vapor pressure deficit in irrigated, urban trees. *Oecologia.* 156:13–20.
- Ewers, BE, Mackay, DS, Gower, ST, Ahl, DE, Burrows, SN, Samanta, SS. 2002. Tree species effects on stand transpiration in northern Wisconsin. *Water Resour Res.* 38:10.1029/2001WR000830.
- Gebauer, T, Horna, V, Leuschner, C. 2012. Canopy transpiration of pure and mixed forest stands with variable abundance of European beech. *J Hydrol.* Available from <http://dx.doi.org/10.1016/j.jhydrol.2012.03.009>.
- Granier, A. 1987. Evaluation of transpiration in a Douglas-fir stand by means of sap flow measurements. *Tree Physiol.* 3:309–320.
- Jackson, RB, Carpenter, SR, Dahm, CN, McKnight, DM, Naiman, RJ, Postel, SL, Running, SW. 2001. Water in a changing world. *Ecol Appl.* 11:1027–1045.
- Litvak, E, McCarthy, HR, Pataki, DE. 2012. Transpiration sensitivity of urban trees in a semi-arid climate is constrained by xylem vulnerability to cavitation. *Tree Physiol.* 32:373–388.
- McCarthy, HR, Pataki, DE. 2010. Drivers of variability in water use of native and non-native urban trees in the greater Los Angeles area. *Urban Ecosyst.* 13:393–414.

- McCarthy, HR, Pataki, DE, Jenerette, GD. 2011. Plant water-use efficiency as a metric of urban ecosystem services. *Ecol Appl.* 21:3115–3127.
- Pataki, DE, Boone, CG, Hogue, TS, Jenerette, GD, McFadden, JP, Pincetl, S. 2011a. Socio-ecohydrology and the urban water challenge. *Ecohydrology.* 4:341–347.
- Pataki, DE, Carreiro, MM, Cherrier, J, Grulke, NE, Jennings, V, Pincetl, S, Pouyat, RV, Whitlow, TH, Zipperer, WC. 2011b. Coupling biogeochemical cycles in urban environments: ecosystem services, green solutions, and misconceptions. *Front Ecol Environ.* 9:27–36.
- Pataki, DE, McCarthy, HR, Litvak, E, Pincetl, S. 2011c. Transpiration of urban forests in the Los Angeles metropolitan area. *Ecol Appl.* 21:661–677.
- Peters, EB, McFadden, JP. 2010. Influence of seasonality and vegetation type on suburban microclimates. doi: 10.1007/s11252-11010-10128-11255.
- Peters, EB, McFadden, JP, Montgomery, RA. 2010. Biological and environmental controls on tree transpiration in a suburban landscape. *J Geophys Res.* 115:1–13.
- Sabo, JL, Sinha, T, Bowling, LC, Schoups, GHW, Wallender, WW, Campana, ME, Cherkauer, KA, Fuller, PL, Graf, WL, Hopmans, JW, Kominoski, JS, Taylor, C, Trimble, SW, Webb, RH, Wohl, EE. 2010. Reclaiming freshwater sustainability in the Cadillac Desert. *Proc Natl Acad Sci.* 107:21263–21270.
- Schipka, F, Heimann, J, Leuschner, C. 2005. Regional variation in canopy transpiration of Central European beech forests. *Oecologia.* 143:260–270.
- Taneda, H, Sperry, JS. 2008. A case-study of water transport in co-occurring ring- versus diffuse-porous trees: contrasts in water-status, conducting capacity, cavitation and vessel refilling. *Tree Physiol.* 28:1641–1651.
- Wilson, KB, Hanson, PJ, Mulholland, PJ, Baldocchi, DD, Wullschleger, SD. 2001. A comparison of methods for determining forest evapotranspiration and its components: sap-flow, soil water budget, eddy covariance and catchment water balance. *Agric For Meteorol.* 106:153–168.
- Wullschleger, SD, Hanson, PJ. 2006. Sensitivity of canopy transpiration to altered precipitation in an upland oak forest: evidence from a long-term field manipulation study. *Glob Chang Biol.* 12:97–109.
- Wullschleger, SD, Meinzer, FC, Vertessy, RA. 1998. A review of whole-plant water use studies in trees. *Tree Physiol.* 18:499–512.

Table 5.1

Species, year, and measurement site information for study trees.

Site name	Year	Species	Common name	Xylem type	n
North campus	2003	<i>Gleditsia triacanthos</i>	Honey locust	Ring-porous	10
North campus	2003	<i>Platanus acerifolia</i>	London plane	Diffuse-porous	10
Williams	2003	<i>Quercus gambelii</i>	Gambel oak	Ring-porous	10
Williams	2003	<i>Quercus rubra</i>	Red oak	Ring-porous	10
Williams	2003	<i>Acer platanoides</i>	Norway maple	Diffuse-porous	10
Library	2007	<i>Carpinus betulus</i>	European hornbeam	Diffuse-porous	7
Practice field	2007	<i>Celtis occidentalis</i>	Common hackberry	Ring-porous	7
Practice field	2007	<i>Sophora japonica</i>	Japanese pagoda	Ring-porous	7
Golf course	2007	<i>Fraxinus americana</i>	White ash	Ring-porous	5
Sunnyside	2007	<i>Tilia cordata</i>	Littleleaf linden	Diffuse-porous	7

Table 5.2

The stand characteristics of measurement trees. The mean \pm the standard error are given.

Species	DBH (cm)	Sapwood depth (cm)	Sapwood area (cm ²)	Basal area (cm ²)	Canopy area (m ²)
<i>Gleditsia triacanthos</i>	20.8 (1.1)	0.17 (0.02)	10.1 (1.2)	347.7 (38.1)	54.4 (3.7)
<i>Platanus acerifolia</i>	25.0 (1.8)	8.70 (0.90)	440.8 (52.8)	515.4 (76.4)	64.5 (8.6)
<i>Quercus gambelii</i>	13.5 (0.5)	0.08 (0.01)	3.2 (0.3)	144.3 (11.2)	6.3 (0.4)
<i>Quercus rubra</i>	21.4 (1.1)	0.21 (0.02)	12.7 (1.3)	367.0 (35.7)	54.1 (7.9)
<i>Acer platanoides</i>	26.5 (0.7)	8.76 (0.62)	483.6 (33.4)	554.4 (31.2)	53.5 (2.9)
<i>Carpinus betulus</i>	14.5 (0.7)	7.25 (0.34)	167.3 (15.9)	167.3 (15.9)	6.1 (0.9)
<i>Celtis occidentalis</i>	46.0 (3.7)	0.30 (0.03)	42.2 (6.7)	1726.2 (244.3)	64.7 (10.8)
<i>Sophora japonica</i>	40.8 (3.0)	0.23 (0.04)	26.9 (3.4)	1346.4 (199.1)	119.7 (12.6)
<i>Fraxinus americana</i>	21.1 (2.3)	0.51 (0.06)	33.7 (6.1)	367.3 (80.4)	13.0 (2.2)
<i>Tilia cordata</i>	37.9 (4.0)	18.9 (1.17)	1147.3 (186.7)	1147.3 (186.7)	73.0 (12.0)

Table 5.3

Mean July water use \pm the standard error for different scaling metrics.

Species	Whole tree water use L d ⁻¹	Water use per basal area L cm ⁻² d ⁻¹	Water use per crown area L m ⁻² d ⁻¹	Site-based water use mm d ⁻¹
<i>Gleditsia triacanthos</i>	117.8 (2.9)	0.39 (0.009)	2.4 (0.06)	2.2 (0.05)
<i>Platanus acerifolia</i>	119.1 (3.0)	0.23 (0.005)	1.9 (0.04)	1.5 (0.03)
<i>Quercus gambelii</i>	15.3 (0.2)	0.11 (0.001)	na	na
<i>Quercus rubra</i>	54.1 (1.2)	0.16 (0.003)	1.2 (0.04)	1.0 (0.02)
<i>Acer platanoides</i>	105.7 (2.0)	0.19 (0.004)	2.0 (0.03)	2.0 (0.04)
<i>Carpinus betulus</i>	46.6 (0.9)	0.30 (0.006)	9.8 (0.19)	2.5 (0.06)
<i>Celtis occidentalis</i>	187.3 (12.1)	0.13 (0.006)	3.2 (0.25)	1.9 (0.11)
<i>Sophora japonica</i>	110.2 (3.1)	0.09 (0.002)	1.0 (0.03)	1.1 (0.03)
<i>Fraxinus americana</i>	133.1 (4.4)	0.38 (0.013)	10.5 (0.35)	2.2 (0.08)
<i>Tilia cordata</i>	164.5 (4.8)	0.14 (0.005)	2.3 (0.07)	1.3 (0.04)



Figure 5.1: The Salt Lake Valley, USA (left panel), showing the location of the measurement sites. Specific measurement sites locations are shown in the right panel.

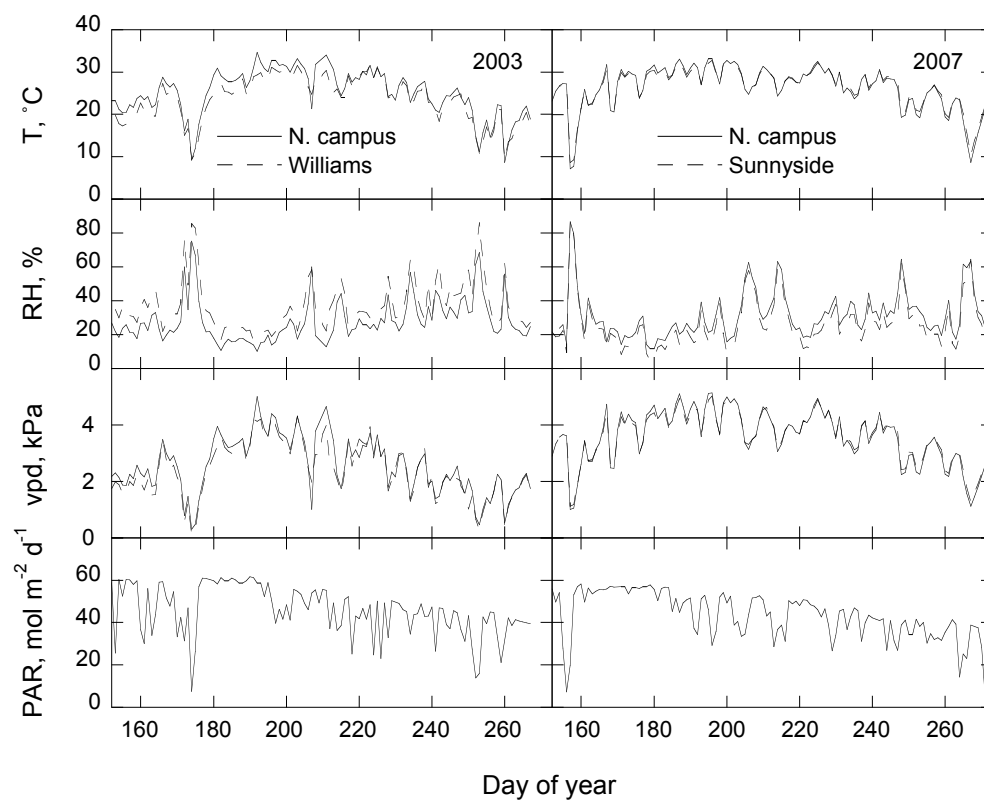


Figure 5.2: Mean daytime temperature (T), relative humidity (RH), vapor pressure deficit (vpd), and photosynthetically active radiation (PAR) for the 2003 and 2007 growing seasons.

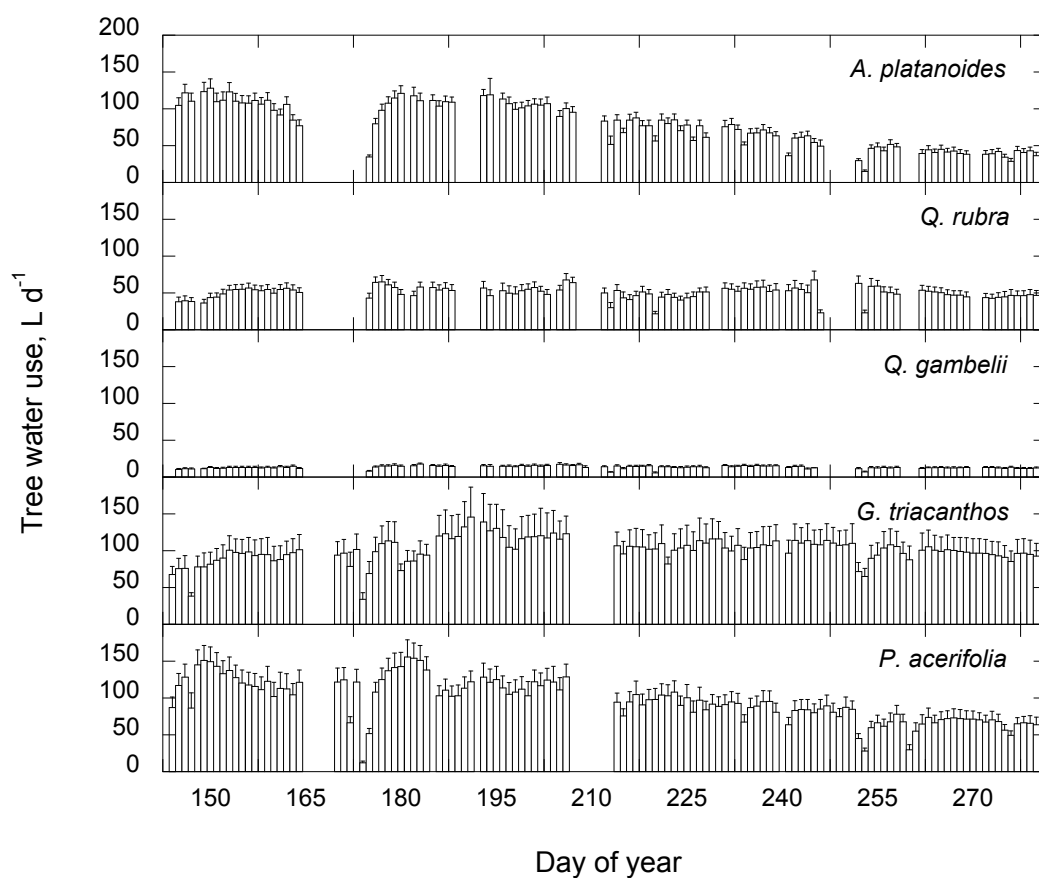


Figure 5.3: Mean whole-tree water use \pm the standard error for trees instrumented during the 2003 growing season.

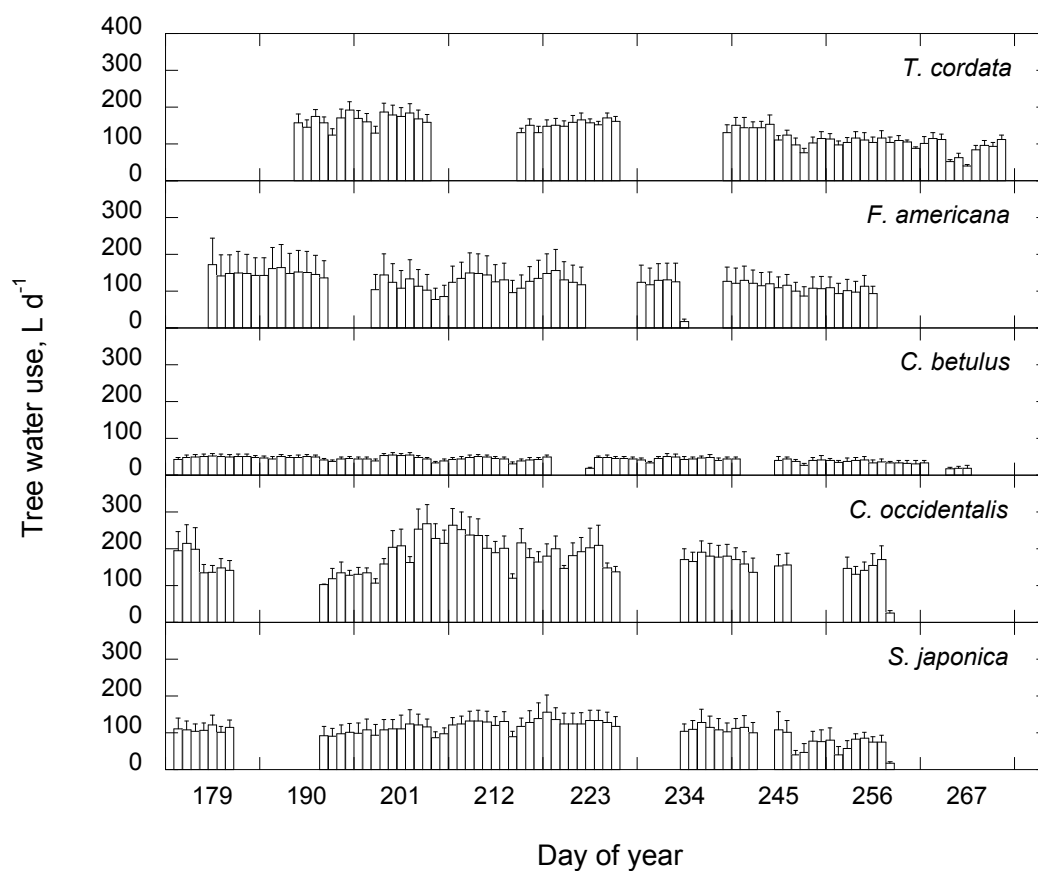


Figure 5.4: Mean whole-tree water use \pm the standard error for trees instrumented during the 2007 growing season.

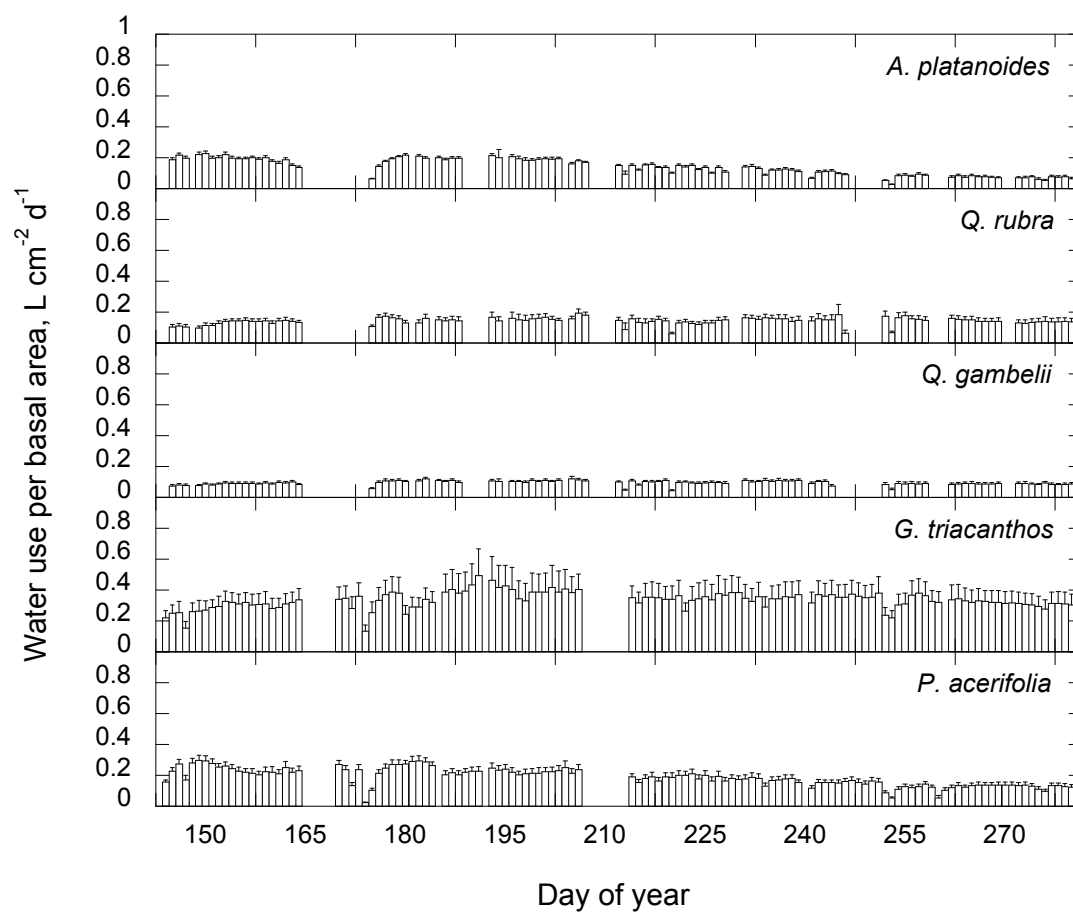


Figure 5.5: Mean whole-tree water use per basal area \pm the standard error for trees instrumented during the 2003 growing season.

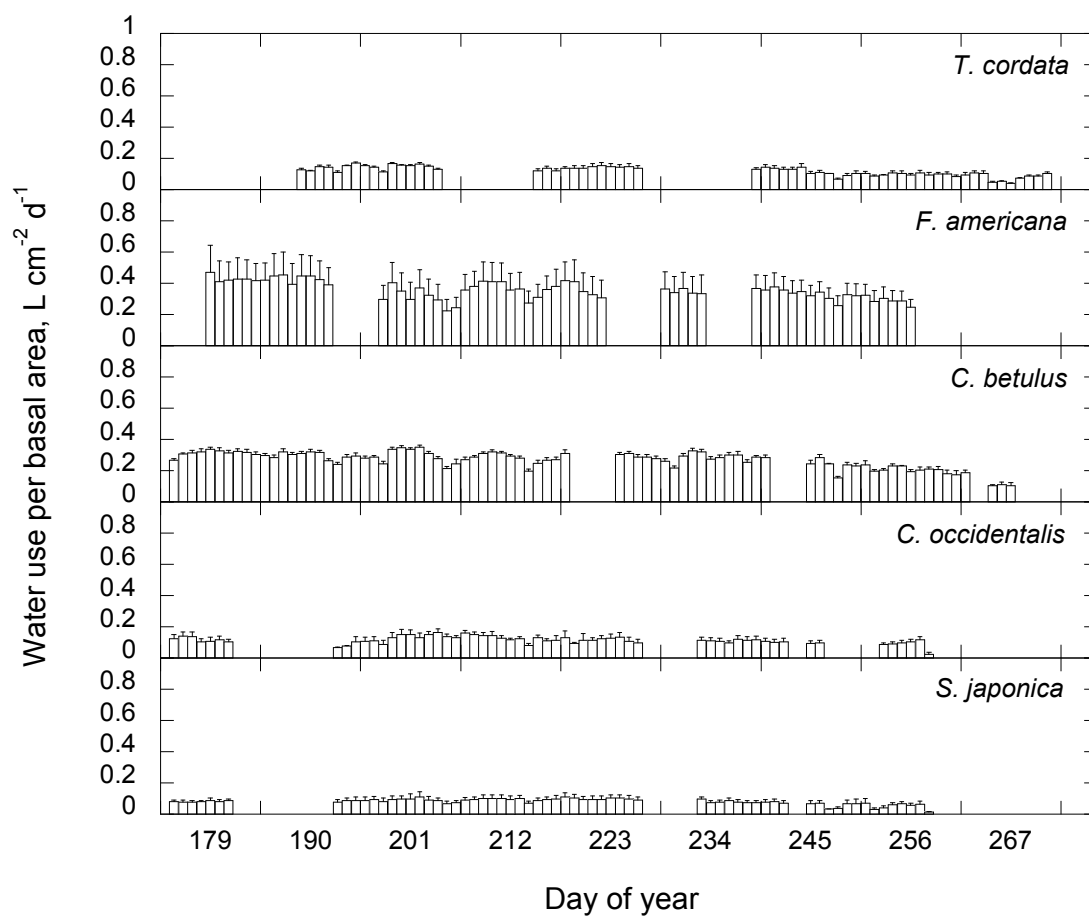


Figure 5.6: Mean whole-tree water use per basal area \pm the standard error for trees instrumented during the 2007 growing season.

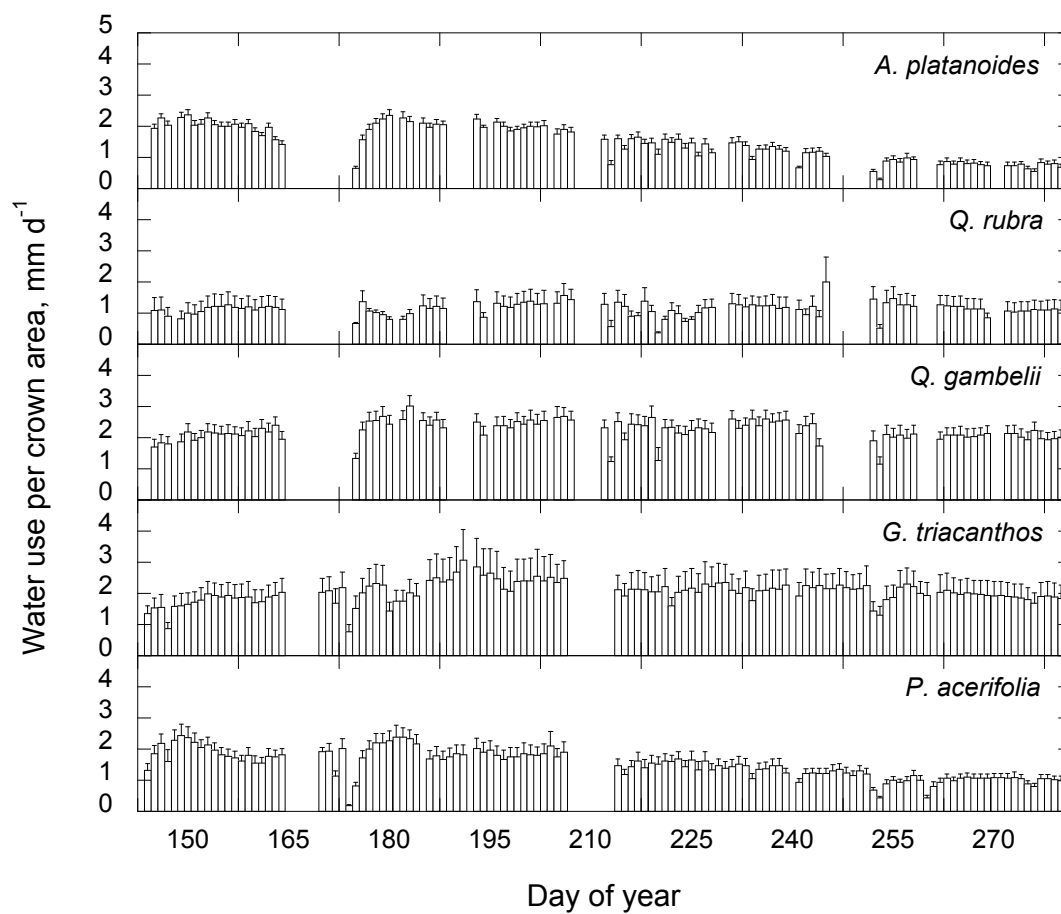


Figure 5.7: Mean whole-tree water use per canopy area \pm the standard error for trees instrumented during the 2003 growing season.

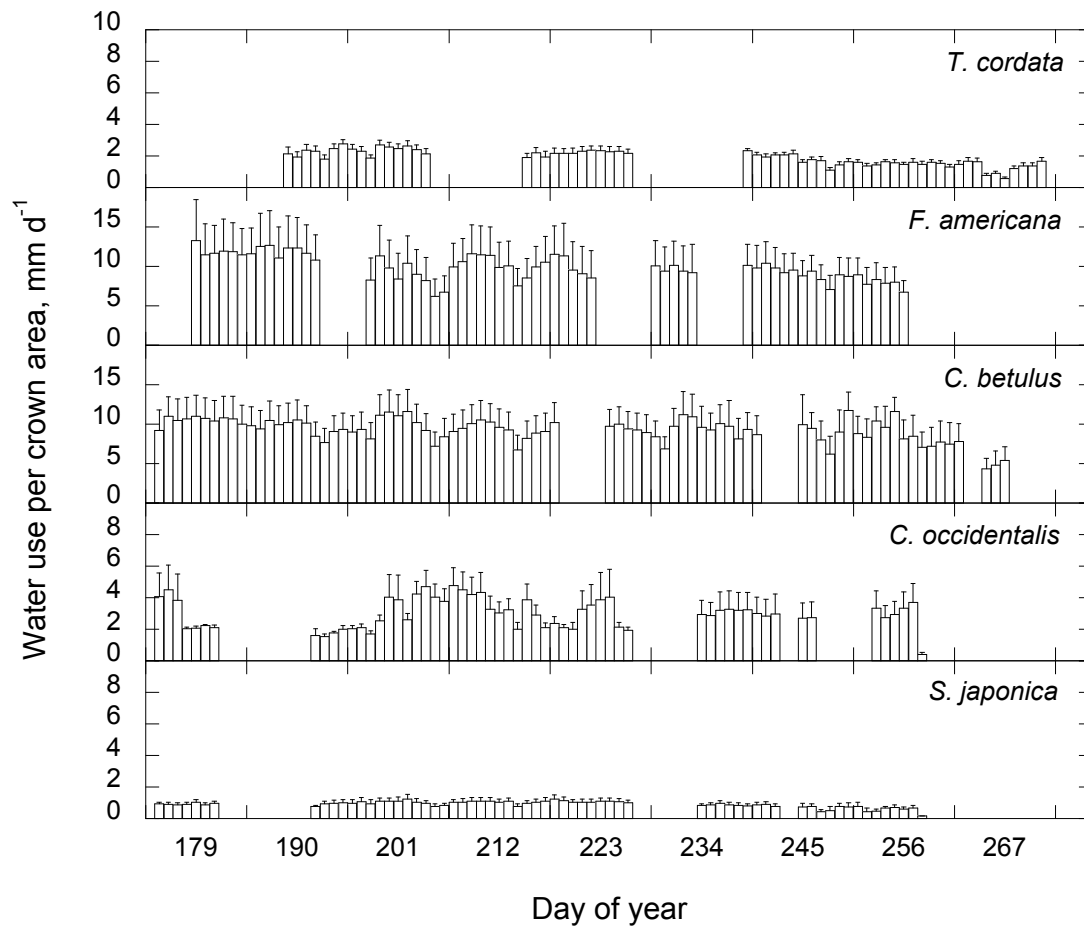


Figure 5.8: Mean whole-tree water use per canopy area \pm the standard error for trees instrumented during the 2007 growing season.

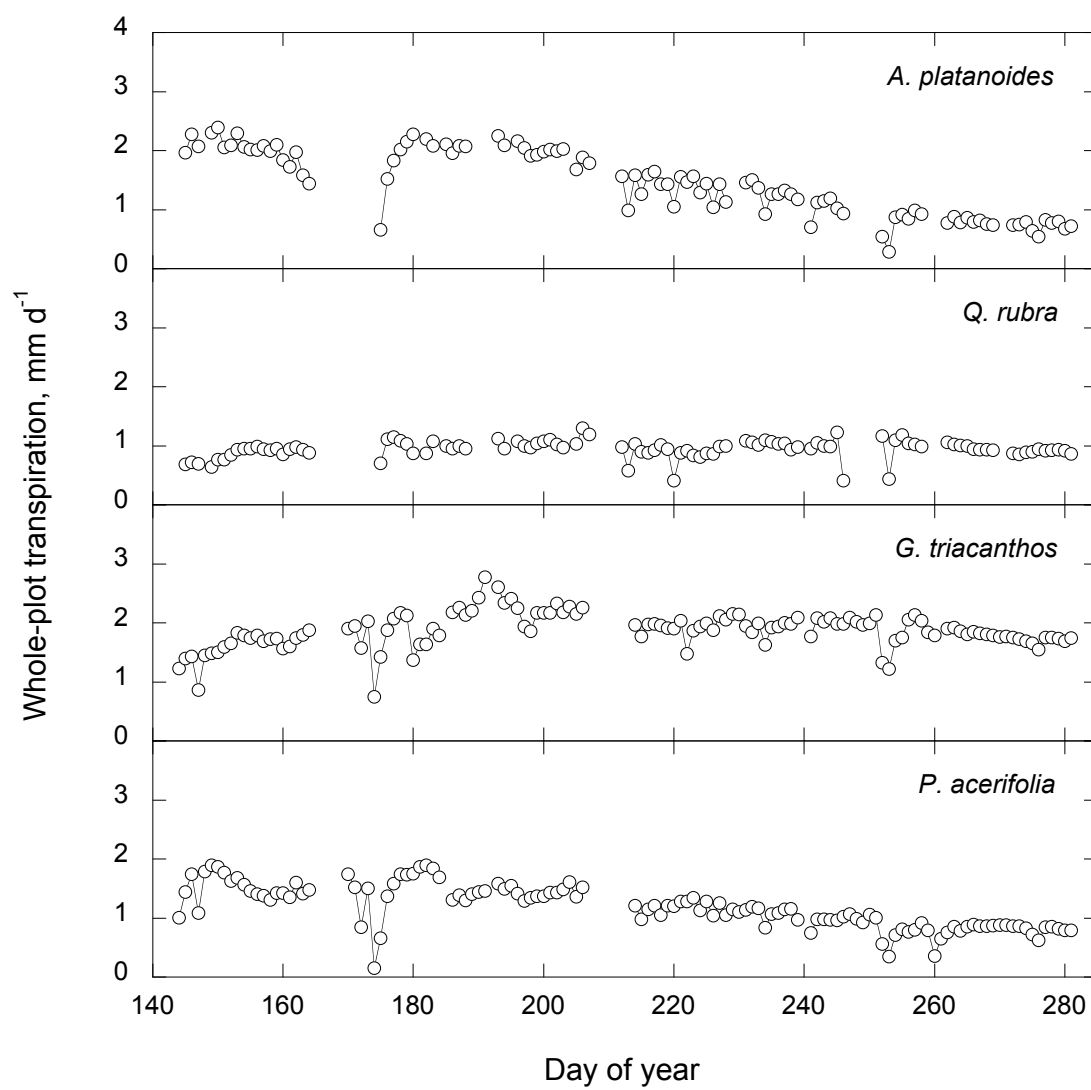


Figure 5.9: Whole-plot transpiration for trees instrumented during the 2003 growing season.

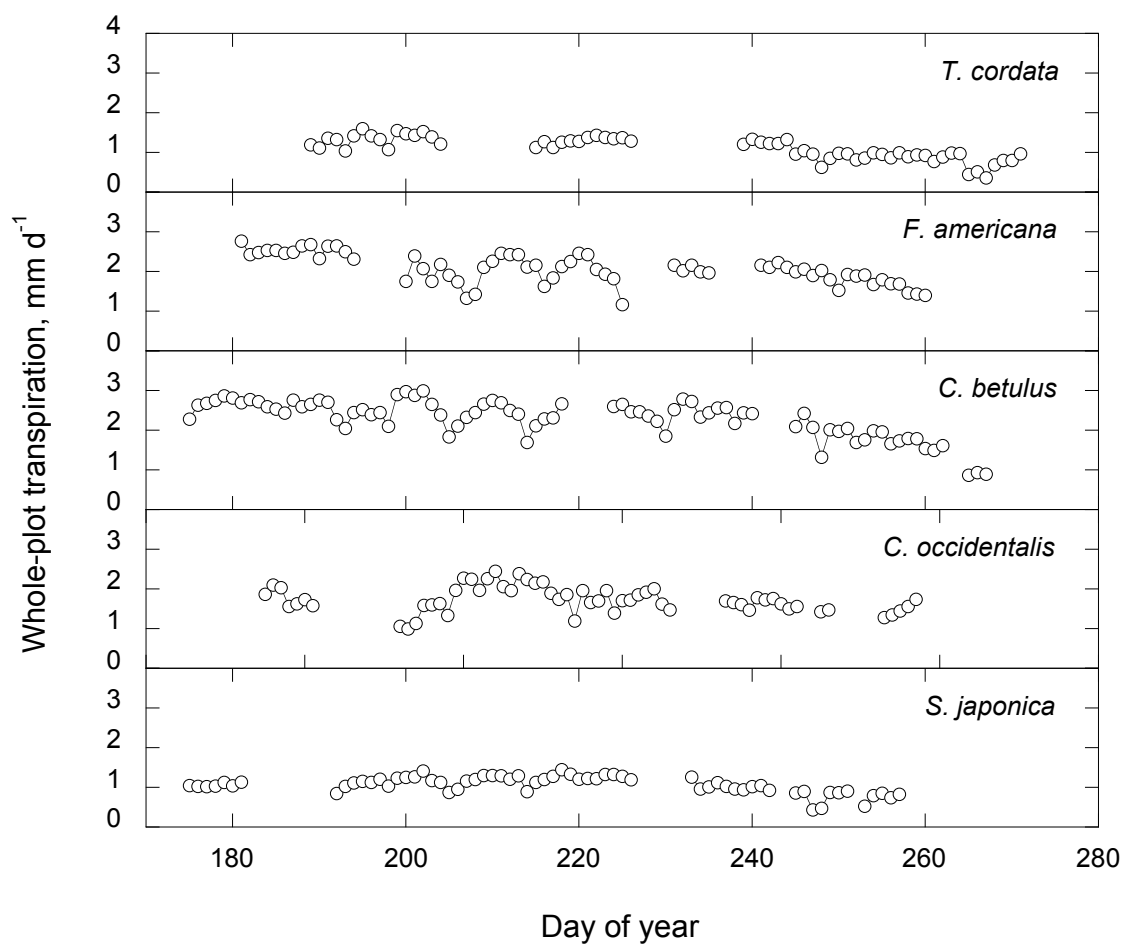


Figure 5.10: Whole-plot transpiration for trees instrumented during the 2007 growing season.

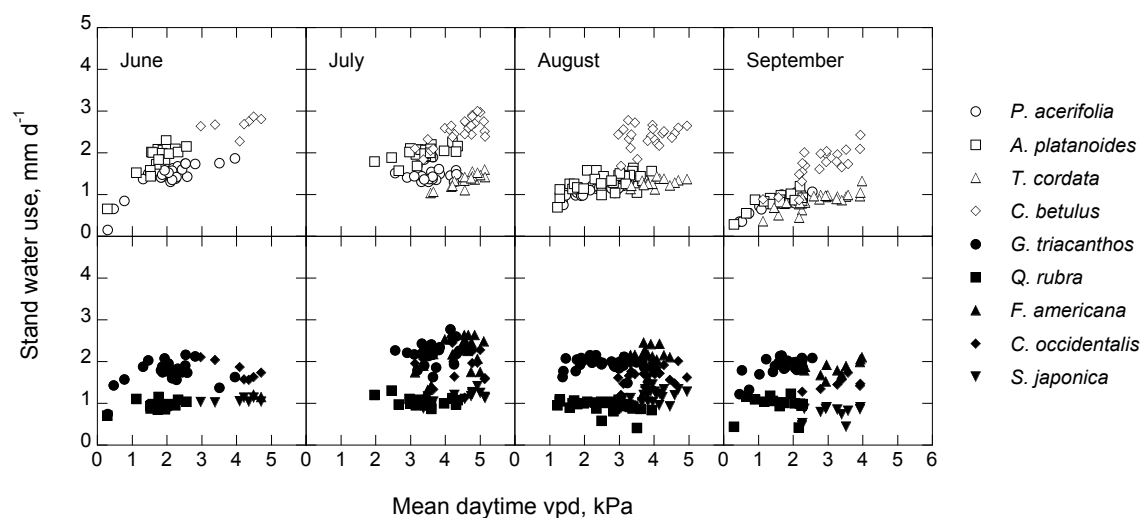


Figure 5.11: Whole-plot water use versus mean daytime vpd for the months of June, July, August, and September. Diffuse-porous species are shown as open symbols in the top panels and ring-porous species are shown as closed symbols in the bottom panels.

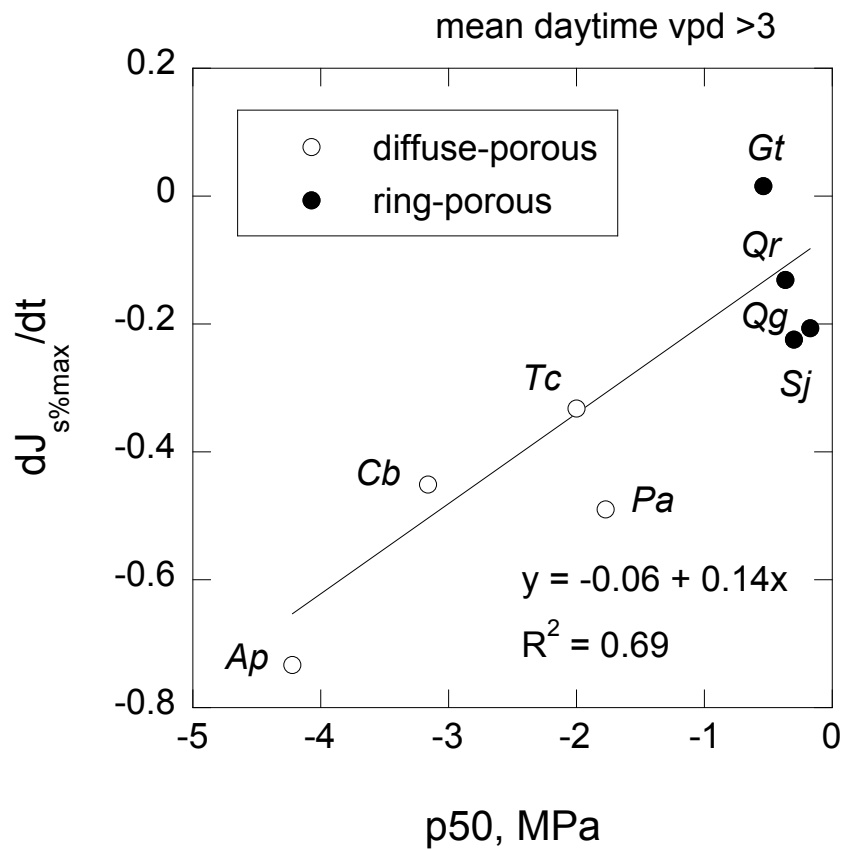


Figure 5.12: The seasonal change in transpiration magnitude versus p50 for atmospheric conditions where mean daytime vpd was greater than 3 kPa. Individual species are identified by letter symbols according to the following: *P. acerifolia* (*Pa*), *A. platanoides* (*Ap*), *T. cordata* (*Tc*), *C. betulus* (*Cb*), *G. triacanthos* (*Gt*), *Q. rubra* (*Qr*), *F. americana* (*Fa*), *C. occidentalis* (*Co*), *S. japonica* (*Sj*).